CHIMIKA CHRONIKA

NEW SERIES

AN INTERNATIONAL EDITION
OF THE ASSOCIATION OF GREEK CHEMISTS

CMCRCZ 20(3-4), 65-178(1991)

ISSN 0366-693X

3-4/91

Volume 20, No 3-4 p.p. 65-178 September-December 1991

CHIMIKA CHRONIKA

NEW SERIES

AN INTERNATIONAL EDITION

Published by the Association of Greek Chemists (A.G.C.)
27 Kaningos str. Athens 106 82 Greece

Correspondence, submission of papers, subscriptions, renewals and changes of address should be sent to Chimika Chronika-New Series, 27 Kaningos street, Athens 106 82, Greece. The Guide to Authors is published in the first issue of each volume, or sent by request. Subscriptions are taken by volume at 2000 drachmas for membres and 3000 drachmas for Corporations in Greece and 50 U.S. dollars to all other countries except Cyprus, where subscriptions are made on request.

Phototypesetted and Printed in Greece by EPTALOFOS S.A.
12, Arditou Str. 116 36 ATHENS Tel. 9217.513

Υπεύθυνος σύμφωνα με το νόμο: Νίκος Κατσαρός, Κάνιγγος 27, Αθήνα 106 82.

Responsible under law: Nikos Katsaros, 27 Kaningos St., Athens 106 82, Greece.

Chimika Chronika, New Series, 20, 65-74 (1991)

293.10

ADDITION D' ORGANOZINCIQUES ALLYLIQUES A DES THIOETHERS PROPARGYLIQUES ET ENYNIQUES

J. AUGER et Y. KOUSSOURAKOS

INSTITUT de BIOCENOTIQUE EXPERIMENTALE des ARGOSYSTEMES UA CNRS 340, Université F. Rabelais, Parc Grandmont 37200 TOURS, FRANCE

(Received February 24, 1986)
Running title: Additions d' organozinciques à des thioéthers.

RÉSUMÉ

Les organozinciques allyliques s' additionnent à la triple liaison des thioéthers propargyliques et ényniques, à fonction acétylénique vraie, par chauffage à reflux durant plusieurs heures dans le THF. Dans certaines conditions, la réaction conduit principalement aux thioéthers diéniques et triéniques résultant d' une monoaddition.

Key - words: Thioethers, organozincincs, plants-insects relations.

INTRODUCTION

Dans le cadre d' une étude de la synthèse et des propriétés de composés soufrés à intérêt biologique, avec application en particulier aux relations entre le poireau (*Allium porrum*) et la teigne (*Acrolepiopsis assectella* Z.)[1], insecte qui lui est inféodé, nous avons envisagé le cas des thioéthers diéniques et triéniques; en effet, de même que les thioéthers, disulfures et trisulfures saturés ou monoinsaturés[2,3], oxydés ou non, les thioéthers diéniques et triéniques sont susceptibles de présenter un intérêt biologique.

Dans ce travail, nous étudions la réaction d' addition entre un organizincique allylique et un thioéther propargylique ou énynique. Il a été montré que les organozinciques allyliques s' additionnent facilement à la triple liaison de carbures acétyléniques vrais[4,5,6,7] d' alcools[5,7,8,9], d' halogénures[8,10,11]

d' éthers-oxydes[8,9,11] et d' amines b-acétyléniques[7,12,13]; il en est de même dans le cas d'énynes conjugués, simples et fonctionnels[4,14,15,16,17,18]. En pratique, lors de l'addition d' un zincique R-ZnBr à la triple liaison d' un composé $HC{\equiv}C\text{-}CH_2Y$, le groupement R se fixe sur l' atome de carbone le plus proche du groupement Y[4,5,7,8,9] sauf lorsque la structure du zincique est encombrée[19,20,21]; en outre, suivant les proportions zincique/composé acétylénique utilisées et suivant la nature du groupement Y, on peut obtenir le produit de monoaddition *1*, le produit de bis-addition *2* et un cyclopropane *3*:

$$HC{\equiv}C-CH_2Y \xrightarrow[2)\ H_2O]{1)\ R\text{-}ZnBr}$$

$CH_2=C(R)-CH_2Y$ *1*

$CH_3-C(R)_2-CH_2Y$ *2*

$(R)_2C$ ——— CH_2 *3*

$\diagdown\ \diagup$

CH_2

R = alk(en)yl

La formation du cyclopropane peut s' expliquer par une réaction de bis - addition sur la triple liaison, suivie d' une réaction d' élimination 1-3 lorsque Y est un bon groupement partant[8,9,10,11].

PARTIE EXPERIMENTALE

— *Thioéthers utilisés:*

Notre étude a été réalisée sur les thioéthers suivants:

4 $HC{\equiv}C-CH_2-S-C_2H_5$; *5* $HC{\equiv}C-CH(CH_3)-S-C_2H_5$;
6 $HC{\equiv}C-C(CH_3)_2-S-C_2H_5$; *7* $CH_3-C{\equiv}C-CH_2-S-C_2H_5$;
8 $HC{\equiv}C-CH_2-S-C_6H_5$; *9* $HC{\equiv}C-CH=CH-S-C_2H_5$ (Z)
10 $HC{\equiv}C-CH=CH-CH_2S-C_2H_5$ (E)

Les composés *4* à *8* et 10 utilisés dans cette étude ont été préparés par action de l' alkyl - (ou du phenyl)thiolate sur le bromure (ou le chlorure) propargylique ou énynque correspondant[22a] (Rdt=60-80%). Le composé *9* a été préparé par action du butadiyne monosodé sur l'éthonethiol [22b] (Rdt=75%).

— *Méthode générale d' addition de l' organometallique sur les thioéthers:*

La réaction est généralement effectuée de la manière suivante: le thioéther acétylénique ou enynique (0,1 mole) est ajouté, à 20°C, au zincique (0,3 mole) préparé dans le THF[2,4], le milieu réactionnel est chauffé sous agitation pendant 15h à reflux. Les résultats obtenus figurent sur le tableau I.

Tableau I: Addition d' organozinciques allyliques aux thioéthers propargyliques et ényniques.

R-ZnBr	Thioéther	Proportions des réactifs	Rdt global	Produits		
				1%	*2%*	*3%*
allyl	*4*	3/1	40%	25	0	75
allyl	*4*	2/1	18%	100	0	0
allyl	*4*	2/1[(a)]	< 5%	100	0	0
crotyl	*4*	3/1	60%	100	0	0
allyl	*5*	3/1	< 5%	100	0	0
allyl	*6*	3/1	0	-	-	-
allyl	*7*	3/1	< 5%	100	0	0
allyl	*8*	3/1	48%	20	0	80
allyl	*8*	2/1	20%	100	0	0
allyl	*9*	3/1	40%	100	0	0
allyl	*10*	3/1	35%	100	0	0
crotyl	*10*	3/1	48%	100	0	0

(a) contact à 20°C pendant 48h; on retrouve une part importante du produit de départ.

Les produits *1* et *3*, liquides, sont isolés à l' état pur, soit par distillation fractionnée, soit par chromatographie en phase vapeur préparative.

Les rendements sont ceux mesurés sur la C.P.V.. Les absorbtions IR sont exprimées en cm^{-1}, les déplacements d des spectres RMN sont exprimés en p.p.m. par rapport au TMS et les constantes de couplage J sont exprimées en Hz.

Lorsque les rendements globaux sont inférieurs à 5% et pour le produit de la réaction sur *10*, qui se polymérise, il n' a pas été possible d' isoler un composé défini. Néanmoins, par analogie avec les autres additions, l' observation de la C.P.V. nous permet de conclure à l' existence d' un produit de monoaddition *1*.

— *Description d' une expérience:*

• *Préparation du bromure d' allyl-zinc*

L' organozincique est obtenu selon Gaudemar[24] à partir de 0,4 at. g (26,2 g) de zinc en poudre, 0,38 mole (46 g) de bromure d' allyle fraichement distillé et 250 cm^3 de T.H.F. anhydre. La température du milieu est maintenue entre 25° et 28°C pendant l' addition goutte à goutte de la solution bromure-THF.

Après 2 h d' agitation à température ambiante et repos d' une nuit, le zincique est utilisé après décantation.

Le rendement (75-80 %) est déterminé par pesée du zinc restant.

Addition de bromure d' allyl-zinc au thioéther 4

A 0,3 mole d' organométallique (54 g), on ajoute goutte à goutte en 15 minutes environ 0,1 mole de thioéther *4* (10 g) dilué dans un volume égal de THF anhydre. La température du milieu s' élève de 10 à 15°C.

On chauffe à température de reflux du solvant (65°C) pendant 15 heures. Le milieu réactionnel est traité par une solution glacée ammoniacale à 20 %.

Après décantation, extraction par 4×100 cm^3 d' éther et sèchage des phases organiques sur K_2CO_3, les solvants sont chassés sous vide et les produits de la réaction sont isolés par distillation sous pression réduite (10 à 15 torrs), au bain d' eau.

Une première fraction qui bout entre 30 et 32°C contient essentiellement le composé *3* (3,6 g soit 0,03 mole) avec un rendement de 30% accompagné d' un peu d' héxène-1 yne-5. Leur séparation s' effectue aisément par CPV préparative.

Une deuxième fraction qui bout entre 35 et 40°C est constituée de disulfure de diéthyle (1,9 g soit 0,15 mole) avec un rendement de 15%.

Une troisième fraction qui bout entre 65 et 68°C contient principalement le produit de monoaddition *1* (1,4 g soit 0,01 mole) avec un rendement de 10%.

Il reste un résidu indistillable qui se polymérise au refroidissement.

— *Produits obtenus*

Allyl Znbr (0,2 mole) + thioéther *4* (0,01 mole)

⟶ Ethylthio-5 methylène-4 pentène-1 (0,01 mole)

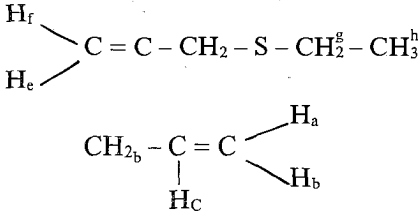

Eb_{12} = 65°C
IR: 910 995 1640 3085
RMN: d = 1,19 (t,3,$\underline{CH_3}$ – CH_2 –) ; 2,35 (q,2,CH_3 – $\underline{CH_2}$ –) ;
2,9 (d,2 – $\underline{CH_2}$ – CH =) ; 3,5 (s,2, – $\underline{CH_2}$ – 5 –) ;
4,82 (m,2, $\underline{CH_2}$ = C) ; 5,15 (m,2, $\underline{CH_2}$ = CH –) ;
5,8 (m,l, – CH_2 – $\underline{CH}$ = CH_2). Jab = 2; Jac = 17; Jbc = 9,5; Jcd = 7;
Jef = 1; Jgh = 7.

Crotyl Znbr (0,3 mole) + thioéther *4* (0,1 mole)
⟶ Ethylthio-5 methyl-3 méthylène-4 pentène-1 (0,06 mole)

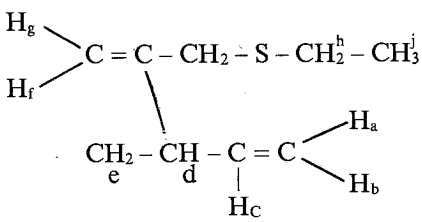

293.11

Eb_{15} = 78-79°C
IR: 910 ; 990 ; 1635 ; 3090
RMN: d = 1,1 (d,3,CH_3 – CH) ; 1,25 (t,3, CH_3 – CH_2 –) ;
2,35 (q,2, CH_3 – CH_2 –) ; 3,1 (s,2, – S – $\underline{CH_2}$ – C) ;
4,8 (s,2 CH_2 = C) ; 5,1 (m,2, CH_2 = CH =) ;
5,7 (m,l, $\underline{CH}$ = CH_2). Jab = 1,5 ; Jac = 17,5 ; Jbc = 9 ; Jcd = 7 ;
Jde = 6,5 ; Jfg = 1 ; Jhj = 5,5.

Allyl ZnBr (0,2 mole) + thioéther *8* (0,1 mole)
⟶ Phénylthio-5 méthylène-5 pentène-1 (0,02 mole)

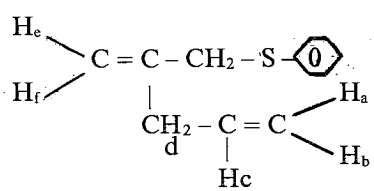

Eb_4 = 130°C
IR: 735 (F) ; 910 (F) CH_2 = C ; 995 (m) ; 1640 (m) ; 3085 (m) C = C

RMN: d = 2,95 (d,2, – CH_2 – CH =); 3,5 (s,2 – CH_2 – S –);
4,9 (m,2, CH_2 = C);
5,4 (m,2, CH_2 = CH –) ; 5,8 (m,l, – CH = CH_4) ;
7,3 (m,5, – 0). Jab = 2 ; Jac = 17 ; Jbc = 9 ; Jcd = 7 ; Jcf = 1.

Allyl ZnBr (0,3 mole) + thioéther *9* (0,1 mole)
⟶ Ethylthio-6 méthylène-4 hexadiène-1,5 (0,04 mole)

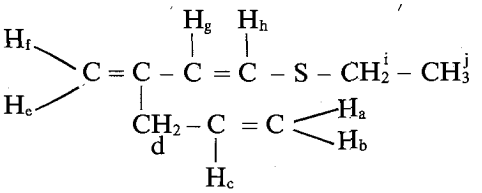

Eb_{24} = 107-110°C
IR : 735 ; 880 ; 910 ; 990 ; 1605 ; 1635 ; 3080
RMN : d = 1,25 (t,3, CH_3 – CH_2 –) ; 2,6 (q,2, CH_3 – CH_2 –) ;
2,95 (d,2, – CH_2 – CH =) ; 4,8 (m,2, CH_2 =) ;
5,0 (m,2, CH_2 =CH –) ;
5,65 (m,l, – CH=CH_2) ; 5,9 (m,2, – CH = CH –).
Jab = 1,5 ; Jac = 18 ; Jbc = 9,5 ; Jcd = 7 ;
Jef = 1,5 ; Jgh = 12 ; Jij = 7.

Allyl ZnBr (0,3 mole) + thioéther *10* (0,1 mole)
⟶ Ethylthio-7 méthylène-4 heptadiène-1,5 (0,035 mole)

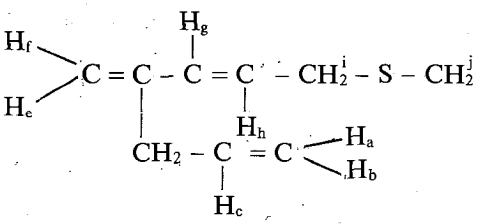

$Eb_{0,1}$ = 65-66°C
IR : 910 ; 990 ; 1600 ; 1640 ; 3090
RMN : d = 1,2 (t,3, CH_3 – CH_2 –) ; 2,4 (q,2, CH_3 – CH_2 –) ;
2,95 (d,2, – CH_2 – CH =) ; 3,1 (d,2, CH – CH_2 – S –) ;
4,85 (m,2, CH_2 =C) ; 5,15 (m,2, CH_2 = CH –) ;
5,75 (m,l, – CH= CH_2) ; 6,0 (m,2, – CH = CH –).
Jab = 1 ; Jac = 17 ; Jdc = 7 ; Jef = 1 ;
Jhg = 15 (E) ; Jhi = 6,5 ; Jik = 7

Allyl ZnBr (0,3 mole) + thioéthers *4* ou *8* (0,1 mole)
⟶ Diallyl-1,1 cyclopropane (0,03 mole)

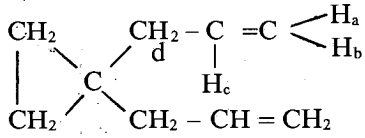

Eb_{71} = 60-62°C
105 = 71°C

IR : 910 (F) ; 995 (F) ; 3080 (F) ; 1640 (F)
RMN : d = 0,3 (s,4, $\underline{CH_2}$) ; 2,0 (d,4, – $\underline{CH_2}$ – CH =) ; 5,8 (m,2, – $\underline{CH}$ =) ;
4,95 (m,4, = $\underline{CH_2}$).
Jab = 2,5 ; Jac = 18 ; Jbc = 9 ; Jcd = 6,5.

DISCUSSION

Cas des thioéthers propagyliques: Lorsque le groupe propargyle ne possède pas de substituants (thioéthers *4* et *8*), la réaction d' addition a lieu comme pour les autres dérivés propargyliques; elle peut conduire à une quantité importante de dérivés cyclopropaniques *3* lorsque l' on utilise un excès de zincique (3/1), mais on obtient uniquement le produit de monoaddition *1* lorsque les réactifs sont dans les proportions 2/1. Avec le bromure de crotyl-zinc, la réaction a lieu avec transposition allylique au niveau de l' organométallique[7,8,12].

Les rendements moyens généralement observés sont dus en partie à l' intervention concurrente de la réaction de substitution qui conduit à l' héxène-1 yne-5, un carbure fréquemment isolé et identifié[11,13].

$$HC \equiv C - CH_2 - S - R' \xrightarrow[2)\ H_2O]{1)\ CH_2 = CH - CH_2 - ZnBr} HC \equiv C - CH_2 - CH_2 - CH = CH_2 + R'SH$$

En plus, lorsque la réaction n' est pas effectuée sous atmosphère rigoureusement inerte, on obtient, à côté du produit d' addition, de 15 à 20% du disulfure R'S – SR', composé provenant vraisemblablement d' une oxydation du thiolate par l' oxygène de l' air[23]:
$2R'S - ZnBr + 1/2\ O_2 \rightarrow R'S - SR' + ZnBr_2 + ZnO$. Ce disulfure est isolé en tête de distillation fractionnée pour chaque expérience réalisée. Il est identifié par comparaison de ses spectres IR et de RMN avec ceux d' un échantillon authentique.

Lorsque la structure propargylique est substituée en α de la triple liaison (thioéthers *5* et *6*), la réaction n' a pratiquement pas lieu, vraisemblablement à cause de l' encombrement stérique[7,8,12].

Lorsque la triple liaison est substituée par un groupement méthyle (thioéther *7*), la réaction n' a pas lieu non plus, ce qui est analogue aux observations faites lors des essais d' addition de zinciques à d' autres dérivés α-acétyléniques substitués[7,8,12,21].

293.12

Cas des thioéthers ényniques: La réaction conduit au produit de monoaddition attendu, avec des rendements moyens (résidus importants). Avec le bromure de crotyl-zinc, la réaction a lieu avec transposition allylique.

Ces résultats sont conformes à ceux observés avec d' autres énynes conjugués fonctionnels[16,17,18] pour lesquels il a été montré que les zinciques s' additionnaient à la triple liaison (en 3, 4), les lithiens à la double liaison (en 1,2) et les magnésiens soit en (1,2) soit en (1,4).

Cette etude nous a permis de préparer par réaction d' addition de zinciques allyliques à des thioéthers possédant une liaison acétylénique vraie, des thiothers diéniques et triéniques:

$CH_2 = C(CH(R') - CH = CH_2) - CH_2 - S - R''$

$R' = H, CH_3$; R'' = alkyle, phényle ;

$CH_2 = C(CH(R') - CH = CH - (CH_2)_n - S - R''$

$R' = H, CH_3$; $n = 0,1$; R'' = alkyle.

Certains de ces composés font l' objet actuellement de tests olfactométriques sur la teigne du poireau *Acrolepiopsis assectella* Z. et sur son parasitoide *Diadromus pulchellus* WSM.

ΠΕΡΙΛΗΨΗ

Σύνθεση Διενικών και Τριενικών Θειαθέρων

Οι αλλυλικές οργανοψευδαργυρικές ενώσεις προστίθενται στον τελικό ακετυλενικό δεσμό των προπαργυλικών και ενυνικών θειαθέρων με βρασμό με κάθετο ψυκτήρα που διαρκεί πολλές ώρες σε τετραυδοφουράνιο.

Σε καθορισμένες συνθήκες η αντίδραση οδηγεί κυρίως σε διενικούς και τριενικούς θειαθέρες οι οποίοι είναι προϊόντα μονοπροσθήκης.

Λέξεις-κλειδιά: Θειαθέρες, οργανοψευδαργυρικές, σχέσεις φυτών-εντόμων.

SUMMARY

Addition of Allylic Organozincics to Propargylic and Enynic Thiothers

Allylic - zinc compounds add on the terminal acetylenic bond of propargylic and enynic thioethers by refluxing a THF solution for several hours. Under suitable conditions, this reaction leads chiefly to dienic thioethers (mono-addition products).

REFERENCES:

1. J. Auger et E. Thibout: Can. J. Zool., *57*, pp. 2223 (1979).
2. Y. Ishikawa, T. Ikeshoji et Y. Matsumoto: Appl. Ent. Zool., *13*, pp. 115 (1978).
3. Y. Koussourakos: Les substances allélochimiques soufrées des Allium: Synthèse d' analogues et action comparée sur le comportement locomoteur d' un insecte spécialiste et d' un généraliste. D.E.A., Tours, 1984.
4. F. Bernadou, B. Mauze, et L. Miginiac: C.R. Acad. Sc., PARIS, 276 C, pp. 1645 (1973).
5. M. Gaudemar: C.R. Acad. Sc., PARIS, 273 C, pp. 1969 (1971). 278 C, pp. 885 (1974).
6. Y. Frangin et M. Gaudemar: Bull. Soc. Chim. Fr., pp. 1173 (1976).
7. G. Courtois et L. Miginiac: J. Organometal. Chem., *69*, pp. 1 (1974).
8. F. Bernadou et L. Miginiac: C.R. Acad. Sc., PARIS, 280 C, pp. 1473 (1975); Tetrahedron Letters, pp. 3083 (1976).
9. Y. Frangin et M. Gaudemar: J. Organometal. Chem., *142*, pp. 9 (1977).
10. Y. Frangin et M. Gaudemar: C.R. Acad. Sc., PARIS, 280 C, pp. 1389 (1975).
11. F. Bernadou et L. Miginiac: J. Organometal. Chem., *125*, pp. 23 (1977).
12. C. Nivert, B. Mauze et L. Miginal: C.R. Acad. Sc., PARIS, 271 C, pp. 698 (1970).
13. C. Nivert, B. Mauze et L. Miginiac: J. Organometal. Chem., *44*, pp. 69 (1972).
14. B. Mauze, G. Courtois et L. Miginiac: C.R. Acad. Sc., PARIS, 274 C, pp. 658 (1972).
15. G. Courtois, B. Mauze et L. Miginiac: J. Organometal. Chem., *72*, pp. 309 (1974).
16. D. Mesnard et L. Miginiac: J. Organometal. Chem., *117*, pp. 99 (1976).
17. G. Courtois et L. Miginiac: J. Organometal. Chem., *117*, pp. 201 (1976).
18. B. Mauze et L. Miginiac: J. Organometal. Chem., *131*, pp. 321 (1977); *134* pp. 1 (1977).

19. M.T. Bertrand, G. Courtois et L. Miginiac: Tetrahedron Letters, pp. 1945 (1974).
20. J. Auger, G. Courtois et L. Miginiac: J. Organometal. Chem., *133*, pp. 285 (1977).
21. G. Courtois et L. Miginiac: C.R. Acad. Sc., PARIS, 285 C, pp. 207 (1977).
22. L. Brandsma: Preparative Acetylenic Chemistry, Elsevier, Amsterdam, pp. 180 (1971 b).
23. S. Patai: The Chemistry of the thiol group, Part. 2, J. Wiley, New-York, pp. 785 à 840 (1974).
24. M. GAUDEMAR, Bull. Soc. Chim. Fr., pp. 974 (1962).

Chimika Chronika, New Series, 20, 75-83 (1991)

GRAM NEGATIVE PSYCHROTROPHIC BACTERIA IN MILK OF EPIROS - GREECE

I.ROUSSIS*, I.KARABALIS**, and C.SARRI***

* *Laboratory of Food Chemistry, Department of Chemistry, University of Ioannina, 451 10 Ioannina*
** *Dairy Industry "Dodoni", Ioannina*
*** *Laboratory of Food Microbiology, Veterinary Service of Ioannina*

(Received July 1, 1986)

SUMMARY

In the present study psychrotrophic bacteria of cow's raw milk in the region of Epiros-Greece were investigated.
The determinations carried out were Total and Psychrotrophic Bacterial Counts (T.B.C. and P.B.C.).
Initial T.B.C. and P.B.C. values were $17.5x10^6$/ml to $110x10^6$/ml and $7x10^6$/ml to $20x10^6$/ml, respectively, the P.B.C. value comprising 18.2 to 40% of the T.B.C. depending on the season of examination. After refrigeration of milk, the above percentage values were significantly increased.
A total of 112 psychrotrophic strains were isolated, 92 of which where found to be Gram negative. From the latter 40 were identified to be of the *Pseudomonas* genus.
Of the Gram negative isolates at 4°C the proteolytic strains comprised the 35,0% and the lipolytic ones the 47.8% whereas at 25°C the corresponding values were 48.9 and 53.2%.

Key words: Psychrotrophs, lipolytic bacteria, proteolytic bacteria.

INTRODUCTION

Today raw bulk milk is stored at 4°C and subsequently delivered to the dairy plant for processing.

The advantages of this handling system are:

a) Elimination of spoilage associated with the growth of lactic acid bacteria and most pathogens,

b) Reduction of unit cost for transport, and

c) Achievement of uniform supply.

However, despite these handling advantages, multiplication of phychrotrophic bacteria introduces a serious problem. These bacteria, of environmental source, degrade important milk constituents by the excretion of heat stable enzymes, mainly proteases and lipases.

The most important respresentative genera of these contaminants are:

a) Gram negatives: *Pseudomonas, Alcaligens, Achromobacter-Acinetobacter, Flavobacterium, Xanthomonas* and members of the *Enterobacteriaceae* family[1]

b) Gram positives: some thermoduric species from genera *Bacillus* and *Clostridium*[2,3]

The significance of psychrotrophic bacteria is well understood and it has been proposed that the presence of psychrotrophs along with the coliforms could comprise an index of production and handling conditions of milk[4].

In the present study psychrotrophic bacteria of cow's milk from several collecting and cooling stations in the region of Epiros-Greece were investigated.

The determinations carried out concerned counts of total and psychrotrophic bacterial flora. In addition, psychrotrophs from milk on the day of sampling were isolated and identified. Proteolytic and lipolytic activities of isolated species among Gram negatives were also examined.

EXPERIMENTAL

Raw cow's milk was obtained from cooling stations in the region of Epiros-Greece. Samples were taken during the four seasons of the year as follows: October-November, January-February, March-April and June-July.

For Total Bacterial Counts (T.B.C.) and Psychrotrophic Bacterial Counts (P.B.C.) plates were incubated at $32\pm1^{\circ}C$ for $48\pm3h$ and $7\pm1^{\circ}C$ for 10 days respectively[5].

The standard plate count method was employed[5] for T.B.C. and P.B.C., determination using quarter strenght Ringer's Solution as diluent[6] and Plate Count Agar as substrate.

Representative single colonies were taken and transferred into Nutrient Broth. They were purified by the streak method on Nutrient Agar and subcultured for a month. Before every use, strains were recovered in Nutrient Broth and subsequently on Nutrient Agar at $25^{\circ}C$ for 18-24h.

To test proteolysis, Skim Milk Agar was used as substrate. Plates were inoculated by streaking and were incubated at $4^{\circ}C$ and $25^{\circ}C$ for 10 and 5 days, respectively. Protein hydrolysis was observed by formation of clear zones around the growing bacterial colonies following addition of 1% HCl[7].

Fat lipolysis was observed by formation of clear zones as above in plates containing Tributyrin Agar[7].

Genus classification was determined on the basis of morphological and biochemical characteristics included in Bergey's Mannual[8], Cowan and Steel[9], Hendriew and Swewan[10], Hayward[11] and Sneath[12] (Table I), as described by Kalogridou[13].

In summary, classification tests were as follows:

Gram stain, cell morphology, oxidation - fermentation (O/F) test, oxidase test, catalase test, growth under aerobic and anaerobic conditions, motility[9], stain of flagella using the modified Montana method[7], diffusion and/or fluorescence of produced pigment[14] and growth spreading[15] (Table I).

TABLE I. Characteristics of Gram negative bacteria genus determination cont'd

Genera	Gram Stain	Cell morph o-logy	Motil ity	Flagella	Diffusible		Non diffusible
					fluorescent	non fluorescent	
Pseudomonas	-	R	+	polar	none or green	none, green, blue, brown,	none, yellow, red,brown,
Xanthomonas	-	R	+	polar	-	rosy, black	blue,rosy,black
Flavobacterium	-	R	+	peritrichous	-	-	yellow, brown
Flavobacterium	-	R	-	-	-	-	yellow
Aeromonas-Vibrio-Plesiomonas	-	R	±	polar	-	- brown	yellow, orange none, yellow, blue,red
Alcaligenes	-	R,RC,	+	peritrichous	-		
Moraxella	-	C		-	-	-	-
Acinetobacter	-	R	-	-	-	-	-
Chromobacterium	-	R,RC	+	polar	-	-	-
Enterobacteriaceae family	-	R	+	peritrichous	-	-	violet
Enterobacteriaceae family	-	R	-	-	-	-	none,yellow,red
Cytophage-Flexibacter	-	R R	-	-	-	-	- yellow,orange,rosy

Genera	O - F				Catalase	Oxidase	Aerobic	Anaer obic	Spread-ing growth
	alcaline reaction	oxid ative	ferment ative	producti-on of gas					
Pseudomonas	±	±	-	-	+	+ rarely - - or (+)	-	-	
Xanthomonas	-	+	-	-	+		+	-	
Flavobacterium	-	±	-	-	+	±	+	-	-
Flavobacterium	-	+	-	-	+	+	+	-	-
Aeromonas-Vibrio-Plesiomonas	-	+	+	±	+	+	+	+	
Alcaligenes	±	±	-	-	+	+	+	-	
Moraxella	-	+	-	-	±	+	+	-	
Acinetobacter	-	±	-	-	+	-	+	-	
Chromobacterium	-	+	±	-	+	+	+	±	
Enterobacteriaceae family	-	+	+	±	+	-	+	+	
Enterobacteriaceae family	-	+	+	±	±	-	+	+	
Cytophage-Flexibacter	-	±	(+)	-	±		+		+

R: Rods
C: Cocci
(+): Weak

RESULTS AND DISCUSSION

Total and Psychrotrophic Bacterial Counts were determined in totally 48 milk samples, 12 from each of the four seasons. The autumn's samples were examined after 0 (initial), 1,2 and 3 days of storage at 4°C, while the rest of them, after 0 (initial) and 3 days of storage at the above temperature.

The initial values of T.B.C., 17.5×10^6/ml to 110×10^6/ml, depending on the season of examination (Table II) were relatively high as compared to most values in the literature, for example 15×10^3/ml[16] and 15×10^4/ml to 29.6×10^4/ml[17], while were similar to other's values, for example 6.1×10^6/ml[18], 25×10^4 to 68×10^7/ml[19].

TABLE II. Changes of T.B.C. and P.B.C. in the four seasons of the year during storage of raw mikl at 4°C for 0 and 3 days

Days of storage		T.B.C.x10^6		P.B.C.x10^6		Percentage of P.B.C. to T.B.C.
		Average	Range	Average	Range	
Winter	0	17.5±5.4*	11.5-25.0	7.0±2.9	3.5-12.0	40.0
	3	50.0±9.2	33.0-68.0	35.0±7.4	20.0-48.5	70.0
Spring	0	28.0±4.6	20.0-36.5	10.0±3.0	4.5-17.5	35.7
	3	82.5±11.8	58.5-117.5	51.0±8.2	37.0-71.5	61.8
Summer	0	110.0±19.4	81.5-144.5	20.0±3.0	13.5-28.0	18.2
	3	260.0±37.5	172.0-324.0	125.0±19.7	81.0-152.0	48.0
Autumn	0	44.0±12.5	31.5-64.0	14.5±4.2	7.5-24.5	32.9
	3	135.0±20.4	102.5-169.0	77.0±11.5	54.5-94.5	57.0

* Errors given are standard deviation of the mean for n=12

The initial counts of psychrotrophs (P.B.C.), 7×10^6/ml to 20×10^6/ml, depending on the season of examination (Table II) were also high as compared to published data. Whang

and Who[20] for example have reported P.B.C. $2.5x10^6$/ml to $10x10^6$/ml while Richard[21] $2.1x10^3$/ml to $7.7x10^3$/ml. Counts of psychotrophs were also somewhat higher than the upper limit suggested by Muir and Phillips[22] for rejection of milk.

The initial percentage ratios of P.B.C. to T.B.C. increased with a high rate for the milk samples stored at 4°C (Table III). The above ratios ranged from 18.2 to 40.0%. The corresponding percentage ratios were ranged from 48.0 to 70.0% after storage of samples for 3 days at 4°C (Table II). Bockelman[23] found initial ratio of P.B.C. to T.B.C. 26% which increased to 65% after refrigeration for 72h, while Kalogridou[13] reported initially 34% and after refrigeration for 2,4,6 and 8 days 49,59,67 and 71% respectively.

TABLE III. Changes of T.B.C. and P.B.C. during storage of raw milk at 4°C for 0,1,2 and 3 days (Period of examination autumn)

Days of storage	T.B.C.x10^6		P.B.C.x10^6		Percentage of P.B.C to T.B.C. (%)
	Average	Range	Average	Range	
0	44.0±2.5*	31.5-64.0	14.5±4.2	7.5-24.5	32.9
1	75.0±5.4	46.5-98.0	35.0±7.0	24.0-46.5	46.7
2	110.0±7.8	78.0-138.5	54.0±9.4	41.5-68.5	49.1
3	135.0±0.4	102.5-169.0	77.0±11.5	54.5-94.5	57.0

* Errors given are standard deviation of the mean for n=12

T.B.C. values after storage of samples for 3 days at 4°C, increased by 2.36 to 3.07 times, depending on the season of examination and P.B.C. by 5.0 to 6.5 times (Table II), while Bloquel and Veillet-Poncet[16] observed increase 1.13 and 8.0 times, respectively, after storage for 4 days at 4°C.

The lowest T.B.C and P.B.C. values were those of winter samples and the highest were those of summer ones. These results are in agreement with those of Whang and Cho[20].

112 strains were isolated from autumn samples, 92 of which were Gram negative. Our interest was focused on Gram negatives, since these mainly introduce problems in dairy products[24], thus, the 20 Gram positive isolates were not further examined.

The percentages of Gram negatives to total isolates (82%), is on the high side among values reported in the literature such as 84.8[14], 66.6[23] and 59%[13].

Gram negative psychrotrophs were present in all milk samples. Their genus, frequency of appearance and number of isolated strains are given in Table IV.

TABLE IV. Frequency of appearance and number of isolates of Gram negative psychrotrophs

Genera	Total isolates		Positive*	
	Number	Percentage	Number	Percentage
Pseudomonas	40	43.5	10	83.3
Acinetobacter	16	17.5	7	58.3
Flavobacterium	8	8.7	5	41.6
Moraxella	4	4.3	2	16.6
Aeromonas-Vibrio-Plesiomonas	8	8.7	3	25.0
Enterobacteriaceae family	16	17.3	9	75.0

12 samples of milk were tested. Those containing the corresponding isolates were characterized as positive

Strains of *Pseudomonas* and *Acinetobacter* genera and of *Enterobacteriaceae* family appeared more frequently comprising 43.5, 17.5 and 17.5% of Gram negative isolates, respectively. Other reported values for *Pseudomonas* include 82.1[25], 65,6[26], 58.0[23] 36.3[27] and 31.2%[13]. As compared to the above values, our value was rather low, although this genus appeared more frequently among the others genera. Reported values for *Acinetobacter* include 21.8[27] and 12.5[13] while for *Enterobacteriaceae* similar values to our own have been reported. [23,28,14,13] The percentage values of the other genera were small
[23,28,14,13] The percentage values of the other genera were small

and in general agreement with literature values[27,13] although there are some differences among them.

Isolated Gram negative strains were examined for proteolytic and lipolytic activity.

Proteolytic strains comprised 35.9 and 48.9% the total Gram negative isolates while lipolytic strains comprised 47.8 and 53.2% at 4°C and 25°C, respectively (Table V).

TABLE V. Number and percentage of proteolytic and lipolytic Gram negative psychrotrophic bacteria of raw milk

Genera	Lipolytic						Proteolytic					
	4°C			25°C			4°C			25°C		
	+	-	%	+	-	%	+	-	%	+	-	%
Pseudomonas	22	18	50	24	16	49	14	26	42	18	22	40
Acinetobacter	10	6	23	10	6	20	8	8	24	10	6	22
Flavobacterium	2	6	4.5	3	5	6	2	6	6	6	2	13
Moraxella	0	4	-	0	4	-	0	4	-	0	4	-
Aeromonas-Vibrio-Plesiomonas	6	2	14	7	1	14	5	3	15	6	2	13
Enterobacteriaceae family	4	12	8.5	5	11	11	4	12	12	5	11	11

+: with lipolytic or proteolytic activity
-: without lipolytic or proteolytic activity

Psychrotrophs excrete larger amounts of protease at room temperature than at 4-7°C[29,30] while often the opposite occurs for lipase excretion. In contrast, both enzymes are more active at room termperatures than at 4-7°C. On the basis that psychrotrophs act by their extracellular enzymes[24], it can be explained why these were found to be more active at 25°C than 4°C.

Pseudomonas strains were both the most active proteolytic and lipolytic among the other genera in agreement with the literature[24,33,34]. *Acinetobacter* strains also showed high proteolytic and lipolytic activity while those of the *Enterobacteriaceae* family did not, in spite of their high frequency of appearance.

In conclusion, since the P.B.C. values appear to be relatively high, there is a possible risk for spoilage of milk and its products, considering the large number of proteolytic and lipolytic bacteria within the P.B.C. population especially at 4°C.

ΠΕΡΙΛΗΨΗ

Gram αρνητικά ψυχρότροφα βακτήρια νωπού γάλακτος περιοχής Ηπείρου.

Μελετήθηκαν τα αρνητικά κατά Gram ψυχρότροφα βακτήρια του νωπού αγελαδινού γάλακτος της περιοχής Ηπείρου.

Προσδιορίστηκαν ο ολικός βακτηριακός πληθυσμός (Ο.Β.Π.) και ο πληθυσμός των ψυχρότροφων βακτηρίων (Ψ.Β.Π.). Ο Ο.Β.Π. αρχικά, ανάλογα με την εποχή εξέτασης ήταν $17,5x10^6$/ml - $110x10^6$/ml και ο Ψ.Β.Π. $7x10^6$/ml - $20x10^6$/ml που αντιστοιχεί σε 18,2-40,0% του Ο.Β.Π. Με διατήρηση του γάλακτος με ψύξη για 1,2 και 3 ημέρες το παραπάνω % ποσοστό αύξανε σημαντικά. Απομονώθηκαν 112 ψυχρότροφα στελέχη, 92 αρνητικά κατά Gram απο τα οποία 40 ήταν του γένους *Pseudomonas*.

Απο τα αρνητικά κατά Gram ψυχρότροφα το 35.0 και 48.9% ήταν πρωτεολυτικά, ενώ το 47.8 και 53.2% λιπολυτικά στους 4°C και 25°C, αντίστοιχα.

ACKNOWLEDGEMENTS

The constructive criticism of the munuscript by Drs. C.Drainas and E.Voudouris is gratefully acknowledged. Thanks are due to Dr. D.Kalogridou for advice on biochemical tests and to Mr. A.Pashali for laboratory assistance.

This study has financed by the Ministry for Industry, Energy and Natural Resources of Greece (6557/7-2-84)

REFERENCES

1. Mikolajcik, E.M. *Cult.Dairy Prod.J.* 14,6 (1980)
2. Larkin, J.M. and Stokes, J.L., *J.Bacteriol.* 91,1667 (1966)
3. Bhadsalve, C.H. Shehata, T.E. and Collins, E.B., *Appl.Microbiol.* 24,699 (1972)
4. Thomas, S.B., Druce, R.C. and Jones, M., *J.Appl.Bacteriol.* 34,659, (1971)
5. American Public Health Association (APHA). *Standar methods for the examination of dairy products* (13rd ed). APHA Washington (1972)
6. British Standard. *Methods of microbiological examination for dairy purposes* (1968)

7. Harrigan, W.E. and Mc Cance, ME., *Laboratory methods in food and dairy microbiology*. Academic Press, London (1976)
8. Buchanan, B.E. and Gibbons, N.E., *Bergey's Mannual of Determinative Bacteriology*. Williams and Wilkins Co. Baltimore (1974)
9. Cowan, S.T. and Steel, I.J., *Mannual for the identification of medical bacteria*. (2nded). Cambridge University Press (1975)
10. Hendrie, M.S. and Shewan, J.M., *In technical Series Soc.Appl.Bacteriol.* 14,1 (1979)
11. Hayward, A.C., *In technical Series Soc.Apppl.Bacteriol.* 14,15 (1979)
12. Sneath, P.H.A., *In technical Series Soc.Appl.Bacteriol.* 1,15 (1966)
13. Kalogridou, D. and Manoklidis, K., *Bulletin National Dairy Committee of Greece.* 1,61 (1984)
14. Dempster, J.F., *J.Appl.Bact.* 31,290 (1968)
15. Hendrie, M.S., Mitchell, T.G., Shewan, J.M., *In technical Series Soc.Appl.Bacteriol.* 2,67 (1968)
16. Bloquel, R. and Veillet-Poncet, L., *XXI Int.Dairy Congress, Vol.1. B.1.* Moscow, USSR (1982)
17. Luck, H., *Dairy Science Abstracts*. 2290 (1983)
18. Kim, J.W. and Kim, N.S., *Dairy Science Abstracts.* 1122 (1982)
19. Pandey, J.N. and Mandal, L.N., *Dairy Science Abstracts*. 1120 (1982)
20. Whang, D.W. and Cho, J., *Dairy Science Abstracts*. 3059 (1982)
21. Richard, J., *Dairy Science Abstracts*. 1121 (1982)
22. Muir, D.D. and Phillips, J.D., *Milchwissenschaft*. 39,7 (1984)
23. Bockelman (Von), J., *XVIII Int.Dairy Congress*, IE 106, Sydney. Australia (1970)
24. Law, B.A., *J. of Dairy Research*. 46, 573 (1979)
25. Kikuchi, M. and Matsui Y., *J.Dairy Food Sci.* 25 (1976)
26. Ergullu, E., *Dairy Science Abstracts*. 3760 (1983)
27. Terada, A., Tanaka, S. and Uchida, K., *Dairy Science Abstracts*. 3035 (1982)
28. Law, B.A., Cousins, C.M., Sharpe, M.E. and Davis, F.C., *In techn.Series Soc.Appl.Microbiol.* 13,137 (1979)
29. Juffs, H.S., *J. of Appl.Bacteriol.* 40,23, (1976)
30. Mayerhofer, H.J., Marshall, R.T., White, C.H. and Lu, M., *Appl.Microbiol.* 25,44 (1973)
31. Alford, J.A. and Elliot, L.E., *Food Res.* 25,296, (1960)
32. Andersson, R.E., *Appl. and Environm.Microbiol.* 39,36 (1980)
33. Fairbairn, D.J. and Law, B.A., *J. of Dairy Research*. 53,139, (1986)
34. Stead, D., *J. of Dairy Research*. 53, 481, (1986)

Chimika Chronika, New Series, 20, 85-95 (1991

PREPARATION OF SPERMIC ACID AND RELATED COMPOUNDS

PANAYIOTIS V.IOANNOU
Department of Chemistry, University of Patras, Patras, Greece

(Received June 17, 1988)

SUMMARY

The preparation of N,N′-bis(β-carboxyethyl)-and N,N,N′,N′-tetra(β-carboxyethyl) derivatives of ethylenediamine, propylenediamine and butylenediamine was effected by adding ethyl acrylate to the parent diamines followed by acidic hydrolysis of the intermediate esters. The procedure was simpler compared to cyanoethylation-hydrolysis route and afforded better yields.

Key words: Spermic acid, N,N′-bis(2-carboxyethyl) diamines, N,N,N′,N′-tetra(2-carboxyethyl) diamines.

INTRODUCTION

Spermine, $H_2N(CH_2)_3NH(CH_2)_4NH(CH_2)_3NH_2$, an important polyamine for a cell, is catabolized mainly[1] by oxidation via its dialdehyde[2] to the diacid, spermic acid, 9.[3] Spermic acid was found only in the brain and spinal cord of rabbit, rat and oxen[3] and in the urine of rats.[1] While spermine and spermine diol stimulate DNA degradation[4,5] and the dialdehyde of spermine is toxic to bacteria and spermatozoa[2] virtually nothing is known about the role of spermic acid in the central nervous system. The catabolic fate of thermine, $H_2N(CH_2)_3NH(CH_2)_3NH(CH_2)_3NH_2$, found in certain thermophilic bacteria, is not known.

The diacids 7-9 and the tetraacids 10-12 can act as complexones, for 7 and 10 form compexes with metal cations[6-8] which are of theoretical[9,10], analytical[11,12] and, probably, of biochemical[13] interest.

From the various routes for the preparation of 7-9 and

NHCH2CH2COOEt
(CH2)n
NHCH2CH2COOEt
2HCl
H2O/HCl
90°C
NHCH2CH2COOH
(CH2)n
NHCH2CH2COOH
2HCl
1 ≈ n = 2
2 ≈ n = 3
3 ≈ n = 4
7 ≈ n = 2
8 ≈ n = 3
9 ≈ n = 4
N(CH2CH2COOEt)2
(CH2)n
N(CH2CH2COOEt)2
2HCl
H2O/HCl
90°C
N(CH2CH2COOH)2
(CH2)n
N(CH2CH2COOH)2
2HCl
4 ≈ n = 2
5 ≈ n = 3
6 ≈ n = 4
10 ≈ n = 2
11 ≈ n = 3
12 ≈ n = 4
NH2
(CH2)n
NH2
OEt
O
2
4

10-12, the cyanoethylation-hydrolysis route for the preparation of 7[6,14-16], 9[2,3,17] and 10[6] and the reaction of β-chloropropionic acid with ethylenediamine for the synthesis of 10[10] have been followed. These procedures are tedious with low to moderate overall yields.

I found that the addition of ethyl acrylate to the aliphatic diamines followed by mild hydrolysis of the purified intermediates, 1-6, was a much simpler procedure for the preparation of 7-12 and the yields were better than those reported in the literature for 7, 9 and 10.

RESULTS AND DISCUSSION

Reaction of the diamine in absolute ethanol (95% ethanol was not a suitable solvent) with two equivalents of ethyl acrylate under high dilution and slow addition conditions gave the desired diester with traces of mono- and triester. The formation of by-products could not be avoided. Isolation of the diester by distillation under reduced pressure led to decomposition[6,18], isolation by dissolving in ether and bubbling hydrogen chloride gave sticky gums which were difficult to work with, while isolation as described in the experimental afforded pure, anhydrous 1-3 in acceptable yields.

For the syntheses of tetraesters, it is important that the triester by-product not be present by more than trace amounts because its removal by recrystallizations leads to considerable loss. The triester was present in large amounts when the reaction was carried out in ether instead of anhydrous ethanol. The salt 4 crystallizes as a hydrate, 6 is anhydrous while 5 could not be crystallized.

The acidic hydrolysis of 1-3 could not be followed by TLC. Isolation of the products as the dihydrochloride salts was effected by adding acetone. The oil which may result crystallized relatively easily. For better yields the water used in the recrystallizations should be kept as little as possible (1.5-0.5 ml/g). For 7 I found a capillary m.p.240-242°C (dec.) as did Haydock and Mulholland[14] while Martell and Chaberek[6] reported 194-198°C (dec.). The m.p. was, however,

211-218°C (dec.) when determined on a hot stage m.p. apparatus.[14] The salt 9 crystallized as a dihydrate which can be dehydrated at 140°C; both salts gave the same m.p.(202-205°C dec.). However, Tabor et al.[2,17] reported a m.p. 221-222°C (dec.) for the anhydrous 9.

The hydrolysis of 4-6 can be followed by TLC (vide infra). Isolation and purification of the products were effected as in the diacid case, without any difficulties except of 11. The salt 10 was anhydrous, 11 was an alcoholate and 12 was a hydrate. When these salts were left at 110°C for 24 h, 10 did not lose weight but its m.p. increased ~20°C, 11·2EtOH decomposed,and 12.5H_2O lost its waters without decomposition with a concomitant increase of its m.p. by ~40°C.

The TLC developing solvents A and B can separate the mono-, di-, tri- and tetraesters and therefore are useful for following their syntheses and the purity of the products 1-6. Solvent C,used in conjuction with non-activated Ca^{2+} —treated silica gel H,did not separate the diesters 1-3 from the diacids 7-9 but did separate the tetraesters 4-6 from the tetraacids 10-12. However it did not separate the intermediates (mono-, di- and triacid) during the hydrolysis of the tetraesters 4-6 even if catalytic amounts of HCl were used to slow down the hydrolysis. Various other developing systems were tried (acidic, e.g. AcOH/H_2O; neutral, e.g. EtOH/H_2O; basic e.g. $CHCl_3$/MeOH/conc. NH_3) for silica gel and for cellulose TLC supports in order to achieve the desired separations but without any success.

EXPERIMENTAL

General

The diamines and stabilized ethyl acrylate were used as such.[19] TLCs were run on microscope slides coated with Merck silica gel H with developing systems: A:$CHCl_3$/MeOH 6:1 v/v (for the esters); B:$CHCl_3$/MeOH/conc.NH_3 60:10:1 v/v (for the hydrochlorides of the esters) and with non-activated silica gel H containing $CaCl_2$ with conc. NH_3 as developing solvent (solvent C) for the hydrochlorides of all acids.Visualization

was effected by spraying with 35% H_2SO_4 and charring. Melting points were taken in open capillaries and are uncorrected. Infrared spectra were recorded as KBr discs with a Perkin Elmer model 577 spectrophotometer and ^{1}H-NMR spectra were taken on a Varian EM-60 spectrometer at 60 MHz in D_2O with DSS (dimethylsilapentanesulphonate) as internal standard.

Preparation of the esters 1-6

N,N'-bis(2-carbethoxyethyl)-1,2-diaminoethane dihydrochloride, 1

To a solution of ethylenediamine (30.00g, 0.5 mol) in 300 ml absolute ethanol was added dropwise over 25 h a solution of ethyl acrylate (100.00 g, 1 mol) in 500 ml absolute ethanol. The yellow solution was stirred at room temperature for 10 h. TLC of the pink solution (solvent A) showed the product, R_f 0.30, and traces of mono-, R_f 0.03, and triester, R_f 0.50. After cooling to 0°C, 94 ml conc. hydrochloric acid was added and the system was left at 0°C for 1 h. Filtration and washing with absolute ethanol gave virtually pure, by TLC (solvent B), product (R_f 0.27) as small flakes, which was recrystallized from 95% EtOH (300 ml) to yield 82.96 g (50%) of product 1 as big white flakes after drying in vacuum at room temperature. M.p. 206-208°C. Calcd for $C_{12}H_{28}N_2O_8.2HCl$: C 43.25, H 7.86, N 8.41%; found C 43.74, H 7.63, N 8.34%. IR: 1270 cm^{-1}. ^{1}H-NMR(δ): 1.3(t, J = 6Hz, 6H, $\underline{CH}_3$), 3.0(m, 4H, $\underline{CH}_2CO$), 3.50(m, 8H, $C\underline{H}_2\overset{+}{N}C\underline{H}_2$), 4.3(q, 4H, $OC\underline{H}_2$).

N,N'-bis(2-carbethoxyethyl)-1,3-diaminopropane dihydrochloride, 2

Prepared as in 1 (0.5 mol scale) and recrystallized from 420 ml 95% EtOH. Yield 84.03 g (49%) of pure 2 as big white flakes, m.p. 231-234°C. Calcd for $C_{13}H_{26}N_2O_4.2HCl$: C 44.96, H 8.13, N 8.07%; found C 44.41, H 8.33, N 8.71%. IR : 1720 cm^{-1}. ^{1}H-NMR (δ) : 1.3 (t, J = 6Hz, 6H, $\underline{CH}_3$), 2.35 (m, 2H, $CH_2C\underline{H}CH_2$), 3.0(m, 4H, $\underline{CH}_2CO$), 3.3(m, 8H, $C\underline{H}_2\overset{+}{N}C\underline{H}_2$), 4.3(q, 4H, $O\underline{CH}_2$).

N,N'-bis(2-carbethoxyethyl)-1,4-diaminobutane dihydrochloride, 3

Prepared on a 0.244 mol scale as in 1 but using twice as

high dilution. Yield 57.47 g (65%) of white crystals, pure by TLC. M.p. 238-240°C (lit. 237-8°C [16]). Calcd for $C_{14}H_{28}N_2O_4.2HCl$: C 46.54, H 8.37, N 7.76%; found C 46.13, H 8.49, N 7.45%. IR : 1720 cm^{-1}. ^{1}H-NMR (δ): 1.3(t, J = 6Hz, 6H, $\underline{CH_3}$), 1.80(m,4H, $CH_2\underline{CH_2}CH_2\underline{CH_2}CH_2$), 2.9(m, 4H, $\underline{CH_2}CO$), 3.3(m, 8H, $\underline{CH_2}\overset{+}{N}\underline{CH_2}$), 4.2(q, 4H, $O\underline{CH_2}$).

N,N,N',N'- tetra (2-carbethoxyethyl)-1,2-diaminoethane dihydrochloride hydrate, 4. $\frac{3}{2}$ H_2O

To a cold solution of ethylenediamine (15.00 g, 0.25 mol) in 75 ml absolute ethanol, ethyl acrylate (130 ml, 1.2 mol) was added dropwise over 1 h in such a way that the temperature did not exceed 40°C.[19] The yellow solution was then stirred at room temperature for 9 days i.e. till disappearance of the triester (TLC solvent A : triester R_f 0.50, tetraester R_f 0.68). The dark red solution was cooled to 0°C and 47 ml conc. hydrochloric acid was added. Addition of 300 ml acetone and cooling at -20°C for 12 h gave a precipitate which was filtered, washed with acetone (3 x 30 ml) and ether (2 x 50 ml) and recrystallized from 500 ml absolute ethanol warmed to 40°C, and cooling at 0°C overnight. Filtration and washing with ether afforded the pure by TLC product (109 g, 78%) as white thin needles after drying in vacuo at room temperature. M.p. 137-141°C. Calcd for $C_{22}H_{40}N_2O_8.2HCl.3/2\ H_2O$: C 47.14, H 8.09, N 5.00%; found C 47.15, H 8.71, N 4.23%. IR : 3490, 1705, 1715 cm^{-1}. ^{1}H-NMR (δ) : 1.2(t, J = 6Hz, 12H, $\underline{CH_3}$), 3.0(m, 8H, $\underline{CH_2}CO$), 3.5(m, 12 H, $\underline{CH_2}\overset{+}{N}(\underline{CH_2})_2$), 4.2(q, 8H, $O\underline{CH_2}$).

N,N,N',N'-tetra(2-carbethoxyethyl)-1,3-diaminopropane dihydrochloride, 5

Crude 5 was prepared as in 4 (0.51 mol scale) after 4 days reaction. Addition of 94 ml conc. hydrochloric acid and evaporation of the solvents afforded a pink oil which could not be crystallized.

N,N,N',N'-tetra(2-carbethoxyethyl)-1,4-diaminobutane dihydrochloride, 6

Crude tetraester was prepared as in 4 (0.186 mol scale) after 3 days reaction. After the addition of 35 ml conc. hydrochloric acid, absolute ethanol was added to give a 5 ml EtOH: 1 g product ratio and cooled at -20°C overnight. Filtration afforded virtually pure by TLC product which was recrystallized from 400 ml absolute ethanol, warmed at 70°C, and leaving at room temperature for 24 h. Pure 6 (needles, 85.73 g, 82%) m.p. 167-169°C. Calcd for $C_{24}H_{44}N_2O_8.2HCl$: C 51.33, H 8.26, N 4.99%; found C 50.89, H 8.59, N 4.38%. IR : 1705, 1715 cm^{-1}. ^{1}H-NMR (δ) : 1.3(t, J = 6Hz, 12H, $\underline{CH_3}$), 1.9(m, 4H, $CH_2\underline{CH_2}CH_2CH_2$), 3.0(m, 8H, $C\underline{H_2}CO$), 3.5(m, 12H, $C\underline{H_2}\overset{+}{N}(\underline{CH_2})_2$), 4.3(q, 8H, $OC\underline{H_2}$).

Preparation of the acids 7-12

N,N'-bis(2-carboxyethyl)-1,2-diaminoethane dihydrochloride, 7

A solution of 1 (76.59 g, 0.23 mol) in 153 ml water and 38 ml 6 M hydrochloric acid was stirred at 90°C for 7 h. TLC (solvent C) did not differentiate between reactant and product. Addition of 1150 ml acetone, leaving at room temperature overnight, filtration and washing with acetone yielded 63 g white shiny microcrystals. These were dissolved in 95 ml boiling water, 190 ml warm 95% EtOH was added and the system left to crystallize at room temperature overnight. Filtration and drying in vacuo at room temperature yielded pure 7 (54.79 g, 86%). M.p.240-242°C (dec.) (lit.[6] : 194-8°C, [14] : 238-240°C). Calcd for $C_8H_{16}N_2O_4.2HCl$: C 34,67, H 6.55, N 10.11%; found C 34.21, H 6.77, N 9.83%. IR : 1720 cm^{-1}. ^{1}H-NMR(δ) : 2.8(m, 4H, $\underline{CH_2}CO$), 3.5(m, 8H, $\underline{CH_2}\overset{+}{N}C\underline{H_2}$).

N,N'-bis(2-carboxyethyl)-1,3-diaminopropane dihydrochloride, 8

Prepared as in 7 on a 0.23 mol scale and recrystallized from boiling water (0.75 ml/g) and warm 95% EtOH (4 ml/g). Yield 53.37 g (80%). M.p. 203-204°C. Calcd for $C_9H_{18}N_2O_4.2HCl$: C 37.24, H 6.92, N 9.62%;found C 37.24, H 6.99, N 9.48%.

IR : 1710 cm^{-1}. ^{1}H-NMR(δ) : 2.3(m, 2H, $CH_2\underline{CH}_2CH_2$), 2.9(m, 4H, $C\underline{H}_2CO$), 3.3(m, 8H, $C\underline{H}_2\overset{+}{N}C\underline{H}_2$).

N,N'-bis(2-carboxyethyl)-1,4-diaminobutane dihydrochloride, 9

Prepared as in 7 on a 0.144 mol scale. Recrystallization from boiling water (0.5 ml/g) and warm 95% EtOH (2 ml/g) gave big white crystals which on prolonged drying in vacuo at room temperature collapsed to the dihydrate (powder, 40.27 g, 82%). M.p. 201-205°C (dec.). IR : 3400, 1710 cm^{-1}. The product on drying at 140°C for 66 h loses 9.29% H_2O which corresponds to a loss of $2H_2O$. M.p. 202-206°C (dec.)(Lit.[2,17]:221-2°C dec.). Calcd for $C_{10}H_{20}N_2O_4.2HCl$:C 39.35, H 7.27, N 9.18%; found C 39.68, H 7.33, N 9.14%. IR : 1710 cm^{-1}. ^{1}H-NMR(δ) : 1.8(m, 4H, $CH_2C\underline{H}_2C\underline{H}_2CH_2$), 2.8(m, 4H, $C\underline{H}_2CO$), 3.3(m, 8H, $C\underline{H}_2\overset{+}{N}C\underline{H}_2$).

N,N,N',N'-tetra(2-carboxyethyl)-1,2-diaminoethane dihydrochloride, 10

A solution of 4 (109.00 g, 0.1946 mol) in 218 ml water and 65 ml 6M hydrochloric acid was stirred at 90°C for 7 h. TLC (solvent C) showed only the product 10 (R_f 0.50) and no 4 (R_f 0.00) after 1 h reaction. Addition of 2L acetone gave a precipitate which was left at room temperature overnight. Filtration, washing with acetone gave white shiny microcrystals (63 g) which were recrystallized from 63 ml boiling water by adding 136 ml warm 95% EtOH and leaving at 0°C overnight. Filtration and drying in vacuo at room temperature yielded 10 (48.39 g, 59%). M.p. 204-208°(dec.). Calcd for $C_{14}H_{24}N_2O_8.2HCl$: C 39.91, H 6.22, N 6.65%; found C 40.06, H 6.46, N 6.81%. IR : 1720 cm^{-1}. ^{1}H-NMR(δ) : 3.0(m, 8H, $C\underline{H}_2CO$), 3.8(m, 12H, $C\underline{H}_2\overset{+}{N}(C\underline{H}_2)_2$). The product can be dried at 110°C for 22 h without decomposition or loss of weight but its m.p. rises to 226-229°C.

N,N,N',N'-tetra(2-carboxyethyl)-1,3-diaminopropane dihydrochloride dialcoholate, 11.2 *EtOH*

The impure 5 was treated as in 10. Addition of acetone (4L) gave an oil which was separated by decantation and dis-

solved in 300 ml absolute ethanol. Addition of ether (1L) gave a gum which did not crystallize. The solvents were decanted and 200 ml absolute ethanol was added. Heating to boiling while stirring and scratching induced the transformation of the gum to a white microcrystalline solid. After 24 h at room temperature it was filtered and dried in vacuo at room temperature to give 84.14 g (35% overall yield based on the diamine) of white microcrystalline, hygroscopic product, m.p. 116-119°C. Calcd for $C_{15}H_{26}N_2O_8.2HCl.2C_2H_5OH$: C 43.26, H 7.64, N 5.31%; found C 43.41, H 7.58, N 6.06%. IR : 3400, 1710 cm^{-1}. ^{1}H-NMR(δ) : 1.2(t, J = 6Hz, 6H, $C\underline{H}_3CH_2OH$), 2.5(m, 2H, $CH_2C\underline{H}_2CH_2$), 3.0(m, 8H, $C\underline{H}_2CO$), 3.6(m, 16H, $C\underline{H}_2\overset{+}{N}(C\underline{H}_2)_2$ and $C\underline{H}_2OH$). The product cannot be dried at 110°C because it decomposes to a sticky, transparent, glassy mass.

N,N,N',N'-tetra (2-carboxyethyl)-1,4-diaminobutane dihydrochloride, 12

Prepared as for 10 on a 0.1426 mol scale. Drying in vacuo at room temperature gave 62.55 g (82%) of white crystalline $12.5H_2O$, m.p. 138-140°(dec.) (premelting at 85°C). IR : 3500, 3360, 1710 cm^{-1}. This product can be dried at 110°C for 22 h without decomposition. It loses 9.03% H_2O corresponging to a loss of $5H_2O$. M.p. 180-182°C(dec.).Calcd for $C_{16}H_{28}N_2O_8.2HCl$: C 42.77, H 6.73, N 6.23%; found C 42.67, H 6.99, N 6.44%. IR : 1710 cm^{-1}. ^{1}H-NMR(δ) : 2.0(m, 4H, $CH_2C\underline{H}_2C\underline{H}_2CH_2$), 3.0(m, 8H, $C\underline{H}_2CO$), 3.5(m, 12H, $C\underline{H}_2\overset{+}{N}(C\underline{H}_2)_2$).

ΠΕΡΙΛΗΨΗ. Σύνθεση του σπερμικού οξέος και συγγενών ενώσεων.

Στην εργασία περιγράφεται η παρασκευή των N,N'-δις(β-καρβοξυαιθυλ)- και N,N,N',N'-τετρα(β-καρβοξυαιθυλ)-παραγώγων της αιθυλενοδιαμίνης, προπυλενοδιαμίνης και βουτυλενοδιαμίνης με προσθήκη ακρυλικού αιθυλεστέρα στις μητρικές διαμίνες και όξινη υδρόλυση των εστέρων που προκύπτουν. Η μεθοδολογία αυτή είναι πειραματικώς απλούστερη από αυτήν της κυανοαιθυλιώσεως-υδρολύσεως με συνέπεια την αύξηση των αποδόσεων.

ACKNOWLEGMENTS

I would like to thank the Alexander S.Onassis Public Benefit Foundation for financial support and Dr.Mantzos, of the National Hellenic Research Foundation, for the elemental analyses.

References

1. Van den Berg, G.A., Elzinga, H., Nagel, G.T., Kingma, A.W. and Muskiet, F.A.J., *Biochim. Biophys. Acta*, 802, 175 (1984).
2. Tabor, C.W., Tabor, H. and Bachrach, H., *J.Biol.Chem.*, 239, 2194 (1964).
3. Imaoka, N. and Matsuoka, Y., *J.Neurochem.*, 22, 859 (1974).
4. Yanagawa, H., Ogawa, Y. and Egami, F., *Z.Allg.Mikrob.*, 16, 627 (1976).
5. Yanagawa, H., Ogawa, Y. and Egami, F., *J.Biochem.*, 80, 891 (1976).
6. Martell, A.E. and Chaberek, Jr., S., *J.Amer.Chem.Soc.*, 72, 5357 (1950).
7. Courthey, R.C., Chaberek, S. and Martell, A.E., *J.Amer. Chem.Soc.*, 75, 4814 (1953).
8. Kodama, M., *Bull. Chem. Soc. Japan*, 43, 2259 (1970).
9. Radanovic, D.J., Djuran, M.I., Stamenovic, D.C. and Grujic, S.A., *Glas. Hem. Drus. Beograd*, 49, 315 (1984);
10. Radanovic, J.J., Djuran, M.I. and Douglas, B.E., *Inorg. Chem.*, 24, 4239 (1985).
11. Sanderson, I.P. and West, T.S., *Talanta*, 9, 71 (1962).
12. Ferreira, R.A.L., Laino, M.C.C. and Martinez, F.B., *Rev. Port. Quim.*, 27, 511 (1985).
13. Jones, M.M., Basinger, M.A. and Weaver, A.D., *J.Inorg. Nucl. Chem.*, 43, 1705 (1981).
14. Haydock, D.B. and Mulholland, T.P.C., *J.Chem.Soc.* (C), 2389 (1971).
15. Egorova, L.G., Serebryakova, N.V. and Tyurenkova, G.N., *J. Gen. Chem. U.S.S.R.*, 41, 1816 (1971).
16. Wasserman, H.H. and Berger, G.D., *Tetrahedron*, 39, 2459 (1983).

17. Tabor, H. and Tabor, C.W., *Methods in Enzymology*, 94, 418 (1983).
18. Johnson, M.R., *J.Org. Chem.*, 51, 833 (1986).
19. Mozingo, R. and McCracken, J.H., *Org. Synth. Coll. Vol*, 3, 258 (1955).

Chimika Chronika New Series, 20, 97-106 (1991)

CONFORMATIONAL CHANGES OF THE INTERACTION BETWEEN PEPSIN AND POLYIONS BY CIRCULAR DICHROISM STUDIES

CHRISTOS I MEKRAS*
Department of Chemistry, Imperial College of Science Technology and Medicine, University of London, London SW7 2AY, ENGLAND - UK.

(Received October 20, 1988)

ABSTRACT

A study has been made of the effects of selected polycations on the circular dichroism (CD) spectrum of the enzyme pepsin A(E.E. 3.4. 23.1) in the wavelength range 240nm to 310nm where the polycations did not have a CD spectrum. The polycations were: polybrene, protamine, poly (L-lysine), spermine and spermidine, and each had been shown previously[1] to inhibit the enzyme. Each of the polycations had a definite effect on the CD spectrum, showing strong binding to the enzyme. The neutral polymer, polyvinylpyrrolidone (PVP) was also found to modify the CD spectrum of pepsin. **The strengths of the interactions as indicated by the** magnitudes of the changes in the CD spectrum of pepsin at 270nm were: polybrene > protamine > poly (L-lysine) > PVP > spermidine > spermine.

Key Words: Circular Dichroism, Enzyme, Pepsin, Protamine Sulphate, Polybrene, Poly(L-lysine), Spermine, Spermidine, Polyvinyl Pyrrolidone.

ABBREVIATIONS AND SYMBOLS

CD	Circular dichroism
θ	Elipticity in radians
$[\theta]$	Molecular elipticity
λ	Wavelength in nm
K_L	Imaginary part of the complex refractive index for left circularly polarized light
K_R	Imaginary part of the complex refractive index for right circularly polarized light
ϵ	Decadic molar extinction coefficient (litre/mole-cm or (Molar absorbance index)
C	Molar concentration of the sample (moles/litre)
l	Light pathlength through the sample (cm)
T	Transmittance of sample
M	Gram-molecular weight of the sample
C'	Concentration in grams per cm^3
A	Absorbance difference of a sample for left- and right-circularly polarized light: $A=A_L-A_R$

* Correspondence:
Dr. Christos I Mekras, BSc, PGDip, MSc, PhD, LRSC, ASC, CBiol, MIBiol.
Department of Chemical Engineering, South Bank Polytechnic, 103 Borough Road, London SE1 0AA

h Planck constant (h=6.62 X 10^{-27} ergs)
N_1 Number of optically active molecules per cm^3
$\theta_K( )$ Measured circular dichroism (elipticity) per unit pathlength due to the Kth transition (radians/cm)
R_K Rotational strength of the Kth optically active transition
PAGE- Polyacrylamide Gel Electrophoresis
SDS Sodium Dodecyl Sulphate

INTRODUCTION

Recently I have shown that porcine pepsin (E.C. 3.4.21.1) is inhibited by the polycations: protamine, polybrene, spermine and spermidine. This is in agreement with the earlier reports of the inhibitory action of poly(L-lysine)[2-4]. Evidence has also been presented to show that protamine, polybrene and poly (L-lysine) form complexes with pepsin[5-7]. In an attempt to obtain a clearer understanding of the nature of the pepsin - polycation complexes, a study has been made of the circular dichroism (CD) of pepsin alone and in the presence of each of the polycations. Previous CD studies of pepsin have reported the effects of pH variations[8,9] and the changes caused by two slightly different forms of the naturally occurring, low molecular weight inhibitor, pepstatin[9,10]. The present work reports for the first time the influence of polycations on the CD spectrum of pepsin.

Historical Role of Circular Dichroism (CD)

Considerable information concerning the structure of proteins in solution can be obtained from measurement of their optical activity. Because of the small volume and low concentration required, a protein sample of less than 0.1 mg is often sufficient for a CD determination[11].

CD is extraordinarily sensitive probe of conformational changes in polynucleotides. There is a huge change in CD relative to absorbance of the same sample and conentration[12]. Furthermore, with computer techniques, it is possible to determine the nearest-neighbour frequencies from a CD spectrum, which is of tremendous practical value in determining base sequences. The precision of CD analysis is no greater than that of standard enzymatic methods, but to obtain a CD spectrum requires a few hours, whereas the enzymatic analysis would take about a week provided the pure enzymes were available. Changes such as these can be used to study:

1. The loss of helical structure of single-stranded polymers by various agents such as high temperature of extremes of pH;
2. the transition from single- to double-stranded polynucleotides and vice versa;
3. structural changes introduced by the binding of cations, peptides, proteins, and so forth.

In the present study the changes in circular dichroism of the enzyme, pepsin, in the presence of polyions such as poly (L-lysine), polyvinyl-sulphate, polyvinyl pyrrolydone, protamine sulphate, spermidine, spermine, polybrene and Kappa-carrageenan,

have been investigated using the modified Cary 61 CD instrument. Different polyions concentrations were used and interpreted as evidence of binding to the enzyme under the experimental conditions.

All optical measurements including circular dichroism were performed in 1-cm pathlength quartz cells, at 25-27°C temperature.

Circular dichroism spectra were recorded on a modified Cary 61 spectropolarimeter[15]. The enzyme spectra as well as the spectra involving the polycations used in this work were run with a 100-second time constant. The cell compartment was flashed with dry nitrogen and the sample cavity was thermostated at 27°C. Spectra were routinely corrected for base-line shifts by running samples of the solvent (water). The circular dichroism scans were generally run in duplicate. Results are expressed as molecular elipticity $[\theta]$ in degrees $-cm^2$ per decimole and also as the difference in the extinction coefficients of the sample for left- and right-circularly polarized light $A = \epsilon_L - \epsilon_R$ in litre/mole-cm. The circular dichroism curves were measured in the wavelength range 240-310nm; wavelength readings were reproducible to ± 0.5nm. All CD measurements were checked by reference to a solution (0.1%) of camphor-d-10-sulphonic acid[16].

Molecular Weight Determination of Pepsin and Investigation of the Degradation on its Own and in the Presence of Protamine Sulphate

The molecular weight has been determined in two ways. The first was by the calibration curve of phosphorus, using the molybdenum blue method, assuming that the pepsin has one phosphate group, and the second by PAGE-SDS electrophosesis[17].

Both methods gave a satisfactory value of the molecular weight of pepsin of 34,440 and 34,640 respectively, which agrees well with the literature value 34,700 Daltons. The pepsin is not degraded by various temperatures 25°, 37° and 100°C neither in the presence of protamine sulphate as PAGE-SDS.

pH Measurement

pH measurements were carried out using a Radiometer Copenhagen pH M 64 research pH meter or a Pye Unicam model 292 Mk II. pH meter was calibrated with standard buffers each time before measurement taken. The buffers used in this work were prepared using standard tablets.

MATERIALS

Pepsin A (E.C.3.4.23.1), from porcine stomach mocosa had been twice crystallized and the lyophilized powder was obtained from the Stigma Chemical Company and stored at 0-5°C in a desiccator. Haemoglobin which had been prepared from washed, lysed and dialysed bovine erythrocytes, was obtained from Sigma (Type II) and stored at 0-5°C in a desiccator. Sigma also supplied protamine sulphate (Grade X) which had been obtained from salmon and gave a negative millon text. The material was used in extensive gel electrophoresis experiments and found it to be homogeneous. Poly (L-lysine) hydrobromide, molecular weight 2,500 Daltons; and Polybrene (poly(dimethylimino)-1,3-propanediyl(dimethylimino)-1,6-

hexanediyl dibromide)) were both of synthetic origin and were obtained from Sigma, as were spermine tetrachloride; spermidine trichloride, Polyvinyl-pyrrolidon (PVP-40) and Folin and Ciocalteu's phenol reagent. All these materials were stored under appropriate conditions. The other chemicals used were of analytical purity (AR).
Note: Concentrations of each polycation have been expressed as "base moles per litre" where one base mole is the mass of a polycation associated with one positive charge.

METHODS

The activity of the sample of pepsin used in these studies has been reported previously[1]. The purity of the enzyme was further checked by three methods. The first was by estimation of the phosphorus content of the pepsin using the method given by Cohen et al[13]. The second was by the use of polyacrylamide gel electrophoresis (PAGE) using a method based on that of Weber and Osbourne[14]. The third was by estimation of the nitrogen content. This was carried out by Butterworths Laboratories of Teddington, Middlesex.

For most of the experiments, especially the studies of circular dichroism, all the solutions were made up using triply distilled water.

RESULTS

The phosphorus content was found to be 0.09% and since pepsin contains only one phosphorus atom per mole[18], the molecular weight of the pepsin was calculated to be 34,440 compared with the generally accepted value of 34,700. The 'PAGE' method gave a value of 34,640. The nitrogen content of the pepsin was 16.4% (theoretical value = 16.9%). The effects of the selected polycations (10^{-4} to 4×10^{-4} base mole l^{-1}) on the CD spectrum of pepsin (1.18 or 1.20mg cm^{-3}) are shown in Figures 1 to 6, in the range 240-310nm. The main bands at 280nm and 271nm may be attributed to tryptophan, or tyrosine residues in the pepsin and the band at 265nm to phenyl alanine residues.

Figure 1 shows the effect of adding poly(L-lysine hydrobromide) to the pepsin. A change occurred in the intensity of each of the main CD bands at 280, 271 and 265nm, indicating a strong interaction between the enzyme and the polycation.

Figure 2 shows that the neutral polymer polyvinylpyrrolidone (PVP) has a similar effect on the CD spectrum of pepsin. (Other work[17] has shown that PVP is an effective inhibitor of pepsin).

Protamine sulphate (Figure 3) showed similar effects, although in this case the changes in the spectrum were more pronounced.

Polybrene (Figure 4) showed the largest changes in the CD spectrum of pepsin that were observed in the present experiments.

Figure 1 Circular dichroism spectra of Pepsin (1.18 mg/ml)in the presence of Poly (L-lysine) (P-L-L) in aqueous solution 27°C and pH6.2 (____) Pepsin; (....) and (-.-.) Pepsin + P-L-L of 10^{-5} and $2.0X10^{-5}$ base mol/litre, respectively.

Figure 2 Circular dichroism spectra of Pepsin (1.18 mg/ml) in the presence of Polyvinyl-pyrrolidone (PVP) in aqueous solution at 27°C and pH 6.2 (____) Pepsin; (....) and (-.-.) Pepsin PVP of $2.0X10^{-5}$ and $4.0X10^{-5}$ base mol/litre, respectively.

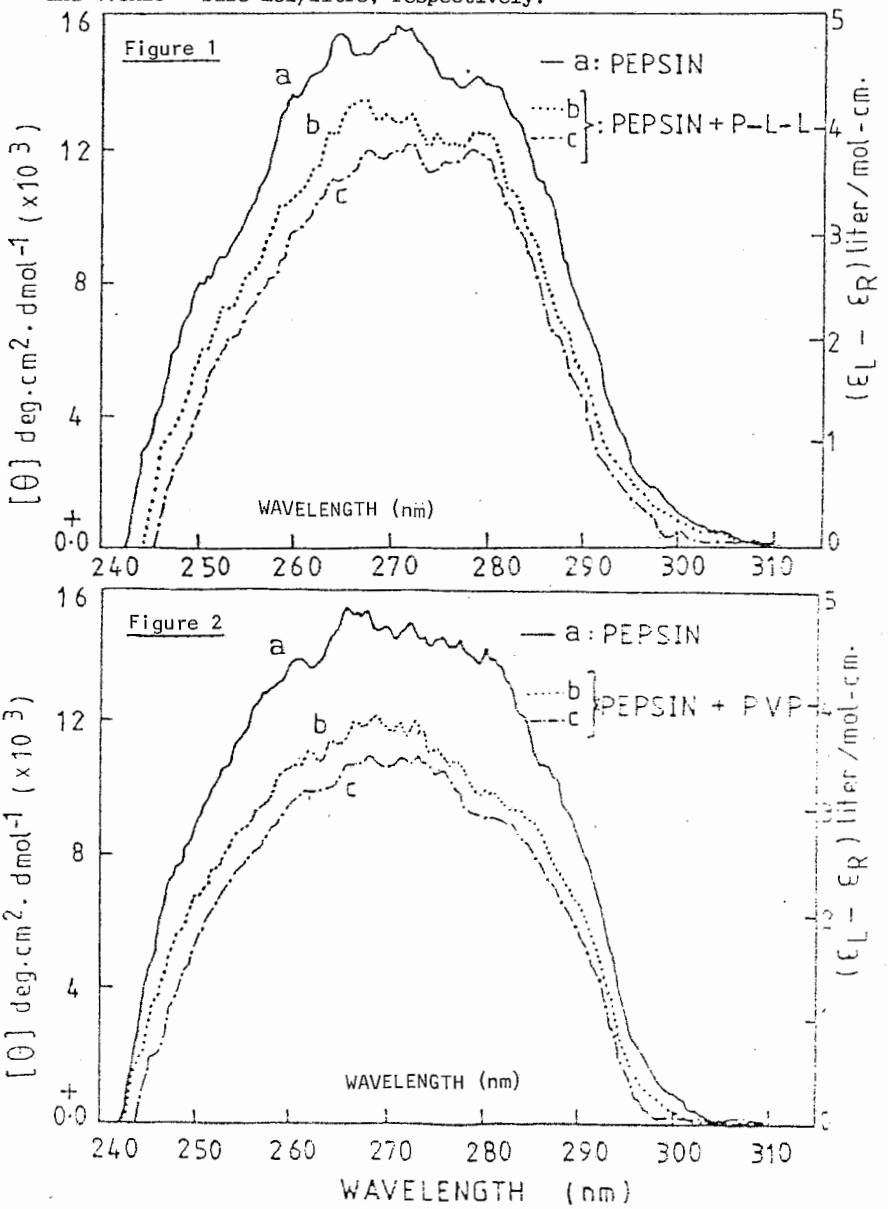

Figure 3 Circular dichroism spectra of Pepsin (1.18 mg/ml in the presence of Protamine sulphate in aqueous solution at 27° and pH 6.2. ( ) Pepsin; ( ) and (-.-.) Pepsin + Protamine of 10^{-5} and $0X10^{-5}$ base mol/litre, respectively.

Figure 4 Circular dichrosm spectra of Pepsin (1.2 mg/ml) in the presence of Polybrene in aqueous solution at 27°C and pH 6.2 ( ) Pepsin; ( ) and (-.-.) Pepsin + Polybrene of 10^{-5} and $2.0X10^{-5}$ base mol/litre, respectively.

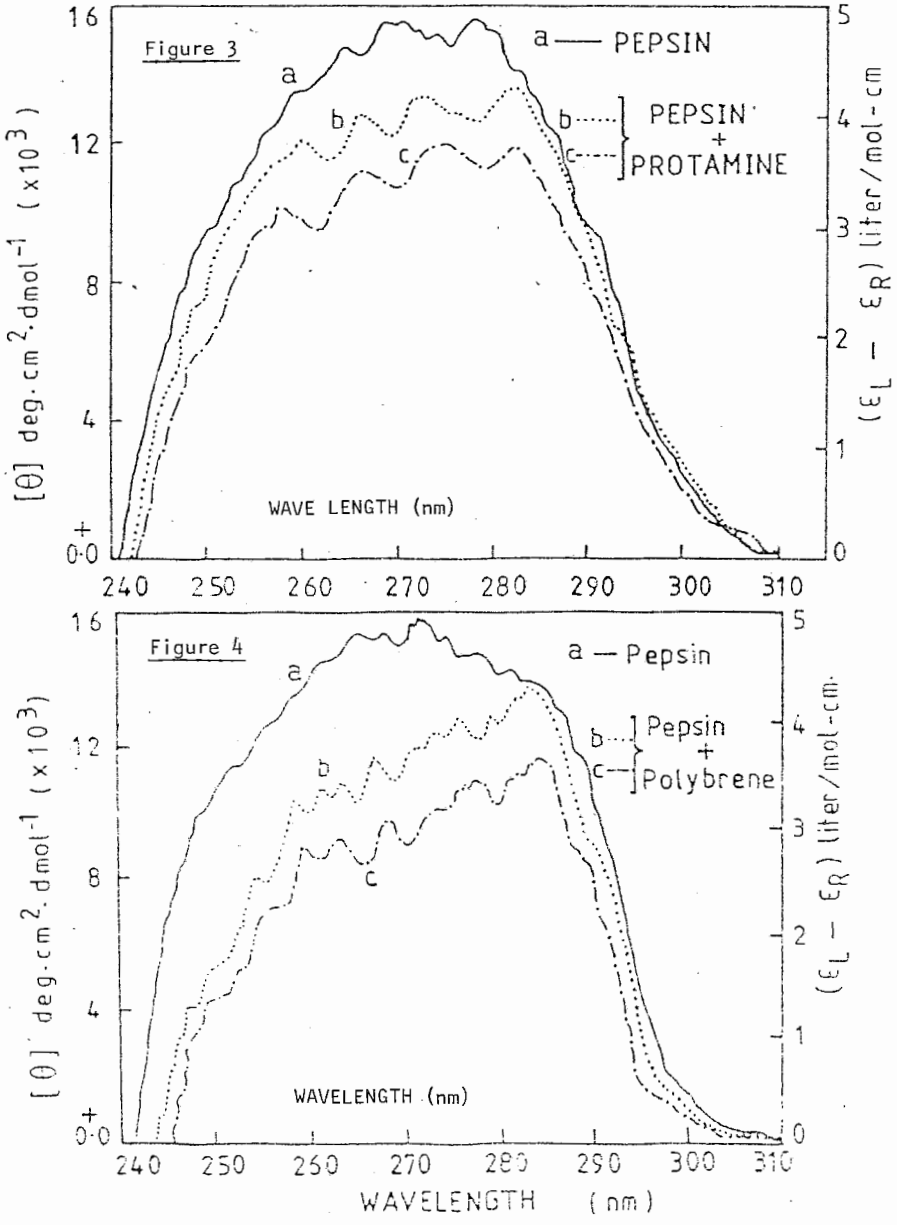

Figure 5 Circular dichroism spectra of Pepsin (1.18 mg/ml in the presence of Spermidine in aqueous solution at 27°C, and pH6.2. ( ) Pepsin; ( ) and (-.-.) Pepsin + Spermidine of 2.0^{-5} base mol/litre.
Figure 6 Circular dichroism spectra of Pepsin (1.2 mg/ml) in the presence of Spermine in aqueous solution at 27°C, and pH612 ( ) Pepsin; (....) and (-.-.) Pepsin + Spermine of $2.0X10^{-5}$ and $4.0X10^{-5}$ base mol/litre, respectively.

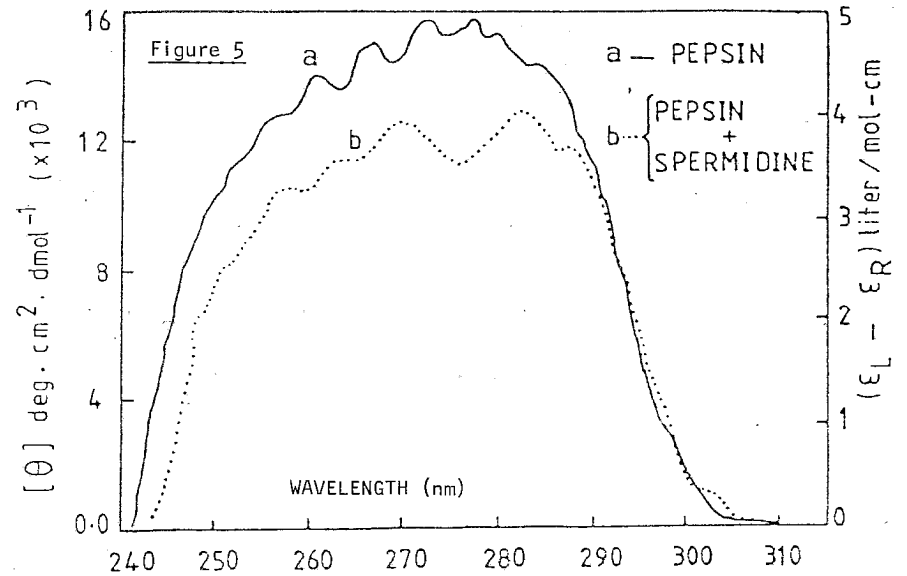

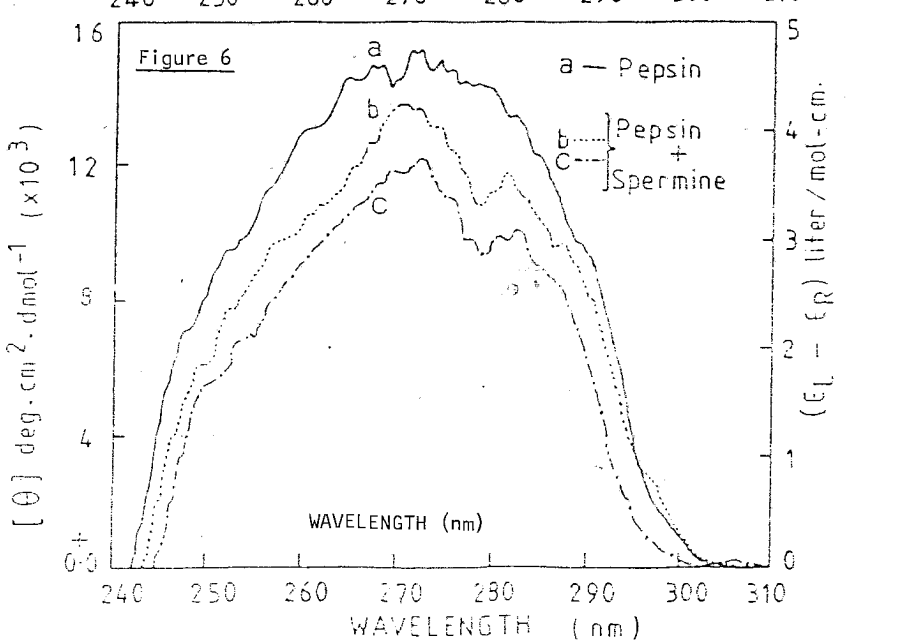

Spermidine (Figure 5) and spermine (Figure 6) were expected to behave similarly, but in fact were quite different, although each interacted quite strongly with the pepsin.

A summary of the quantitative changes caused by the polycations in the CD spectrum of pepsin are given in Table 1 for the wavelength of 270nm.

It is important to note that none of the polycations showed any CD spectrum in the range of wavelengths used when they were run in aqueous solutions alone.

DISCUSSION

The results show that each of the polycations causes definite changes in the CD spectrum of pepsin. Since the enzyme used had a high degree of purity, it follows that these effects must be caused by changes in the conformation of the pepsin as it interacts with the polycations. (If no conformational change had taken place, the CD spectrum would have been unchanged, as for example, Kuramoto et al[19] reported recently for the interaction of polyacrylic acid and bovine serum albumin).

Several features are of interest, especially the fact that the best inhibitors[1]: protamine and polybrene, caused similar changes in the CD spectrum of the pepsin. The spectra of the pepsin, the presence of these polycations (Figures 3 and 4) resembles that given by Kozlov et al[9] for pepsin at pH 1-5 and by Turk et al[8] for pepsin at pH 3.5. (A similar effect is also shown by spermidine in Figure 5). The changes in the CD spectrum shown in Figures 3, 4 and 5 on the addition of the polycations, resemble very closely the changes that Kozlov et al[9] reported when pepsin was taken from pH 6 to a lower pH, and may indicate that the polycations caused similar conformational changes to those accompanying protonation of the pepsin.

The other polycations and PVP had a different type of effect on the CD spectrum of pepsin, and that may indicate that they act as inhibitors by a different mechanism.

It is of interest to note that spermidine (Figure 5) with three positive charges per molecule, behaved differently to spermine (Figure 6) which has only one more positive charge per molecule.

The two previous CD studies of pepsin-inhibitor interactions by Kozlov et al[9] and Nakatani et al[10] showed that the binding of the inhibitor had the effect of enhancing the elipticity values, slightly at pH 3[9] and ph 5[10]. The spectrum given by Kozlov et al[9] for pepsin plus pepstatin is very similar to our spectra for pepsin plus polybrene (Figure 4), or protamine (Figure 3), although we worked at pH 6.2 and then at pH 3.0.

The data in Table 1, which shows the percentage of the elipticity of the pepsin that remains in the presence of the polycations, allows us to list the polycations in order of their effectiveness in changing the CD spectrum of pepsin.

TABLE 1
The Effect of Polycations on the Circular Dichroism of Pepsin (1.18mg ml^{-1}) in Aqueous Solutions at 25°C and pH 6.2

Polycation	Concentration of Polycation (base mol l^{-1}	Percentage of Elipticity Remaining at 270 nm in Presence of Polycation
Polybrene	10^{-5}	76
Polybrene	2 X 10^{-5}	58
Protamine	10^{-5}	80
Protamine	2 X 10^{-5}	69
Polyvinylpyrrolidone	2 X 10^{-5}	80
Polyvinylpyrrolidone	4 X 10^{-5}	72
Poly(L-lysine)	10^{-5}	82
Poly(L-lysine)	2 X 10^{-5}	76
Spermidine	2 X 10^{-5}	87
Spermine	2 X 10^{-5}	94
Spermine	4 X 10^{-5}	81

The order is:
polybrene > protamine > poly(L-lysine) > PVP > spermidine > spermine.

In previous studies using fluorescence depolarisation[19] and dye-displacement[6], we have shown that pepsin forms definite complexes with protamine[11] and polybrene[6]. The present CD studies have confirmed those results and also shown evidence of strong interactions between pepsin and poly)L-lysine), polyvinylpyrrolidine, spermine and spermidine.

ACKNOWLEDGEMENTS

The author is indebted to Dr. R P F Gregory (University of Manchester, Medical School) and to Dr. J B Lawton (University of Salford) for valuable assistance during this study. The author also expresses his gratitude to Miss Breda O' Connor (UCL) for typing this manuscript on a special paper provided by the Journal.

CONCLUSION

Considerable information concerning the structure of pepsin in the presence of polyions has been obtained from the studies of the circular dichroism of pepsin-polycation complexes. The results for the interaction of poly(L-lysine), plyvinyl sulphate, protamine, spermidine, spermine and polybrene are shown in Figures 1-6.

It appears to be a change in circular dichroism spectra due to binding of pepsin to polyions. The spectra of the polyions when run alone, did not show any change at all in the range of wavelengths used, thus indicating that the observed changes are due to changes in the conformational structure of pepsin. These results have been taken as a further evidence for a strong interaction between the pepsin and each of the polycations.

ΠΕΡΙΛΗΨΗ

Μεταβολές της διαμόρφωσης από αλληλεπίδραση πεψίνης και πολυκατιόντων στα φάσματα κυκλικού διχροϊσμού.

Μελετάται η επίδραση επιλεγμένων πολυκατιόντων στο φάσμα του οπτικού διχροϊσμού (CD) της πεψίνης A (E.E. 3.4. 23.1) στην περιοχή κύματος 240nm έως 310 nm, στην οποία τα πολυκατιόντα δεν δίδουν φάσμα CD.Τα πολυκατιόντα polybrene,protamine,poly(L-lysine), spermine και spermidine αναστέλλουν το ένζυμο. Κάθε πολυκατιόν επηρεάζει το φάσμα CD, εμφανίζοντας ισχυρή σύνδεση με το ένζυμο Επίσης το ουδέτερο πολυμερές πολυβυνιλοπυρρολιδόνη (PVP) τροποποιεί το φάσμα CD της πεψίνης. Η ισχύς των αλληλεπιδράσεων, όπως εκδηλώνεται από το μέγεθος των αλλαγών του φάσματος CD της πεψίνης στα 270 nm είναι:polybrene protamine poly(L-lysine) PVP spermidine spermine

REFERENCES

1. J B Lawton, C I Mekras, J. Pharm. Pharmacal. 37, 396 (1985).
2. E Katchalski, A Berger, H Newman, Nature 173, 998 (1954).
3. E E Dellert, M A Stahmann, Nature 176, 1028 (1955).
4. W Anderson, J E Harthill, R Rhamatalla, J. Pharm. 32, 248 (1980).
5. J B Lawton, C I Mekras, Int. J. Biol. Macromol. 7, 2248 (1985).
6. J B Lawton, C I Mekras, Makromol. Chem. 186, 2397 (1985).
7. C I Mekras, MSc Thesis, University of Salford, UK, (1982).
8. V Turk, V Puizdar, T Lah, I Kregar in "Cell Function and Differentation", Part C, Alan R Liss, Inc., P.81 (1982).
9. L V Kozlov, E A Meshcheryakova, L L Zavada, E S Efremov, L G Rashkovetskii, Biokhimiya 44, 338 (1979).
10. H Nakatani, K Kitagishi, K Hiromi, Biochim. Biophys. Acta, 452, 521 (1976).
11. J A Alder, L Grossman and G D Fasmale Biochemistry 7, No. 11, 3836 (1968).
12. V Turk, V Puizdar, T Lah and I Kregar, Progress in Clinical and Biological Research 102, (c) (1982).
13. L E Cohen, F W Czech, Chemiet-Analyst 47, 86 (1958).
14. K Weber, M Osborn, J. Biol. Chem. 244, 4406 (1969).
15. R P F Gregory, G Borbély, S Demeter, A. Faldi-Dániel Biochem. J. 202, 25 (1982).
16. W C Krueger, L M Pschigoda Anal. Chem. 43, 675 (1971).
17. C I Mekras, Unpublished results, PhD Thesis, University of Salford, UK (1985).
18. R M Herriot, J. Gen. Physiol. 45, 57 (1962).
19. N Kuramoto, M Salamoto, J Komiyama, T Iijima. Makromal. Chem. 185, 1419 (1984).

Chimika Chronika, New Series, 20, 107-128 (1991)

CATALYTIC DECOMPOSITION OF FORMIC ACID ON HYDROTHERMALLY TREATED POROUS ANODIC ALUMINA FILMS

G. PATERMARAKIS

Department of Chemical Engineering, Laboratory of Physical Chemistry and Applied Electrochemistry, National Technical University of Athens, Greece

(Received March 20, 1990)

SUMMARY

The catalytic dehydration reaction of HCOOH over porous anodic alumina films on Al metal substrate, prepared in a 15% w/v H_2SO_4 bath at 30°C bath temperature and 3.5 A/dm² current density and which were treated hydrothermally in boiling water prior to catalysis, was studied at reaction temperatures 290-350°C. The kinetic parameters activation energy, frequency factor and catalytic activity at constant temperature of the HCOOH dehydration reaction, were found to be significantly higher in the case of hydrothermally treated than those of dry anodic aluminas. The catalytic promotion factor was found to decrease sharply with decreasing reaction temperature as well as with anodization time at constant reaction temperature until the time at which the maximum in activity is observed and beyond which the promotion factor remains constant. It is believed that the microcrystalline nature of anodic Al_2O_3 is responsible for this particular catalytic behaviour. Hydrothermal treatment of dry anodic aluminas results in the addition of OH groups and H_2O molecules on the surface of microcrystallites followed by the separation of the latter. During heating in catalysis experiments and although some shrinking of the hydrated and therefore swelled layer takes place on the pore wall surface, on removal of the greater portion of H_2O uptaken, 74%, a significantly larger and catalytically more active surface, i.e. that of separated microcrystallites, is exposed. The variation of microcrystallite size and p-semiconductivity across pore wall oxide emerged as the determining factors for the kinetic parameter changes with anodization time for hydrated as well as for dry oxide films. Although a significant amount of protons remains during catalysis experiments, corresponding to H_2O which amounts to 3.8% of the mass of the dry oxide, they do not behave as active centers for HCOOH dehydration. Instead, Lewis acid sites appear as the active centers for HCOOH dehydration on both hydrated and dry anodic alumina catalysts.

Key words: Catalysis, hydrothermally treated anodic alumina, formic acid decomposition.

INTRODUCTION

The catalytic decomposition of HCOOH on porous anodic aluminas prepared by the anodic oxidation of Al metal in a 15% H_2SO_4 bath was previously investigated[1-4] in a laboratory microreactor while this reference reaction was also used for examining the applicability of anodic aluminas in a semiindustrial catalytic reactor[5]. The HCOOH decomposition test reaction was employed for the reason that its dehydration/dehydrogenation relation is widely used as a model in catalyst selectivity[6]. The decomposition of HCOOH over anodic porous aluminas was found to be, up to 350°C reaction temperature, an exclusively dehydration reaction[1,2]. They showed a much higher activity as compared to that of bulk γ-Al_2O_3 chemically prepared[1] despite the fact that the catalytic real surface of porous anodic aluminas is much smaller, about 10-20 m^2/g,[3] than that of chemically prepared γ-Al_2O_3 which usually has a specific real surface around or above 100m^2/g. The Al metal underlying the Al_2O_3 film does not influence the HCOOH decomposition[2]. The reaction order was found to be zero for HCOOH partial pressure above a certain value for each reaction temperature employed which increases with reaction temperature, being i.e. 0.38 and 0.55 at 320 and 350°C respectively. The conditions of anodic Al_2O_3 film preparation such as anodization time, current density and bath temperature significantly affect the catalytic activity of alumina[2-4]. Two factors were suggested to be of importance for this effect: microcrysallite size and oxygen surplus (p-semiconductivity) which change across the pore wall oxide and are considerably affected by anodic oxidation conditions. The catalytic effect of chemically prepared γ-Al_2O_3 in the HCOOH decomposition reaction was also studied earlier[7-9] at reaction temperatures $\leq$190°C and an almost exclusively dehydration reaction was also reported.

Porous anodic alumina has been reported as being unhydrous[4] and of microcrystalline nature[2,10,11]. Microcrystallite size determined by NMR spectroscopy studies was found to be around 25 Å[11]. An amount of electrolyte anions is

always incorporated into the film depending on electrolyte choise, this amount being higher in the case of H_2SO_4. This amount is located at the deep end of pores and can be easily removed on film neutralization; it is also present on the crystallite surfaces or intercrystallite spaces. The hydrothermal treatment of porous anodic aluminas in boiling water is essentially a process by means of which the crystallite surfaces adsorb water converting it to surface OH groups which in return adsorb molecular water (physical adsorption) or molecular water is trapped in the intercrystallite voids[10,11]. The hydroxylation of crystallite surfaces replaces the surface electrolyte anions[12] and anions present in the intercrystallite spaces are certainly removed. As H_2SO_4 is a good dehydrative agent for HCOOH and as the surface protons supplied by the HCOOH dissociative adsorption on chemically prepared γ-Al_2O_3 were suggested to be the main active centers for HCOOH dehydration at reaction temperatures $\leq 190^{\circ}C$[7-9], then, the hydroxylation of crystallite surfaces of anodic aluminas, on hydration, could reveal the influence of both SO_4^{2-} anions and OH groups on the catalytic properties of anodic aluminas. This together with the effort to optimise the catalytic activity of anodic aluminas, besides that achieved by varying the conditions of their preparation, is the scope of the present work. Hydrothermally treated anodic aluminas, prepared in a 15% H_2SO_4 bath, were used without pretreatment in the HCOOH decomposition reaction. Although the largest portion of the adsorbed OH or H_2O is expected to be removed on heating at the catalytic reaction temperatures (290-350°C) employed, a significant amount of OH groups is expected to remain, sufficient to produce the OH effect on the HCOOH catalytic dehydration.

EXPERIMENTAL

The materials and procedure for the preparation of the Al strips carrying the anodic Al_2O_3 film catalyst were outlined in detail earlier[2-4]. Anodic Al_2O_3 films of varying film thickness using different anodization times

were prepared at 30°C bath temperature and 3.5 A/dm^2 current density. The neutralization of anodized Al specimens with NaOH 0.1 N as previously described[2] was performed carefully in order to remove H_2SO_4 accumulated at the depth of pores and the maximum possible amount of SO_4^{2-} anions adsorbed on the pore wall surface. Anodized specimens were then hydrothermally treated in boiling water, 100°C, for time intervals varying from 0.5 up to 20 min. The experimental set up and procedure for both HCOOH catalytic decomposition in the Schwab laboratory microreactor and reaction rate measurments at reaction temperatures 290-350°C which were also employed in the present study were outlined in detail earlier[2,4]. The hydrated Al_2O_3 films were used for the catalysis experiments exactly as they were without any further treatment. The weight gain during hydrothermal treatment and loss after catalysis experiments and the concomitant neutralization of spent catalysts with NaOH 0.1 N for removing adsorbed HCOOH were measured gravimetrically. The thickness and mass of dry oxide films prepared at different anodization times for calculating the %age of H_2O gained during hydrothermal treatment, the weight changes after catalysis experiments and catalyst neutralization and the relevant reduced kinetic parameters (per gram of dry oxide) in the HCOOH dehydration reaction were taken from previously published data[2].

RESULTS

During hydrothermal treatment of porous anodic alumina films water is gained either in the form of OH groups adsorbed on the surface of microcrystallites constituting the compact pore wall Al_2O_3 or it is physically adsorbed on the hydroxylated surfaces[10,11] or in the form of free water molecules in the vacuum space inside pores. The %age of water gained and calculated on the basis of the mass of the dry initially produced Al_2O_3 films increases with hydrothermal treatment time (h.t.t.) in boiling water as shown in Fig. 1 concerning a film prepared at 27 min anodization

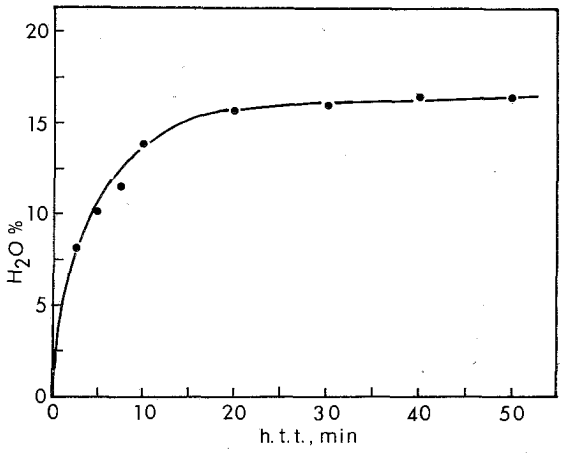

FIG. 1. *Dependence of %age of water uptaken by an anodic Al_2O_3 film, prepared at anodization conditions: bath temperature 30°C, current density 3.5 A/dm² and anodization time 27 min (27 μm thickness), on the time of hydrothermal treatment.*

time. The water uptake was essentially completed within 20 min of hydrothermal treatment. Fig. 2 depicts a section of a row of cells parallel to the pore axis. The porous anodic alumina is essentially a close packed array of approximately hexagonal columnar cells[1-3]. The barrier layer, porous layer, pore wall material and conical pore shape[4] are clearly indicated in Fig. 2. After introducing the Al_2O_3 film in boiling water the pores begin being filled by it and a "reaction" with pore wall Al_2O_3 sets on. This process is fast at the very early stages. Hydration of pore wall crystallite surfaces causes their separation and the water adsorbed on them in the form of OH groups or physically adsorbed molecular H_2O causes also the swelling of the hydrated layer of pore wall Al_2O_3 and a narrowing of pores. The diffusion of H_2O in the direction along the pore axis as well as to the innermost layers of pore wall Al_2O_3 is retarded with h.t.t. probably because of the narrowing of pores. the delayed diffusion of water through the dense, swelled hydrated layer and the change in intercrystallite

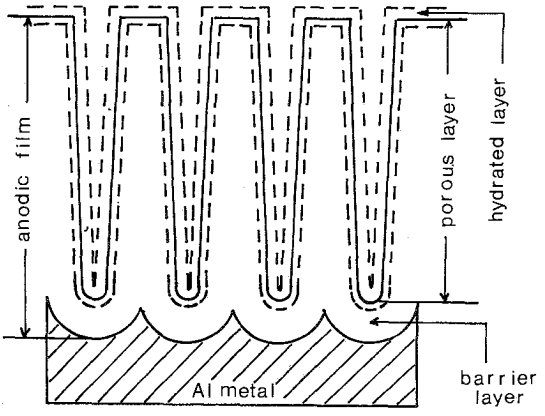

FIG. 2. *Idealized section of a row of cells, parallel to the pore axis, where the barrier layer, porous layer, conical pore shape, pore wall surface prior to hydration (——) and the swelled, hydrated layer of pore wall Al_2O_3 during hydrothermal treatment (---) are distinguished.*

spaces across pore wall Al_2O_3 owing possibly to the increase of crystallite size along the same direction. The depletion of dry material at some points, i.e. pore wall material at the mouths of pores which has thinned down, could also be a cause for the retardation of H_2O uptake. Hydration stops when the swelled layer of Al_2O_3 fills the initial pore void volume to the greatest possible extent, at a pore depth from its base at which the depletion of pore wall dry Al_2O_3 is complete and the increase in the volume occupied by the hydrated layer due to its swelling becomes identical to pore initial void volume at this point.

Hydrated Al_2O_3 during heating for the catalysis experiments are quickly and extensively dehydrated and OH groups and physically adsorbed H_2O on crystallite surfaces as well as free H_2O are easily removed. Although some shrinking of the hydrated, swelled layer must occur, the microcrystallites must remain separated to some extent around the pore wall surface and a significantly higher surface than the

initial pore wall surface is exposed to the gaseous HCOOH molecules. Hence, the catalytic activity of hydrated Al_2O_3 films must increase in comparison to that of non-hydrated ones.

The HCOOH decomposition on hydrated anodic alumina films was found to be an exclusively dehydration reaction of zero order under the experimental conditions employed. Hence the reaction rate (r in mol/s) is identical to the reaction rate constant (k). HCOOH catalytic dehydration reaction experiments were carried out on hydrated anodic alumina films prepared at 27 min anodization time (t). The films had a thickness of 27 μm and the total mass (m) of the dry oxide present on the 20 strips of the Al_2O_3/Al catalyst used was 119 mg. The duration of hydrothermal treatment varied from 0.5 up to 20 min. The Arrhenius kinetic parameters activation energy (E in kJ/mol), frequency factor (A in mol/s) and reduced frequency factor per gram of dry oxide (A/m in mol/s·g) which were calculated from the reaction rate measurements at various reaction temperatures, varied with hydrothermal treatment time as shown in Fig. 3(a). The corresponding changes in both total activity exhibited by the film present on the 20.2 cm^2 of anodized geometric surface of the 20 strips of Al_2O_3/Al catalysts used[22,4] and specific activity at constant reaction temperature 350°C (k(350°C) and k(350°C)/m respectively) are shown in Fig. 3(b). All the above parameters increase considerably with h.t.t. in the same fashion. By comparing Figs 1 and 3 it is observed that these parameters increase together with the %age amount of water uptaken or the average thickness of hydrated layer of compact pore wall Al_2O_3. The fact that the kinetic parameters remained essentially constant after 3 min of h.t.t., eventhough the water uptake increased appreciably further, probably denotes that the hydrated layer does not participate in the HCOOH dehydration "en masse". Since a shrinking of the hydrated layer takes place during heating, then, the catalytically effective surface of microcrystallites, accessible to HCOOH molecules, must be that of crystallites

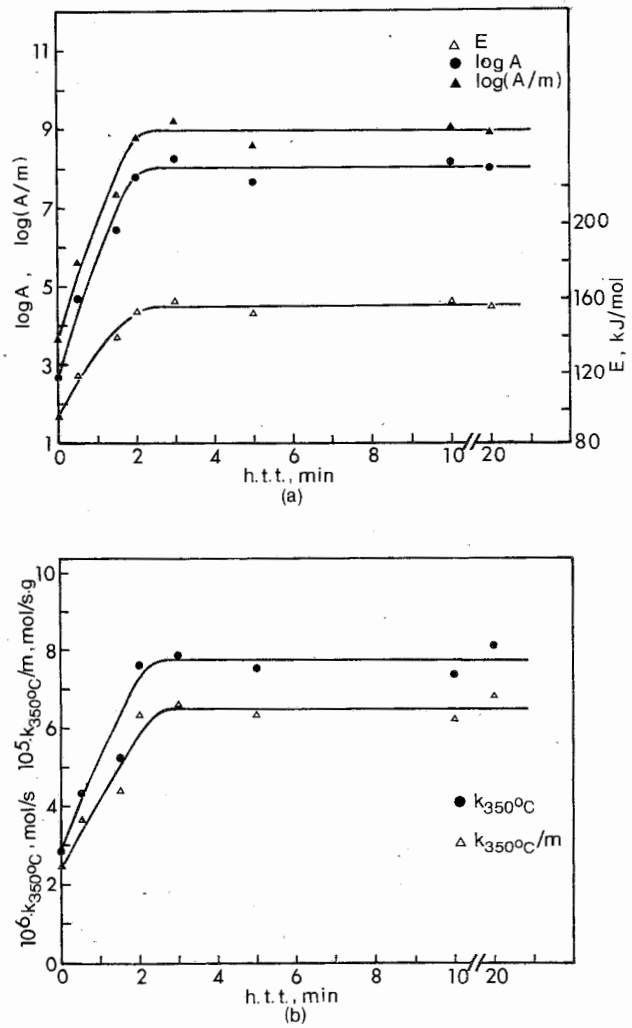

FIG. 3. *Effect of hydrothermal treatment time on the kinetic parameters of the HCOOH catalytic dehydration reaction: activation energy (E), frequency factor (A), frequency factor reduced per gram of dry oxide (A/m), (a), and total and specific activity at reaction temperature 350°C (k(350°C) and k(350°C)/m), (b).*

belonging to the outermost sublayer of the initially hydrated layer. Another reason for this phenomenon could be

the quick depletion of Al_2O_3 material around pore mouths during hydrothermal treatment. It was previously reported[4] that the extent of catalytic effectiveness of the pore wall surface is mainly determined by the part of the surface which neighbours pore mouths, this becoming more intense as the thickness of film increases, due to the increase in pore diameter and catalytic surface along the pore axis from pore base to pore mouths as well as to the strong increase of kinetic parameters and activity of Al_2O_3 along the pore wall/cell boundaries direction. The latter suggestion also partially explains the significantly increased catalytic parameter values of hydrated films in comparison to those of dry Al_2O_3 films. The hydration of microcrystallite surfaces and their subsequent separation makes Al_2O_3 crystallites situated at the innermost layers of pore wall Al_2O_3, which display higher values in kinetic parameters[4], accessible to HCOOH molecules. The separation of crystallites gives rise to the catalytic surface and thus to the oxide activity whether total or specific. The greater number and intensity of unsaturated bonds present on the surface of collapsed crystallites gives rise to the number and intensity of active centers for HCOOH adsorption and subsequent reaction and explains the higher frequency factor and activation energy. Since the enthalpy of HCOOH dissociative adsorption increases, the activation energy will also increase[22]. Hydrothermal treatment could also release the surplus oxygen present on the microcrystallite surfaces followed by a diminution in p-semiconductivity. Since the oxygen atoms surplus is responsible for the depression in the activity, frequency factor and activation energy values[22,4], hydrothermal treatment reduces its influence. Hence the values of the above parameters rise despite the fact that by hydrothermal treatment crystallites of greater size are revealed. This tendency increases along the pore wall/cell boundaries direction and causes a certain depression in kinetic parameter values[4].

Anodic Al_2O_3 films of various thicknesses, prepared at different anodization times, were also hydrothermally

treated. Since prolonged treatment, longer than 3 min, does not exert any significant effect on the catalytic activity of Al_2O_3 the hydrothermal treatment intervals applied were 5 min for films prepared at anodization times ≤27 min, but for anodization times longer than 27 min the applied h.t.t. was 15 min since the increase in film thickness up to 48 $min^{\frac{1}{2}}$ probably demands a more extensive treatment time, falling into the time interval region at which constant catalytic parameters are observed. The kinetic parameters E, A and A/m obtained from catalysis experiments over these hydrated aluminas are given in Figs 4(a, b and c) where they are also being compared to those yielded by the dry Al_2O_3 films. Although dry Al_2O_3 films yield maxima with respect to all these parameters at anodization time interval being close to that at which the limiting maximum mass and thickness are first achieved $(48\ min)^{\frac{1}{2}}$, hydrated films yield also maxima clearly displaced nevertheless at lower anodization time value. Two regions are observed: one corresponding to anodization times <48 min inside which the effect of hydrothermal treatment on parameter values is remarkable and one corresponding to anodization times ≥48 min where the same effect is observed but of much lower intensity. Activation energy increases up to 75.5 kJ/mol are observed. The dependence of total and specific activity, the latter being based on dry oxide mass, at constant reaction temperatures 350 and 330°C, on anodization time is depicted in Figs 5(a and b) respectively where a comparison with dry Al_2O_3 catalysts is also made. In both cases a maximum in activity is observed at an identical anodization time, 48 min, for both dry and hydrated oxide catalysts. As it was earlier stated[4] the appearance of maxima in kinetic parameters cannot be attributed solely to a film thickness distribution on the Al specimen surface, which in any case is insignificant, or to the specific position on the specimen from which the 20 Al_2O_3/Al strips of catalyst were taken (around the middle of the specimen). Maxima must be attributed rather to changes in the nature of Al_2O_3 across the pore wall material for both hydrated and dry oxide as

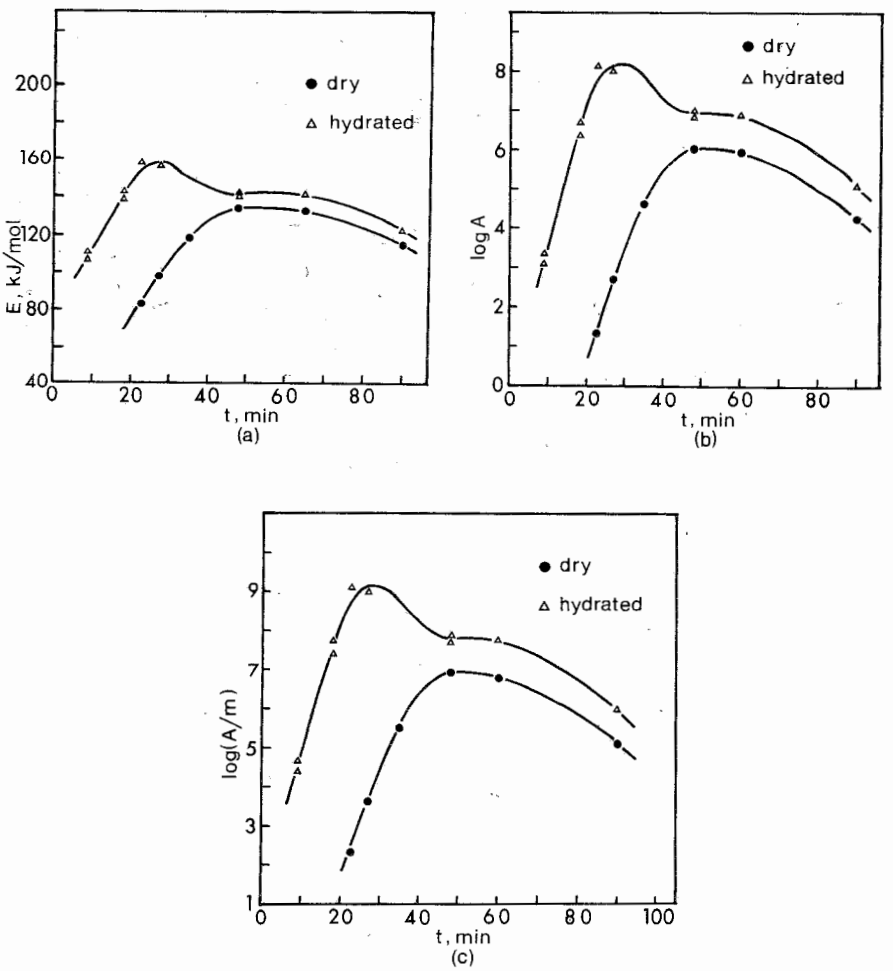

FIG. 4. *Plots of activation energy (a), frequency factor (b) and frequency factor reduced per gram of dry oxide (c) of HCOOH dehydration on both dry and hydrothermally treated Al_2O_3 films vs anodization time of Al_2O_3 preparation.*

it has been shown[2-4].

The promotion of oxide activity is much higher at short anodization times or film thicknesses. The ratio of the activity of hydrated Al_2O_3 to that of dry oxide, i.e. the

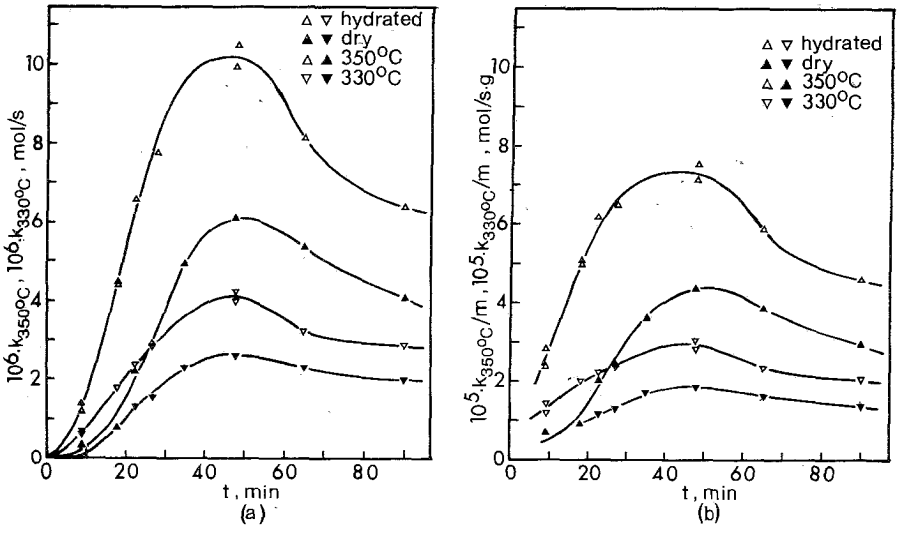

FIG. 5. *Plots of total (a) and specific (b) activities of both dry and hydrothermally treated porous anodic Al_2O_3 films at constant reaction temperatures, 350 and 330°C, in the HCOOH catalytic dehydration vs anodization time of Al_2O_3 preparation.*

promotion factor (p.f.), at reaction temperatures 350 and 330°C are depicted in Fig. 6. Initially, at 350°C reaction temperature the promotion is much higher than at 330°C, but after 48 min they become almost equal. The promotion factor falls abruptly with anodization time or film thickness up to 48 min while beyond 48 min the promotion factor remains constant for both reaction temperatures. At the lower Al_2O_3 film thickness used, 9 μm, the promotion factor in the HCOOH dehydration reaction at 350°C is four times that corresponding to films with maximum thickness, 33 μm, achieved at anodization times ≥48 min[22].

The more intense effect on kinetic parameters displayed by the low thickness Al_2O_3 film catalysts on hydrothermal treatment can also be explained on the basis of the theory formulated previously[22-24]. The decrease in p-semiconductivity with concomitant increase in microcrystallite size across the pore wall oxide in the pore wall to cell bound-

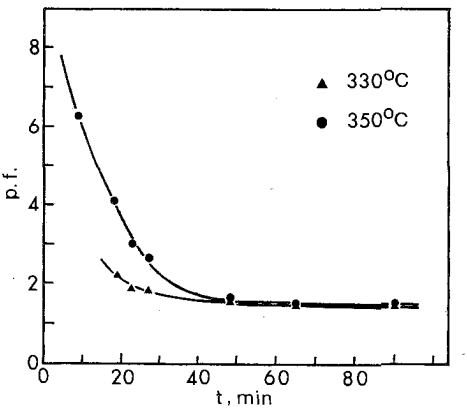

FIG. 6. *Plots of the ratio of the activity displayed by the hydrothermally treated Al_2O_3 films to that displayed by dry films (promotion factor, p.f.) at reaction temperatures of HCOOH dehydration 350 and 330°C vs anodization time of Al_2O_3 preparation.*

aries direction. Fig. 2, means that the pore wall conical surface of lower thickness films possesses on average a greater oxygen surplus and exhibits a smaller crystallite size. Therefore the expected extensive removal of oxygen surplus from crystallite surfaces during hydrothermal treatment and the separation of the smaller crystallites around the pore wall surface increase the number and intensity of catalytically active centers more appreciably at lower than at higher film thicknesses. Hence the effect on kinetic parameters upon hydration of pore wall surfaces becomes much more remarkable, it being also the case for the activation energy, frequency factor and oxide activity at a given reaction temperature. The displacement of the maxima of E, A and A/m to the left, Figs 5(a, b and c), is owed probably to the different way in which the heterogeneity of the pore wall surface is established in comparison to that of dry Al_2O_3 catalysts along the pore axis, due first of all to the variable thickness of the pore wall hydrated layer and hence to the variable thickness of its catalytically effective sublayer. Although this displace-

ment takes place in the case of the activation energy and frequency factor, the maximum in activity appears at about 48 min anodization time as in the case of the dry oxide. For the higher Al_2O_3 film thicknesses, in which the catalytic behaviour is determined primarily by the zone of pore mouths[4], the hydrated layer at pore mouths is much thinner and the influence of hydrothermal treatment is much lower. This is also consistent with the fact that pore wall Al_2O_3 in cell boundaries has the lowest oxygen surplus and the highest crystallite size; then, the effect of hydration on the catalytic parameters is not very significant. It also appears that the results of the present study essentially confirm the formulated theory in previous works[2,4], the basic aspect of which was the determination of catalytic behaviour of porous anodic Al_2O_3 films with respect to two factors namely oxygen surplus (p-semiconductivity) and microcrystalline film nature both of which vary across the pore wall material.

The presence of SO_4^{2-} anions around microcrystallite surfaces, removed on hydrothermal treatment, appears to have no significant effect on the oxide catalytic effectivity. An increase in the activity should be expected on SO_4^{2-} anions removal since they occupy Lewis acidic centers on the surface, although it might have some dehydrative effect on HCOOH. Concentrated H_2SO_4 is a known dehydrative agent for HCOOH but its dehydrative action could be attributed rather to protons attached to the SO_4^{2-} anions. The possible effect due to the presence of the SO_4^{2-} must then be small and overshadowed by the strong influence of hydrothermal treatment "per se" on the catalytic effectiveness of the oxide.

The water gained during hydrothermal treatment was on average 14.5% above the mass of the dry oxide initially produced and varied roughly between 10 and 15.5% correspondingly for the lower (9 μm) and higher (33 μm) oxide thickness of Al_2O_3 films used. The weight of oxide catalysts after catalysis experiments was on average 5% higher than that of dry oxide while after neutralization it was

about 3.8% higher than that of dry oxide, the difference of 1.2% corresponding to the HCOOH adsorbed and subsequently removed on neutralization. The 3.8% weight remaining above the weight of the dry oxide after catalysis corresponds roughly to 26% of the water uptaken during hydrothermal treatment. This approximate estimation of the amount of water remaining after catalysis experiments represents water which is strongly bound to crystallite surfaces, not removed on heating up to 350°C and existing mainly in the form of OH groups. Catalysis on dry oxide catalysts produced almost no change in their weight[4]. This reinforces the above mentioned reasoning that most of the H_2O uptaken either as OH groups or as H_2O molecules is removed on heating revealing active centers for subsequent HCOOH decomposition. The strongly bound water retained during catalysis, existing rather as OH groups and for the additional reason that H_2O is not appreciably adsorbed under the catalytic reaction conditions as shown by the zero order of reaction, was not consistent with the variation of catalytic activity. The portion of water remaining after catalysis in the case of hydrated oxides was smaller for low-thickness oxide catalysts whereas their catalytic promotion was much greater compared to that of high-thickness films. Hence the direct participation of OH groups as active centers in the mechanism of HCOOH catalytic dehydration must be rather excluded.

DISCUSSION

The catalytic decomposition of HCOOH on γ-Al_2O_3 chemically prepared was also examined by other workers[7-9] at reaction temperatures ≤190°C, by means of IR spectroscopy. It was stated that, when γ-Al_2O_3 is exposed to HCOOH vapour, formate ions and protons are formed as a result of the dissociative adsorption of HCOOH. During formic acid decomposition on γ-Al_2O_3 the chemisorbed species were formate ions, protons and water while no carbon monoxide nor formic acid molecules were adsorbed under the reaction conditions[9]. A nearly complete dehydration reaction of

HCOOH on γ-Al_2O_3 was noted[8]. Formate ions on the alumina surface do not decompose directly to reaction products while a fraction of them rapidly desorbs by exchange with formic acid[7]. The decomposition of HCOOH takes place in two stages[7]. First, carbon monoxide is evolved at a considerable rate probably at the Lewis acidic sites on the surface. The reaction rate is given by $r=kP_{HCOOH}(1-a[H_2O]_{ads})$, where P_{HCOOH}=ambient partial pressure of HCOOH, a=constant and $[H_2O]$=fraction of surface sites occupied by H_2O molecules. The reaction mechanism provided involves gaseous HCOOH molecules colliding with formate ions adsorbed on Lewis acidic sites producing carbon monoxide while the Lewis acidic sites are destroyed by the water produced. Secondly, during the stationary state of the reaction the decomposition takes place between HCOOH molecules and Brönsted acidic sites i.e. the surface protons which are supplied from the dissociative adsorption of HCOOH. The reaction rate is given by $r=k'P_{HCOOH}[H^+]/(1+b[H_2O]_{ads})$, where $[H^+]$=surface concentration of protons and b=constant. Hence, the formate ion present on the catalyst surface does not behave as the main intermediate. The surface formate ion is stable and in vacuum decomposes mainly to H_2O and CO only at temperatures considerably higher than those at which formic acid decomposition takes place. The decomposition rate of the formate species on the alumina catalyst in vacuum is about two orders of magnitude slower than the rate of decomposition of HCOOH vapour at the same reaction temperature and coverage[7]. Although the basic tenet extracted from these works was that HCOOH decomposition takes place mainly between HCOOH molecules in the ambient gas and protons supplied to the surface from the dissociative adsorption of HCOOH, the possibility of HCOOH decomposition via a formate ion under other reaction conditions was not excluded. Since the decomposition of HCOOH via a formate ion has seemingly a higher activation energy than the decomposition via the interaction of HCOOH with the surface protons, the decomposition may proceed through the formate ion at much higher temperatures[7].

In a previous work by the author[2] it was demonstrated that, under the experimental conditions employed, a mechanism of HCOOH dehydration on dry anodic alumina via the decomposition of formate ions on Lewis acidic sites must be adopted. The results of the present study strengthen this view for the following reasons: (i) The reaction temperatures at which the catalytic effectivity of anodic aluminas either dry or hydrated was examined were considerably high i.e. 290–350°C. (ii) The reaction order under experimental conditions was found to be zero for both dry and hydrated Al_2O_3 catalysts; this denotes that the catalytically effective surface of pore walls or that of separated crystallites is saturated by the dissociatively adsorbed HCOOH and that H_2O does not inhibit the reaction or that H_2O produced is quickly desorbed. (iii) It has been shown that the small quantity of water initially contained in the dry oxide diminishes during catalysis experiments in cases where the changes in weight become measurable i.e. for oxide films prepared at bath temperatures greater than 30°C[4]. This also denotes that not only water produced during HCOOH decomposition is not being adsorbed or incorporated into the oxide, but even the initially contained water is removed to a great extent during catalysis experiments. This is also consistent with the results of the present study, although a significant amount of water remains after catalysis over the hydrated oxide owing to the considerably higher catalytic surface of separated crystallites as compared to that of pore wall surface in the case of dry oxide and probably to some increased tendency for H_2O adsorption or enclosure at some sites on their surface or in the bulk. (iv) The activation energy is always sufficiently high depending on the conditions of anodic Al_2O_3 preparation as well as on its hydrothermal treatment and varies between 83.5 and 167.5 kJ/mol[2–4]. (v) The amount of water retained on hydrated oxides during catalysis experiments is not produced during HCOOH decomposition but exists prior to it as indicated by the zero order reaction. Since molecular water is easily

removed from the catalyst surface the remaining water gain exists rather in the form of OH groups on the Al_2O_3 surface. Its amount does not correspond quantitatively to the promotion of catalytic activity followed by the hydration of Al_2O_3 films prepared at different anodization times and having thus varying thickness and porosity. The OH groups remaining on the surface of crystallites are strongly bound on it since they persist to adhere even at 350°C. Hence protons are strongly bound to oxygen atoms and cannot in anyway behave as Brönsted acidic sites. Then, the dehydration of HCOOH is excluded from taking place on Brönsted acidic sites, i.e. OH groups present on the surface of anodic aluminas are not implicated in the HCOOH dehydration mechanism. The catalytic effect of hydrothermally treated anodic aluminas on HCOOH dehydration must be attributed to the Lewis acidic sites (Al^{3+}) present on the catalyst surface. Since HCOOH molecules are not present on Al_2O_3 surfaces during the HCOOH dehydration reaction[9] even for reaction temperatures significantly lower than those employed in the present work, the reaction must take place via the decomposition of formate ions adsorbed on Lewis acidic sites. This is valid for both hydroxylated and dry anodic aluminas.

The part played by OH groups could be an indirect promotion of catalytic effectivity. Their presence in crystallite surfaces probably helps crystallites to remain separated. The complete removal of OH groups on heating at temperatures much higher than 350°C could cause a packing of crystallites whereafter a diminution of oxide activity could probably be observed.

CONCLUSIONS

From the results of the present study the following conclusions can be drawn.

1.Hydrothermal treatment of porous anodic Al_2O_3 films significantly affects their catalytic efficiency during the HCOOH dehydration reaction. Water uptake during treatment

in boiling water increases with treatment time at a continuously decreasing rate. The kinetic parameters activation energy, frequency factor and activity at constant reaction temperature displayed by the hydrothermally treated anodic Al_2O_3 films during the HCOOH catalytic dehydration significantly increase with treatment time up to a particular time interval from which onwards they remain constant although the H_2O uptaken during hydrothermal treatment still increases. This is due to the fact that the hydrated layer on pore walls does not participate "en masse" in the promotion of catalytic activity.

2.During the HCOOH decomposition, hydrothermally treated anodic Al_2O_3 prepared at bath temperature 30°C, current density 3.5 A/dm^2 and various anodization time intervals yielded kinetic parameters which vary with anodization time in a similar way to that displayed by the dry anodic Al_2O_3. Activation energy and frequency factor displayed by the hydrated Al_2O_3 as well as by dry Al_2O_3, gave a maximum. In the case of hydrated Al_2O_3 the maximum was displaced at an anodization time value which is lower than that at which the limiting maximum values of film thickness, mass and porosity are first achieved (48 min) and at which the dry oxide exhibited maxima. Total and specific activity values also showed a maximum but at exactly the anodization time interval at which the dry oxide yielded a maximum in activity (48 min).

3.The ratio of the catalytic activity of hydrated Al_2O_3 to that of dry Al_2O_3 at constant reaction temperature, or promotion factor, decreases with anodization time up to 48 min beyond which the promotion factor remains constant. At reaction temperature 350°C the promotion factor was 6.5 and 1.5 for the lower (9 μm) and the higher (33 μm) thickness of Al_2O_3 films employed respectively. The promotion factor strongly increased with increasing reaction temperature for

films prepared at anodization times <48 min, but it was rather independent of reaction temperature for anodization times ≥48 min, being 1.5.

4.The cited catalytic behaviour is owed to the microcrystalline nature of porous anodic Al_2O_3 films. The hydrothermal treatment of the oxide adds to the crystallite surfaces OH groups and H_2O molecules while crystallites become separated. During heating in the catalytic process the largest amount of water uptaken ($\simeq$74%) is removed. Despite shrinking of the hydrated layer around pore walls, to some extent, crystallites remain predominantly separated, exhibiting a surface much greater and more active than the pore wall surface of dry oxides.

5.The OH groups remaining on crystallite surfaces are not implicated as Brönsted acidic sites in the HCOOH dehydration reaction mechanism. The Lewis acidic sites (Al^{3+}) are indeed implicated in the HCOOH dehydration mechanism via a formate ion intermediate decomposition in both dry and hydrothermally treated anodic aluminas.

ΠΕΡΙΛΗΨΗ

ΚΑΤΑΛΥΤΙΚΗ ΔΙΑΣΠΑΣΗ ΤΟΥ ΜΥΡΜΗΚΙΚΟΥ ΟΞΕΟΣ ΣΕ ΥΔΡΟΘΕΡΜΙΚΑ ΚΑΤΕΡΓΑΣΜΕΝΕΣ ΜΕΜΒΡΑΝΕΣ ΠΟΡΩΔΩΝ ΑΝΟΔΙΚΩΝ ΟΞΕΙΔΙΩΝ ΤΟΥ ΑΡΓΙΛΙΟΥ.

Στην εργασία αυτή μελετήθηκε η καταλυτική διάσπαση του μυρμηκικού οξέος πάνω σε μεμβράνες πορώδους Al_2O_3 ηλεκτρολυτικά παρασκευασμένου, που προηγουμένως είχαν κατεργασθεί υδροθερμικά σε νερό 100°C. Οι μεμβράνες Al_2O_3 παρασκευάστηκαν με ανοδική οξείδωση του Al σε λουτρό H_2SO_4 15%, πυκνότητα ρεύματος 3.5 A/dm^2 και σε διάφορους χρόνους ανοδικής οξείδωσης. Η διάσπαση του HCOOH που μελετήθηκε στην θερμοκρασιακή περιοχή 290–350°C βρέθηκε να είναι αντίδραση αφυδάτωσης, μηδενικής τάξης στις πειραματικές συνθήκες που χρησιμοποιήθηκαν. Οι κινητικές παράμετροι της αντίδρασης, ενέργεια ενεργοποίησης, παράγοντας συχνότητας και σταθερά της ταχύτητας διάσπασης ή δραστικότητα του καταλύτη σε σταθερή θερμοκρασία αντίδρασης βρέθηκε ότι είναι σημαντικά μεγαλύτερες από αυτές που βρέθηκαν σε μη ενυδατωμένο, ξηρό ανοδικό Al_2O_3. Αυτές γενικά αυξάνονται με την ποσότητα του προσλαμβανόμενου νερού κατά την κατεργασία του Al_2O_3 μέχρι κάποια τιμή της, μετά από την οποία παραμένουν σταθερές, ανεξάρτητες από την παραπέρα αύξηση

της ποσότητας του προσλαμβανόμενου νερού. Αυτό δείχνει ότι το ενυδατωμένο στρώμα Al_2O_3 γύρω από την επιφάνεια των πόρων του οξειδίου δεν είναι καταλυτικά ενεργό σ' όλη του την έκταση. Υδροθερμικά κατεργασμένες μεμβράνες πορώδους Al_2O_3 που παρασκευάστηκαν σε διάφορους χρόνους ανοδικής οξείδωσης, έδοσαν ποιοτικά την ίδια μεταβολή των κινητικών παραμέτρων της καταλυτικής αφυδάτωσης του HCOOH με αυτή των μη κατεργασμένων. Όλες οι παράμετροι εμφάνισαν μέγιστο στις τιμές τους σε χρόνο ανοδικής οξείδωσης ίδιο με αυτόν (ολική δραστικότητα που δίνεται από μεμβράνες Al_2O_3 σταθερής γεωμετρικής επιφάνειας και ειδική δραστικότητα) ή μικρότερο από αυτόν (ενέργεια ενεργοποίησης και παράγοντας συχνότητας) στον οποίο οι μέγιστες οριακές τιμές του πάχους, της μάζας και του πορώδους της μεμβράνης αρχικά επιτυγχάνονται και στον οποίο το μη ενυδατωμένο Al_2O_3 εμφανίζει μέγιστο σ' όλες τις κινητικές παραμέτρους. Ο βαθμός ενίσχυσης της καταλυτικής δραστικότητας του Al_2O_3 με την υδροθερμική κατεργασία βρέθηκε ότι μειώνεται δραστικά με τη θερμοκρασία διάσπασης του HCOOH καθώς επίσης και με το χρόνο ανοδικής οξείδωσης για σταθερή θερμοκρασία αντίδρασης μέχρι το χρόνο εμφάνισης της μέγιστης τιμής στη δραστικότητα πέρα από τον οποίο παραμένει σταθερός και ανεξάρτητος της θερμοκρασίας της αντίδρασης. Η μικροκρυσταλλική φύση του πορώδους ανοδικού Al_2O_3 είναι υπεύθυνη γι' αυτήν την καταλυτική του συμπεριφορά. Η υδροθερμική κατεργασία προσθέτει στην επιφάνεια των κρυστάλλων υδροξύλια και μοριακό νερό που συντελούν στο διαχωρισμό τους. Κατά τη θέρμανση των οξειδίων στη διάρκεια της καταλυτικής διάσπασης του HCOOH η απομάκρυνση του μεγαλύτερου ποσοστού του αρχικά προσλαμβανόμενου $H_2O \simeq 74\%$ αποκαλύπτει μια σημαντικά μεγαλύτερη και πιο δραστική καταλυτική επιφάνεια, αυτή των διαχωρισμένων μικροκρυστάλλων, παρ' όλο που κάποια συρρίκνωση του ενυδατωμένου και διογκωμένου στρώματος Al_2O_3 στην επιφάνεια των πόρων του οξειδίου συνοδεύει αυτή την απομάκρυνση H_2O. Το μέγεθος των μικροκρυστάλλων και η περίσσεια ατομικού οξυγόνου (p-ημιαγωγιμότητα) που μεταβάλλονται κατά μήκος της τομής του αρχικά συμπαγούς Al_2O_3 που αποτελεί τα τοιχώματα των πόρων, αναδεικνύονται σαν οι κύριοι παράγοντες για την μεταβολή των κινητικών παραμέτρων της καταλυτικής διάσπασης του HCOOH με τον χρόνο ανοδικής οξείδωσης, όπως και στην περίπτωση των μη ενυδατωμένων ανοδικών οξειδίων. Παρ' όλο που μια σημαντική ποσότητα πρωτονίων που αντιστοιχεί σε $H_2O \simeq 3.8\%$ της μάζας του μη ενυδατωμένου Al_2O_3 παραμένει κατά τη διάρκεια της κατάλυσης δεν φαίνεται ότι αυτά συμπεριφέρονται σαν ενεργά κέντρα για την διάσπαση του HCOOH. Τα όξινα κατά Lewis κέντρα της επιφάνειας εμφανίζονται σαν τα ενεργά κέντρα πάνω στα οποία γίνεται η αφυδάτωση του HCOOH στο ενυδατωμένο όπως επίσης και στο μη ενυδατωμένο Al_2O_3. Η καταλυτική αφυδάτωση τοι HCOOH γίνεται δια μέσου της διάσπασης του μυρμηκικού ανιόντος πάνω σ'αυτά τα ενεργά κέντρα.

REFERENCES

1. Skoulikidis, Th. and Sarropoulos, C. :*Proc. ICSOBA, 4th, Athens*, Vol. 3, pp. 356-374 (1978).
2. Patermarakis, G. :*Chimika Chronika (N.S)*, **16**, 141 (1987).
3. Patermarakis, G. :*Ibid*, **18**, 115 (1989).
4. Patermarakis, G. :*Ibid*, in press.
5. Skoulikidis, Th. and Patermarakis, G. : *Aluminium*, **65**, 185 (1989).
6. Trillo, J., Munera, G. and Criado, J. :*Catalysis Rev.*, **7**, 51
7. Noto, Y., Fukuda, K., Onishi, T. and Tamaru, K. :*Trans. Faraday Soc.*, **63**, 2300 (1967).
8. Fukuda, K., Noto, Y., Onishi, T. and Tamaru, K. :*Trans. Faraday Soc.*, **63**, 3072 (1967).
9. Tamaru, K. :*Dynamic Heterogeneous Catalysis*, pp. 115-121, Academic Press, London (1978).
10. O Sullivan, J., Hockey, J. and Wood, G. :*Trans. Faraday Soc.*, **65**, 535 (1969).
11. Baker, B. and Pearson, R. :*J. Electrochem. Soc.*, **119**, 160 (1972).
12. Murphy, J. :*Proceedings Anodizing Symposium;* p. 3, Birmingham (1967).
13. Diggle, J., Downie, T. and Goulding, C. :*Chem. Rev.*, **69**, 365 (1969).

Chimika Chronika, New Series, 20, 129-138 (1991)

THE INFLUENCE OF OIL PHASE ON THE STABILITY OF DILUTE O/W EMULSIONS. THE ROLE OF ζ-POTENTIAL.

ANTONIS AVRANAS [1] and GEORGE STALIDIS [2]

Laboratories of [1]Physical Chemistry and [2] General and Inorganic Chemical Technology, Aristotle University of Thessaloniki, 54006, Thessaloniki, Greece.

(Received November 29, 1989)

ABSTRACT

The stability of dilute oil-in-water emulsions prepared using a range of oils is studied. Three surfactants are used as emulsifying agents, sodium dodecyl sulfate (SDS), cetyldimethylbenzylammonium chloride (CDBACl) and cetyltrimethylammonium bromide (CTAB). The time needed for the appearance of traces of oil phase onto the surface of the emulsion, indicating the breaking of emulsion, is measured. The ζ-potential of the droplets is calculated from microelectrophoretic measurements. The great differences observed in the stability of the emulsions cannot be attributed to the small differences in ζ-potential nor can entirely be explained by the molecular diffusion theory.

key words: Surfactants, emulsions, demulsification, zeta potential.

INTRODUCTION

An emulsion is an unstable heterogeneous system of a liquid in another in the form of droplets. The types of instability are creaming, flocculation and coalescence which may lead to phase separation[1]. Instability in emulsions is normally detected by changes in droplet size or phase separation. According to the conventional theories[2,3], the addition of a surfactant which is adsorbed from the continous phase upon the internal interface ensures the stability of the emulsions. The repulsive double-layer forces together with hydration forces are considered to be responsible for the stability when the surfactant is ionic, and steric repulsion as well as hydration forces are involved in

stability when the surfactant is nonionic. The ionic surfactants impart a surface charge to the dispersed droplets. This charge enhances emulsion stability by hindering the approach of emulsion droplets because of electrostatic repulsive forces between them. ζ- potential is used to characterize the surface charge of emulsion droplets.

In some cases emulsions of long-term stability are needed whereas in other cases emulsions of limited stability are required. There are also cases where unwanted stable emulsions have to be broken down, ie the O/W emulsions that arise in effluent waters. It is thus obvious that the predicting of emulsion stability is of practical importance. However no rules are available today for predicting the stability of an emulsion and the trial and error method is considered necessary. Many factors are known to affect emulsion stability. Among them, the nature of the oil phase has received little attention and some authors have considered it to be of no consequence [4-7].

In this parer the stability of dilute oil-in-water emulsions was studied. Experiments were carried out by using nine oils having different polarity and solubility in water. Three ionic surfactants have been chosen among the surfactants available to serve as emulsifying agents which are among the more commonly used. An anionic one, sodium dodecylsulfate (SDS) and two cationics, cetyldimethylbenzylammonium chloride (CDBACl) and cetyltrimethylammonium bromide (CTAB). The ζ-potential of the emulsion droplets was calculated from microelectrophoretic mobility data in order to correlate this value with the stability of emulsions. The molecular diffusion theory[8] and some other parameters were further examined to explain the stability data.

EXPERIMENTAL

The anionic surfactant was of Merck puriss quality (≥ 99%) and used as received. The two cationic surfactants were of Fluka purum quality (> 98%) and were

recrystalized from acetone. Purity was checked by measurements of the surface tension of their aqueous solutions around the critical micellar concentration (CMC)[9]. The CMC from a surface tension-log concentration curve was 8.1 ± 0.2 X 10^{-3}M for SDS, 5.0 ± 0.2 X 10^{-4} M for CDBACl and 9.4 ± 0.3 X 10^{-3}M for CTAB.

The oil phases used were cyclohexane, methylcyclohexane, heptane, isooctane, octanol-1, toluene, ethylbenzene and benzylacetate. They were of Fluka purum quality and were further purified[10]. Their solubility in water and the interfacial free energy between them and water in the absence of surfactant are given in Table I [11,12]. Water was taken

TABLE I: Some properties of pure oil phases at 25°C [11,12].

O i l	Interfacial free energy γ_{ow},[mN m^{-1}] at 25°C	Solubility in water [% w]
Cyclohexane	50.2	5.5 X 10^{-3}
Methylcyclohexane	50.8	11.6 X 10^{-3}
Heptane	50.2	2.9 X 10^{-4}
Octane	50.8	6.6 X 10^{-5}
Isooctane	49.0	2.4 X 10^{-4}
Octanol-1	8.5	5.4 X 10^{-2}
Toluene	36.1	5.2 X 10^{-2}
Ethylbenzene	38.4	1.5 X 10^{-2}
Benzylacetate	20.5	sl.sol.

from a Millipore apparatus; its resistivity was about 100 MΩ cm^{-1} and its surface tension was measured as 72 mN m^{-1} at 25°C. The water remained in equilibrium with the oil phase at least 24 hours before use. NaCl was of Merck analar quality.

The emulsions were prepared by ultrasonic dispersion by suspending 0.5% by volume of oil phase in a 0.01 M NaCl aqueous solution containing the surfactant. The emulsions were stored at 25 ± 0.1°C.

The electrophoretic mobility of oil droplets was measured in a modified demountable microelectrophoretic apparatus as it has already been described[13,14]. The recommended

procedure with regard to the location of the stationary levels, timing of droplets, reversing of the current after each reading, etc. was followed[15]. The results were accurate within 2%.

The time needed for the appearance of traces of oil phase onto the surface of the emulsions, ie breaking of the emulsions was used for the estimation of emulsion stability.

RESULTS AND DISCUSSION

The electrophoretic mobility measurements closely reflect changes in the degree of adsorption. The electrophoretic mobility is directly related to the nature of the mobile part of the electric double layer and may only be interpreted in terms of ζ-potential or the charge density at the surface of shear. For a curved surface such as the droplet surface the shape of the double layer is described in terms of the dimensionless quantity κa, which is the ratio of the radious α of the droplet to double layer thickness, where κ is the Debye-Hückel parameter. $1/\kappa$ has the dimension of length and is a good measure of the extension of the double layer. When $\kappa\alpha$ is large, the double layer is effectively large and may be treated as such. In the present case where $\kappa = 3.28 \times 10^6$ cm^{-1} (for 0.01 M NaCl) and $\alpha \sim 1.5 \times 10^{-4}$ cm the value for $\kappa\alpha$ is 500 ($\gg$ 1). ζ-potential is therefore calculated by using the Helmholtz-Smoluchowski formula

$$\zeta = \frac{u_E \eta}{\varepsilon}$$

where u_E is the electrophoretic mobility, ε the permitivity of the dielectric and η the viscosity of water.

Emulsions prepared without emulsifier are unstable having large droplets of different size with a very low negative ζ-potential (which is due to the preferential adsorption of chloride ions). The ionic surfactants change ζ-potential and increase the stability of the emulsions giving droplets of almost equal size. No changes in ζ-potential are evident upon short-ageing.

The ζ-potential values of cyclohexane and heptane emulsions prepared with SDS or CDBACl are given in Figure 1.

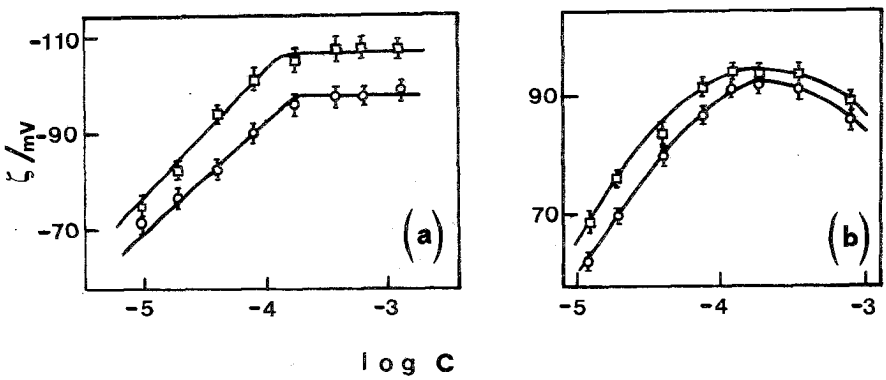

FIG. 1. *Effect of surfactant concentration on ζ-potential of a dilute oil-in-water emulsion: (a) sodium dodecylsulfate, (b) cetyldimethylbenzylammonium chloride. The oil phases are -□- heptane and -○- cyclohexane.*

The addition of SDS increases the absolute value of ζ-potential (which is negative) and reaches a maximum at higher concentrations. This maximum value is thought to represent the point of completion of a closely packed monolayer of molecules on the droplet surface[16]. The plateau value is reached below the CMC (log CMC = -2.09). On increasing the concentration of CDBACl the positive ζ-potential increases and reaches a maximum value before the CMC of CDBACl. At higher concentrations, above CMC, a slight reduction observed in ζ-potential can be explained as a thinning of the double layer, due to ionic strength effects, without a compensating increase in the number of adsorbed ions[3,14]. Similar curves are found for CTAB.

All the emulsions are prepared using 1.5 X 10^{-4} M surfactant concentration where ζ-potential has its maximum value and the oil-water interface is saturated. This concentration is below the CMC value of the surfactants.

The ζ-potential values at 25 ± 0.1 °C are given in Table II. For a given oil phase, ζ-potential has almost the same

TABLE II: ζ-potential values of various oil phases dispersed in 1.5 X 10^{-4}M surfactant solution. Measurements were made at 25 ± 0.1 °C 80 minutes after emulsification.

Oil	SDS	CDBACl	CTAB
Cyclohexane	-95.1	91.2	91.2
Methylcyclohexane	-96.4	92.5	93.8
Heptane	-106.6	93.8	95.1
Octane	-109.2	95.1	95.1
Isooctane	-110.5	93.8	93.8
Octanol-1	-87.4	——	84.8
Toluene	-91.2	89.9	89.9
Ethylbenzene	-91.2	87.4	87.4
Benzylacetate	-107.9	101.5	105.4

value when CDBACl or CTAB are used as emulsifiers while it has a lower value (absolute) when SDS is used as emulsifier. Octanol-1 emulsions prepared with CDBACl are very unstable making measurements of ζ-potential impossible.

It is clear from Table II that ζ-potential show some dependance on the nature of the oil phase, since it determines the compactness of the interfacial film and the distribution of the surface active agent. The same electrokinetic behavior is observed among homologous oil phases like cyclohexane and methylcyclohexane, toluene and ethylbenzene, octane and heptane. The saturated hydrocarbon droplets (methylcyclohexane, cyclohexane) possess greater charge compared to the unsaturated hydrocarbon droplets (ethylbenzene, toluene). Similar results have been reported for emulsions prepared with lauric salts[17]. It must be mentioned that the increase of oil polarity can either decrease ζ-potential (octane, octanol-1) or increase it (ethylbenzene, benzylacetate). The mean volume diameter, estimated from the known phase volume and the number of oil droplets per unit volume, strongly depends upon the nature of the oil phase and the surfactant, ranging from 1 X 10^{-4}cm to 2.2 X 10^{-4}cm (depending on the observation time).

However no relation seems to exist between diameter and ζ-potential.

The time required for the appearance of visible oil phase on the surface of the emulsion is given in Table III.

TABLE III: Time required for the appearance of visible oil phase on the surface of the emulsions. The emulsions were stored at 25 ± 0.1 °C.

Oil	SDS	CDBACl	CTAB
Cyclohexane	4 h	6 h	6 h
Methylcyclohexane	4 h	7 h	7 h
Heptane	24 h	23 h	23 h
Octane	25 h	30 h	30 h
Isooctane	8 h	20 h	20 h
Octanol-1	3 days	10 min	3 h
Toluene	≤ 30 min	7 h	12 h
Ethylbenzene	≤ 30 min	8 h	14 h
Benzylacetate	1 h	1 h	90 min

The emulsion stability is found to be highly dependent on the nature of the oil phase. The stability of SDS emulsions decreases in the order toluene ~ ethylbenzene < benzylacetate < cyclohexane ~ methylcyclohexane < isooctane < heptane ≤ octane < octanol-1. The octanol-1 emulsion prepared with SDS is the most stable studied emulsion, while it is the less stable when it is prepared with CDBACl. The stability of CDBACl and CTAB emulsions is almost the same with the exception of octanol-1. The stability decreases in the order benzylacetate < cyclohexane ≤ methylcyclohexane < toluene ≤ ethylbenzene < isooctane < heptane < octane.

According to the Derjaguin - Landau - Verwey - Overbeek (DLVO) theory of colloid stability there are attractive van der Waall's forces between particles and repulsive forces due to electrostatic repulsion. The attractive potential falls off as the inverse square of the distance apart of the particles while the repulsive term is more complex and of longer term. This theory allows the Gouy-Chapman theory of

the equilibrium double layer to be extended to situations involving double layer overlaps, where surface potential can be replaced by ζ-potential. However not good correlation exists in all the cases studied between stability and ζ-potential. For example heptane and octane emulsions having droplets that carry the highest ζ-potential (with the exception of benzylacetate droplets) are the most stable. However the isooctane emulsion with SDS as emulsifier presents a remarkably less stability despite the high value of ζ-potential. The saturated cyclic hydrocarbons (cyclohexane and methylcyclohexane) that have a lower value of ζ-potential have a decreased stability. The presence of benzene ring (toluene and ethylbenzene) decreases further the ζ-potential as well as the stability. However the high ζ-potential value measured of the polar benzylacetate droplets cannot explain the poor stability. The cause of discrepancies between ζ-potential and stability may be that in an expanded interfacial film the surfactant molecules may be dispelled from the region of closest approach by desorption into the aqueous phase or displacement around the droplet surface[7,18].

Various observations and theories of emulsion stability are further examined. It has been found that the stability of emulsion can be related to the interfacial free energy γ_{ow}, between the oil and water in the absence of surfactant[19] (Table I). Experiments have shown that in general the larger the γ_{ow}, the higher the stability of the emulsion. Since large values of γ_{ow} imply a very hydrophobic oil phase the interactions between the hydrocarbon tails of the surfactant and the organic molecules as well as those between the polar head groups of the surfactant and water are expected to be strong. This stabilizes the interface between the two phases and thus increases the stability of the emulsion. If the organic molecules interact with the polar head group of the surfactant, this weakens the interactions between the polar head group and water, resulting in a decreased stability. The increased stability of aromatic compounds prepared with CTAB compared to those prepared with

CDBACl, where an interaction between the benzene ring of the oil phase and polar group of the surfactant is observed, can thus be explained. However the great differences observed in stability between octane and methylcyclohexane or heptane and cyclohexane cannot be explained.

It is very important not only to consider the interfacial free energy γ_{ow}, but also the rate of decreasing γ_{ow} in the presence of surfactant, since this rate that gives information about the movement of the surfactant molecules to the interface is more important than the steady value.

According to the molecular diffusion theory, very small particles demonstrate deviations in their physical properties as compared to larger particles. This theory predicts that the greater the solubility of the oil in the continous phase the greater the instability due to the preferential dissolution of small droplets onto larger droplets. However the order of stability for the oils considered in Table III does not follow their respective solubility in water given in Table I. It is also impossible to correlate the stability with the polarity of the oil phases used for the preparation of emulsions[6,20].

It is obvious from the above discussion that ζ-potential alone cannot be straightforward correlated with emulsion stability. Some other theories can partly explain the stability and that more parameters are needed to be considered to explain the experimental findings and to provide an apriori estimation of emulsion stability that is of practical importance.

ΠΕΡΙΛΗΨΗ

ΕΠΙΔΡΑΣΗ ΤΗΣ ΕΛΑΙΩΔΟΥΣ ΦΑΣΗΣ ΣΤΗ ΣΤΑΘΕΡΟΤΗΤΑ ΑΡΑΙΩΝ Ε/Υ ΓΑΛΑΚΤΩΜΑΤΩΝ

Στην εργασία αυτή μελετάται η σταθερότητα αραιών γαλακτωμάτων ελαίου σε νερό, χρησιμοποιώντας διάφορες ελαιώδεις φάσεις. Σαν γαλακτωματοποιητές χρησιμοποιούνται τρεις τασενεργές ουσίες, το δωδεκυλοσουλφονικό νάτριο, το δεκαεξυλοδιμεθυλοβενζυλαμμώνιο χλωρίδιο και το δεκαεξυλοτριμεθυλαμμώνιο βρωμίδιο. Ο χρόνος που απαιτείται για την εμφάνιση ιχνών ελαιώδους φάσης στην επιφάνεια του γαλακτώματος (σπάσιμο του γαλακτώματος) χρησιμοποιείται σαν ποιοτικό κριτήριο σταθερότητας. Το ζ-δυναμικό των σταγονιδίων των γαλακτωμάτων υπολογίζεται από μετρήσεις μικροηλεκτροφορητικής ευκινησίας. Παρατηρούνται μεγάλες διαφορές στη σταθερότητα των γαλακτωμάτων που δεν είναι δυνατόν να αποδοθούν στις μικρές διαφορές στο ζ-δυναμικό. Στη συνέχεια εξετάζονται επιπλέον παράμετροι για μια πιο ολοκληρωμένη αντίληψη της σταθερότητας των γαλακτωμάτων.

REFERENCES

1. Becher, P., *Emulsions : Theory and Practice* , 2nd edition, Reinhold Publishing Corporation, New York, 1965.
2. Tadros, T.F., and Vincent, B., *Encyclopedia of Emulsion Technology* Vol. 1 (P.Becher, Ed.) ch. 3, Marcel Dekker inc., New York, 1983.
3. Hunter, R.J. , *Zeta Potential in Colloid Science* , Academic Press, London, 1981.
4. Garrett, E.R., *J. Pharm. Sci.* 54, 1557 (1965).
5. Hallworth, G.W., and Carless, J.E., *J. Pharm. Pharmacol.* 24 Suppl., 71P (1972).
6. Lapan, B.T., Kucher, R.V., Enalev, V.D., and Zhilina, L.G., *Kolloid Zh. SSSR* 35, 175 (1973).
7. Davis,S.S., and Smith, A., *Theory and Practice of Emulsion Technology* (A.L.Smith, Ed.) ch. 19, Academic Press, London, 1976.
8. Higuchi, W.I., and Misra, J., *J. Pharm. Sci.* 51, 459 (1962).
9. Carrol, B.J., and Haydon, D.A., *J. Chem. Soc. Faraday Trans. I* 71, 361 (1975).
10. Perrin, D.D., Armarego, L.F., and Perrin, D.R. , *Purification of Laboratory Chemicals* , 2nd Edition, Pergamon Press, 1980.
11. Riddick, J.A., and Bunger, W.B., *Organic Solvents* Vol. II, 3rd Edition , Wiley-Interscience, 1970.
12. Girifalco, L.A., and Good, R.J., *J Phys. Chem.* 61, 904 (1957).
13. Avranas, A., Stalidis, G., and Ritzoulis, G., *Colloid Polym. Sci.* 266, 937 (1988).
14. Avranas, A., *Thesis*, University of Thessaloniki, 1986.
15. Bowen, B.D., *J. Colloid Interface Sci.* 82, 574 (1981).
16. Lane, A., *Thesis*, University of Bristol, 1970.
17. Cante, C.J., Mc Dermott, J.E., and Saleeb, F.Z., *J. Colloid Interface Sci.* 50, 1 (1980).
18. Elworthy, P.H., and Florence, A.T., *J. Pharm. Pharmacol.* 21 Suppl., 79 S, (1969).
19. Chen, H.H., and Ruckenstein, E., *J. Colloid Interface Sci.* 138, 473 (1990).
20. Vijayendran, B.R., and Bursh,T.P., *J. Colloid Interface Sci.* 68, 383, (1979).

Chimika Chronika, New Series, 20, 139-158 (1991)

LABORATORY EVALUATION PROCEDURES OF FLUID CRACKING CATALYSTS

A.A. LEMONIDOY[1], A.F. PAPADOPOULOU, I.A. VASALOS

Aristotelian University of Thessaloniki, Department of Chemical Engineering and Chemical Process Engineering Research Institute P.O. Box 1517, 54006 Thessaloniki, GREECE

(Received November 18, 1990)

SUMMARY

Fluid Catalytic Cracking (FCC) is of major interest in the petroleum industry. Catalyst evaluation procedure includes steam deactivation and microactivity testing for the determination of catalyst activity and selectivity. Four commercial FCC catalysts with different Rare Earth Oxides (Re_2O_3) content were evaluated. The fresh samples were steam deactivated at different conditions (temperature and duration) and the activity of the artificially deactivated catalyst was measured in a Microactivity Test Unit.

It was found that the steaming conditions affect greatly the catalyst surface area, the feed conversion and the coke yield. At standard steaming conditions Re_2O_3 content also affect feed conversion, coke yield and the quality of the gasoline produced.

Key words: Fluid cracking catalysts, evaluation, zeolites, rare earth oxides, Research Octane Number

INTRODUCTION

Most industrial reactions are catalytic, and many process improvements result from the discovery of better chemical routes, usually involving new catalysts. One of the largest scale catalytic processes practiced today is cracking, the conversion of large petroleum molecules into smaller hydrocarbons, primarily in the gasoline range.

Cracking processes were first carried out in the absence of catalysts, but in the last fifty years a series of continuously improved cracking catalysts has been applied, all of them solid acids. The most important advance in cracking technology in the last three decades has been the development of zeolite catalysts.

---

[1]To whom correspondence should be addressed

One of the desirable characteristics of a commercial cracking catalyst is a high selectivity to gasoline range hydrocarbons especially aromatics and isomeric alkanes, low gas and coke yield. All cracking catalysts lose activity in use by the formation of coke on their surfaces. The coke is both a by product and a poison of catalyst activity. Since the coking reaction is very fast, catalyst activity decreases rapidly and the catalyst has to be removed for regeneration after a relatively short time on stream. Commercial reactors take this into account by circulating the catalyst between the reactor and a regenerator. High circulation rates lead to problems with attrition and consequent catalyst losses in the form of fines. The successful catalyst must therefore have high attrition resistance as well as high gasoline selectivity and stability. Nevertheless, even the best catalysts are fouled by coke and need regeneration. Regeneration is carried out in the presence of air and water vapor, at temperatures higher than those used in cracking. Thus, thermal and hydrothermal stability becomes important.

The first cracking catalysts used commercially on a large scale were synthetic amorphous silica aluminas and silica magnesias[1]. In the early 1960's, zeolites[2,3] with rare earth ions replacing the sodium cation were added to the amorphous matrix to improve catalyst activity and selectivity. The new catalysts had remarkably higher activity, much better selectivity for gasoline, and a higher hydrothermal stability than the amorphous catalysts used up to that time. Typical commercial catalysts of this type consist of 10 to 20% zeolite in an attrition resistant silica alumina matrix which provides the bulk of the catalyst mass. The matrix itself is highly porous and allows access to the crystallites of zeolite embedded in the interior of the particle. In practice the matrix has much lower activity than the zeolitic components; hence, the product distribution and activity of commercial zeolite containing catalysts can be mainly ascribed to the small percentage of zeolite present.

The influence of the zeolite on the yield and selectivity of the cracking catalyst has been reviewed by Magee and Blazek[4]. Their results can be summarized in part by noting that an increase in the amount of zeolite present in the catalyst increases the yield of gasoline and

light cycle oil, while coke and dry gas make is decreased at any given level of conversion. At the same time the aromatic content and the octane number of the gasoline fraction increase.

The type of the zeolite used in the cracking process is faujasite (Zeolite Y) with the chemical formula $0.9\pm0.2\ Na_2O.Al_2O_3.\omega SiO_2.xH_2O$, where $3<\omega<6$ and $x<9$. To act as a cracking catalyst this NaY zeolite must be converted to an acidic form. The sodium content must be reduced to the lowest possible level to obtain high thermal and hydrothermal stability. Both can be achieved by ion exchanging the zeolite to an acidic form and then incorporating it into the matrix.

Rare earth exhanged (REY) catalysts induce hydrogen transfer reactions between alkenes and naphthenes producing alkanes and aromatics, and associated lower octanes due to the lower octane potential of alkanes compared to the boost from the aromatics produced. Since the number of acid sites is proportional to the concentration of framework aluminum, high silica/alumina zeolites have fewer acid sites and therefore lower hydrogen transfer activities than low silica/alumina zeolites. The lower unit cell size (high silica/alumina ratio) decreases the coke yield and the activity of the catalyst, but the gasoline produced has higher octane number. While all catalysts incorporate zeolites as the core, the type and amount vary widely. Differences in catalyst composition can be significant, 0-3 wt % rare earth oxides, 19-40 wt % crystalline zeolite with surface areas ranging from 100-400 m^2/gr.

In general a cracking catalyst must show:

- High activity
- High selectivity that means
  - high octane gasoline
  - low coke yield
  - high $C_3^=/C_3$ and $C_4^=/C_4$ ratios
- Attrition resistance
- Metals resistance, especially to V and Ni

FCC CATALYST EVALUATION

The objectives of the FCC catalyst evaluation includes routine inspections of equilibrium catalysts, preapproval of fresh catalyst shipments, evaluation of commercially available catalysts and the recommendation of catalyst for use in commercial FCC units.

An effort was started a few years ago in the Laboratory of Petrochemical Technology of the Chemical Engineering Department to built a system for complete catalyst evaluation. Laboratory evaluation of the catalytic performance of fresh FCC catalysts involves steaming (hydrothermal deactivation), activity testing (Microactivity Test, MAT) and gasoline RON measurement.

In a commerical unit the fresh catalyst deactivates with time. It is recognized that it is difficult to simulate the conditions of catalyst deactivation in the lab. An approximation of equilibrium catalyst is performed with steam deactivation. Steaming conditions affect the activity and selectivity of the sample catalyst. Hydrothermal deactivation results in changes to matrix and zeolite[5]. High temperature leads to loss of surface area, change in pore volume and pore size distribution. The combined action of high temperature and steam affect greatly the crystalline part of the catalyst, the zeolite. The Si/Al ratio increases because of the dealumination, the concentration of hydroxyl groups decreases and part of the zeolite crystallinity is destoyed.

The artificially deactivated FCC catalysts are tested in the Microactivity Test Unit[6], the most important step of the evaluation procedure. Although the reactor used in MAT unit is fixed bed while in commercial units the reactor is of fluidized type, the results of laboratory testing can provide useful information for predicting commercial catalyst performance. The optimization of test conditions in steam deactivation and microactivity test is essential for the reliable evaluation of new commercial FCC catalysts.

The small quantities of gasoline samples produced from bench scale equipment are not sufficient for RON measurement by CFR engine test[7]. Three classes of octane models have been appeared in the literature, based upon analytical techniques used to characterize

gasoline composition: nuclear magnetic resonance (NMR)[8], fluorescent indicator absorption (FIA)[9] and Gas Chromatography (GC)[10,11,12]. In general, the available models work well for the types of gasolines for which they were developed. The gas chromatography analytical technique was used in our lab for the characterization of FCC gasoline composition and the prediction of gasoline octanes.

While ASTM procedures for both steaming[13] and MAT[6] testing have been established (ASTM D4463 and D3907 respectively) a general survey of the petroleum industry indicates that neither of these methods are specifically practiced. Instead each laboratory has developed individualized steaming and MAT testing procedures that best suit their needs.

EXPERIMENTAL

Steaming

The steaming of a catalyst is conducted in a cylindrical furnace shown in Figure 1. The reactor is made of quartz and is placed in the furnace with the thermocouple positioned in the middle of the catalyst bed.

Nitrogen flow is attached to the bottom of the reactor and the temperature is set to 1200°F. The catalyst is added to the reactor slowly so as to heat shock the catalyst particles. The N_2 flow should be sufficient to keep the bed fluid. When all catalyst is loaded, the temperature is raised to the desired temperature. Nitrogen flow is stopped and water is added to the bottom of the reactor. The water vaporizes as soon as it reaches the hot quartz reactor. The duration of steaming varies between 5 to 10 hrs. The temperature in the fluid bed must be kept constant.

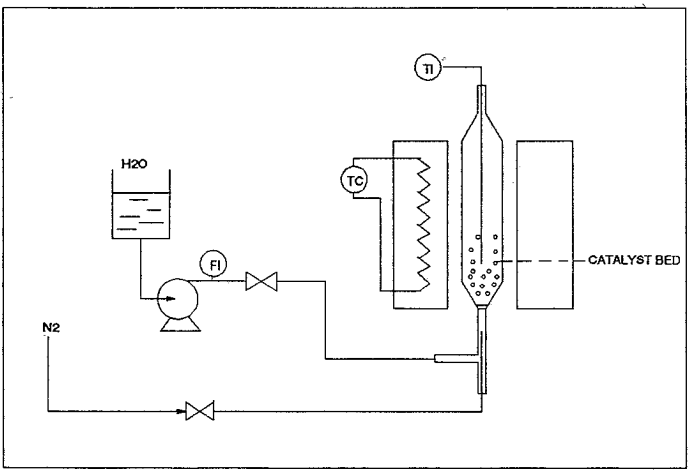

FIG. 1: *Schematic diagram of steam deactivation unit*

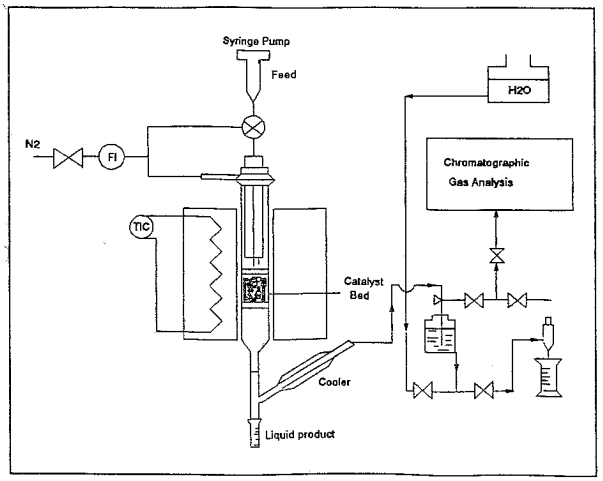

FIG. 2: *Microactivity Test Unit (MAT)*

Microactivity Test

The measurement of activity and selectivity of steam deactivated catalyst samples is performed in the microactivity test unit illustrated in Figure 2. A small amount of catalyst (3 gr) is placed in the quartz reactor and is heated up to 900°F. A three zone furnace equipped with temperature controllers is employed for heating and control of the reactor temperature. The rate of gas oil (feed) injection is controlled by the use of a syringe pump. A stainless steel preheater that fits closely inside the reactor and the heat for preheating the gas oil is supplied by the upper zone of the three zone furnace. Testing conditions are shown in Table I.

TABLE I: MAT operating conditions

Feedstock	: D-32 ASTM standard MAT feed
Feed flow rate	: 0.78 - 0.79 gr/min
Operating time	: 50 sec
Nitrogen flow rate	: 50 cc/min
Temperature	: 900°F
Pressure	: 14.7 psia
Catalyst weight	: 3 gr
WHSV	: 15 - 16 hr^{-1}
C/O	: 3.5 - 4.0

Pyrolysis products at the reactor exit are cooled in a chilled liquid receiver where gasoline and unconverted gas oil are condensed. The gases then flow to a gas collecting system where the volume is measured by water displacement. The analysis of gases is performed with a Gas Chromatograph Varian 3400 refinery gas analyzer. Liquid products are analyzed in a Gas Chromatograph Hewlett Packard 5710A. Analysis conditions are presented in Table II.

TABLE II: Product analysis

Liquid products	
Chromatograph	: HP 5710A (FID)
Column	: 3% OV 101 chromosorb
Components	: C_5 and higher hydrocarbons
Gas products	
Chromatograph	: Varian 3400 refinery gas analysis
Columns	: 20% DC 200/500 20% BEEA Porapak N 2B Chrom 106 Molecular sieve 5A
Components	: H_2, O_2, CO_2, CO, CH_4, C_2H_4, C_2H_6, C_3H_8, iC_4H_{10}, nC_4H_{10}, 1 - & cis & trans C_4H_8, iC_5H_{12}, nC_5H_{12}, C_5H_{10}, C_6H_{14}

The amount of coke on the catalyst is measured in a Leco furnace where it is burned to carbon dioxide, which is adsorbed by ascarite. Liquid products are a mixture of gasoline and unconverted gas oil. All peaks in the chromatogram up to the peak of n-dodecane are assumed to be in the gasoline range. The feed conversion is calculated by the formula:

$$X = \frac{F - L\left(\frac{100-N}{100}\right) - H}{F}$$

where: F: gr of gas oil (BP>430°F)
L: gr of liquid products
N: wt% of gasoline in liquid products
H: gr of residue in transfer line and reactor

The reliability of the experimental unit is checked with testing standard equilibrium ASTM catalysts[6]. The feed conversions measured by the lab are in good agreement with the conversions given by ASTM. The results for the five ASTM catalyst samples are shown in Figure 3.

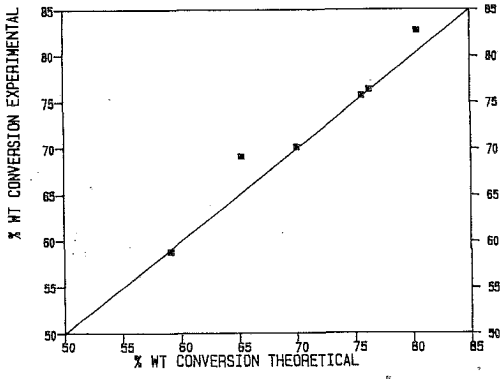

FIG. 3: *Relationship between the experimental and theoretical conversion*

BET Surface Area

The surface area of FCC samples depends greatly on the type of catalyst and on the degree of deactivation. Steaming conditions affect the surface area. Measurement of surface area of the steamed catalyst samples was performed with a Micrometritics Accusorb 2100E surface area analyzer with nitrogen as the adsorbate gas.

Prediction of Gasoline Octanes

The calculation of Research Octane Number (RON) by means of chromatographic analysis of the gasoline produced by the MAT unit is a very useful tool for the complete evaluation of new FCC commercial catalysts.

A chromatographic technique was set up on a Hewlett Packard Model 5880A to separate the gasoline portion of the full boiling range liquid product from the higher boiling components (higher than n-dodecane). This was performed by using a specially modified injection port, an 8 port valve and a prefractionator column[14].

A fused silica cross linked methyl silicone (50 m x 0.2 mm) capillary column was used for the separation of hydrocarbons up to n-dodecane. The chromatographic conditions employed are shown in Table III. The separation of about 300 hydrocarbons is very successful. About 100 peaks have been identified by using individual standards.

TABLE III: GC operating conditions for gasoline analysis

Instrument	: Hewlett Packard 5880A
Column	: 50 m x 0.2 mm ID W.C.O.T. on fused silica crosslinked methyl silicone
Detector	: FID
Carrier gas	: N_2
Split ratio	: 60/1
Sample size	: 1 µl
Injector temperature, °C	: 250
Detector temperature,°C	: 250
Column temperature, °C	: 0-140

The model of Walsh and Mortimer[10] was used for the prediction of Research Octane Numbers (RON). The above method uses linear regression to assign effective octane number to the 31 pseudocomponents of gasoline. These groups have been defined by locating certain key peaks and their areas, and then finding the total area of peaks falling between the "keys". Some of these groups in fact consist of a single compound while others, are mixtures of compounds chosen to be within narrow boiling ranges and to be of like chemical type. Table IV defines the 31 groups used to characterize a gasoline.

TABLE IV: Definition of the 31 groups according to Walsh and Mortimer[10] and regression coefficients

Group No	Compounds in each group	Regression coeff.,a
1	compounds before n-butane	103.9
2	n-butane	88.1
3	n-butane to isopentane excl	144.3
4	isopentane	84.0
5	isopentane to n-pentane excl	198.2
6	n-pentane	67.9
7	n-pentane to 2-methylpentane excl	95.2
8	2-methylpentane to 3-methylpentane incl	86.6
9	3-methylpentane to n-hexane excl	95.9
10	n-hexane	20.9
11	n-hexane to benzene excl	94.9
12	benzene	105.2
13	benzene to 2-methylhexane excl	113.6
14	2-methylhexane to 3-methylhexane incl	80.0
15	3-methylhexane to n-heptane excl	97.8
16	n-heptane	-47.8
17	n-heptane to toluene excl	62.3
18	toluene	113.9
19	toluene to 2-methylheptane excl	115.1
20	2-methylheptane to 3-methylheptane incl	81.7
21	3-methylheptane to n-octane excl	109.7
22	n-octane	10.5
23	n-octane to ethylbenzene excl	96.1
24	ethylbenzene	122.6
25	ethylbenzene to p-xylene excl	45.4
26	p- + m-xylene	102.0
27	m-xylene to o-xylene excl	73.3
28	o-xylene	123.6
29	end o-xylene to end n-nonane	35.0
30	n-nonane to n-decane excl	112.0
31	n-decane and beyond	85.6

The linear model suggested by Walsh and Mortimer is of the form:

$$RON = \sum_{i=1}^{31} \alpha_i w_i$$

where: w_i: weight fraction of group i

α_i: weight blending octane number of group i

The blending octane numbers α_i have been estimated by means of multiple regression analysis and are shown in Table IV[4].

RESULTS AND DISCUSSION

Four catalyst samples with various Rare Earth Oxide (Re_2O_3) content were evaluated. The catalysts tested were Sigma 400, Delta 400 (Katalistics), DA 300 and Super D (Grace). The properties of these samples are presented in Table V.

TABLE V: Catalyst properties

	Delta 400	Sigma 400	Super D	DA 300
Al_2O_3, wt%	34.3	34.2	31.0	45.3
Na_2O, wt%	0.18	0.66	0.40	0.20
Fe_2O_3, wt %	-	-	0.60	0.68
% Re_2O_3 on 100% zeolite	0.2	8.0	12.8	15.9
Apparent bulk density, gr/cm^3	0.69	0.69	0.79	0.84
Pore volume, cm^3/gr	0.35	0.35	0.30	0.25
Surface area, m^2/gr	244.0	216.0	155.0	130.0

At first the effect of steaming conditions on surface area was examined. The surface area decreases rapidly with the steaming temperature as shown in Figure 4 for the catalyst Delta 400. The higher

the steaming temperature, the lower is the catalyst surface area. The duration of steam deactivation affects also the surface area, especially at high temperature (1500°F). The reduction of surface area is due to by the partial loss of the zeolite crystallinity. The effect of steaming conditions on surface area is the same for all catalyst samples tested.

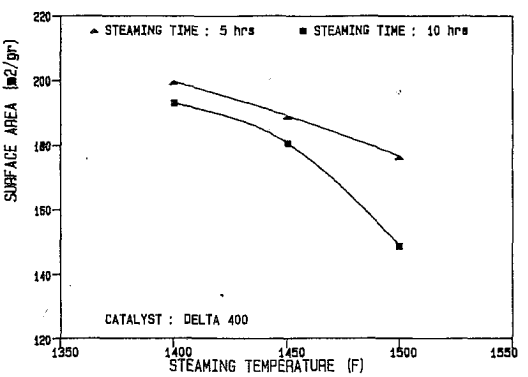

FIG. 4: *Effect of steaming temperature and time on catalyst surface area*

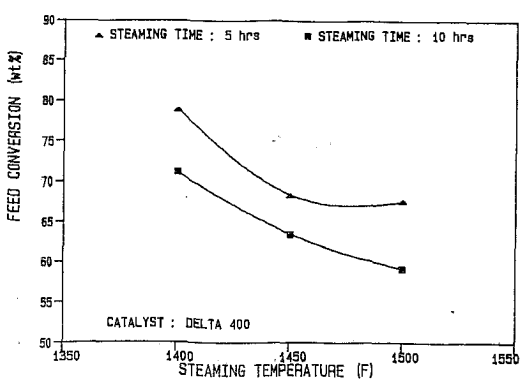

FIG. 5: *Effect of steaming temperature and time on feed conversion*

TABLE VI: Experimental results of catalyst evaluation

Catalyst	: Delta 400	Sigma 400
Steaming conditions		
Temperature, °F	: 1400.0	1500.0
Steaming time, hr	: 5.0	10.0
MAT operation conditions		
Feed flow rate, gr/min	: 0.7368	0.7784
Feed flow rate, sec	: 50.00	50.00
Nitrogen flow rate, cc/min	: 31.00	47.00
Temperature, °C	: 483.00	484.00
Pressure, psia	: 15.050	15.050
Catalyst to oil ratio	: 4.0717	3.8539
WHSV	: 14.7360	15.5688
% wt coke on feed	: 3.1661	1.2194
% wt coke on catalyst	: 0.6480	0.2637
% wt conversion	: 78.9358	59.1445
Product yields, % wt		
C_4 in liquid	: 3.3665	3.6316
C_5 - 421 F	: 48.5929	36.2625
421-626 F	: 20.8665	40.4719
Coke	: 3.1661	1.2194
Hydrogen	: 0.0140	0.0062
Methane	: 0.2745	0.1222
Ethane	: 0.2537	0.1276
Ethylene	: 0.4643	0.1606
Propane	: 0.8339	0.2370
Propylene	: 3.5754	1.6893
i-butane	: 4.5836	1.5039
n-butane	: 0.7616	0.2046
1-butane	: 1.6605	0.9890
trans-butane 2	: 1.4311	0.7286
cis-butene 2	: 0.9153	0.4661
i-pentane	: 4.9499	1.5296
n-pentane	: 0.3124	0.1111
pentene	: 4.0729	2.1461
hexane	: 0.7740	0.8339
Carbon dioxide	: 0.1413	0.0310
% wt recovery	: 96.6210	91.9844

The steam deactivated catalyst samples were tested under the same experimental conditions in the MAT unit. Some representative results are shown in Table VI. The effect of steaming conditions on feed conversion is significant (Figure 5). The conversion decreases as the

steaming temperature and duration increases. The yield of coke is greatly affected by the deactivation procedure as illustrated in Figure 6. Olefinicity ratios $C_3^=/C_3$ and $C_4^=/C_4$ are also affected by the deactivation (Figure 7). As the extent of deactivation increases, the above ratios also increase. Deactivation of catalyst reduces the acid active centers of the catalyst thus inhibiting the hydrogen transfer. Because of the reduced hydrogen transfer, rates the percentage of olefines increases at the expense of paraffins.

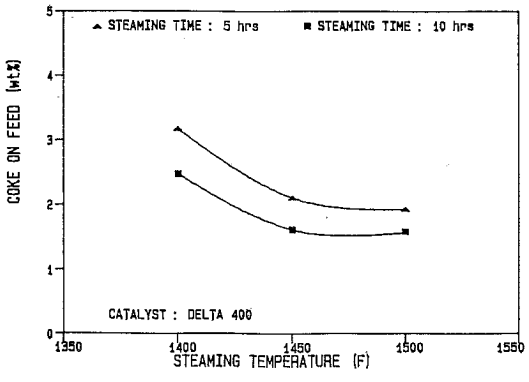

FIG. 6: *Effect of steaming temperature and time on coke production*

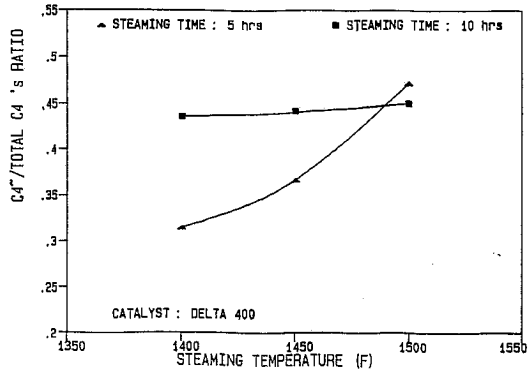

FIG. 7: *Effect of steaming temperature and time on olefinicity ratio*

Zeolites are usually exchanged by rare earth metals. The rare earth cation stabilizes the framework aluminum atoms, thus inhibiting dealumination. Thus, the degree of rare earth oxide content affects greatly the catalyst performance.

As shown in Table V the four catalyst samples have different rare earth oxide content. The catalyst samples were deactivated with steam at 1450°F for 10 hrs and then were tested under the same experimental conditions. Delta 400 catalyst that does not have Re_2O_3 shows low conversion whereas DA 300 with 16 wt% Re_2O_3 (on zeolite) shows higher conversion. There is a strong relation between conversion and Re_2O_3 content (Figure 8).

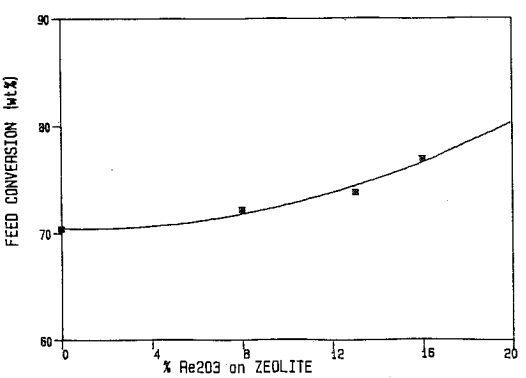

FIG. 8: *Reaction between the Re_2O_3 content of the catalyst and the feed conversion*

Coke yield increases significantly from Delta 400 catalyst to DA 300. Highly exchanged rare earth catalysts have the disadvantage of high coke production (Figure 9). The effect of rare earth oxide content is shown more clearly in Figure 10, where the coke yield is plotted as a function of Re_2O_3 at standard conversion 73 wt%. Olefinicity ratios $C_3^=/C_3$ and $C_4^=/C_4$ are also affected by the rare earth content. The ratio of olefins to total paraffins for C_3's and C_4's decreases with the increase of Re_2O_3 (Figure 11). As it was mentioned the rare earth oxides

inhibit dealumination and consequently the hydrogen transfer rate maintain high. So the formation of olefins is decreased.

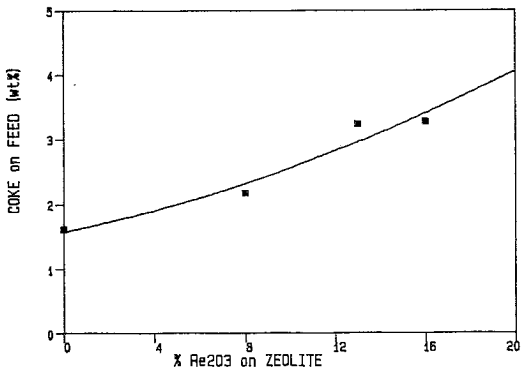

FIG. 9: *The effect of % Re_2O_3 on zeolite on coke production*

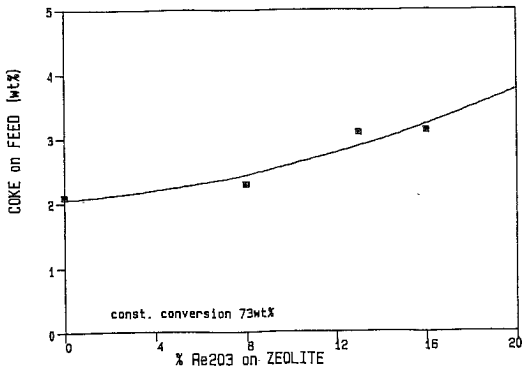

FIG. 10: *Coke on feed as a function of Re_2O_3 on zeolite at constant conversion*

The RON values of the gasoline produced, were calculated by using the model of Walsh and Mortimer. The type of catalyst and the degree of

Rare Earch Oxide content influences the quality of the gasoline. As the Re_2O_3 content increases, the Research Octane Number decreases (Figure 12).

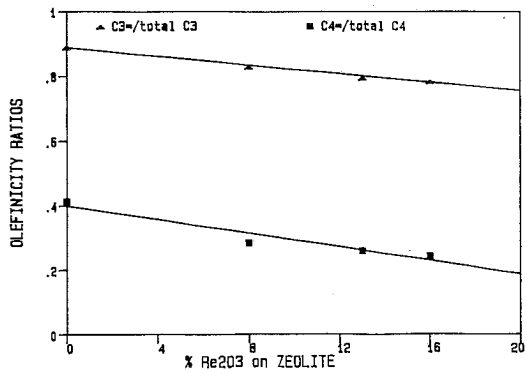

FIG. 11: *Relation between the Re_2O_3 content of the catalyst and the olefinicity ratio*

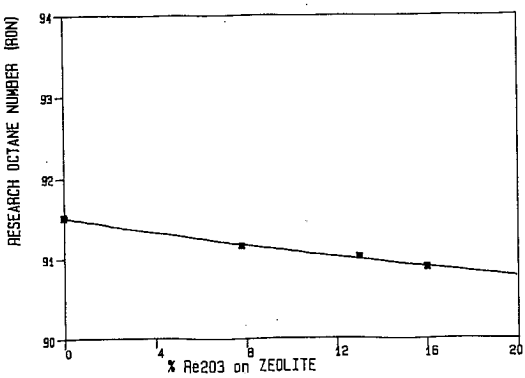

FIG. 12: *Research octane number of gasoline as a function of the Re_2O_3 content of the catalyst*

CONCLUSIONS

Experimental procedures have been established which can be used to evaluate FCC catalyst. As shown, the choice of steaming/MAT procedures selected for evaluation of fresh FCC catalyst can affect the catalyst performance. As the steaming temperature and the duration increases, the catalyst looses activity that means that the conversion and the coke yield decreases.

The rare earth oxide content affects also the catalyst performance. The higher the Re_2O_3 concentration is, the catalyst is more active. The feed conversion and the coke yield increases but the gasoline produced has lower Research Octane Numbers.

ACKNOWNLEDGEMENTS

This work was supported by the Hellenic Aspropyrgos Refineries.

ΠΕΡΙΛΗΨΗ

Πειραματική Διαδικασία Αξιολόγησης Καταλυτών της Μονάδας Καταλυτικής Πυρόλυσης

Η καταλυτική πυρόλυση των βαριών κλασμάτων πετρελαίου είναι μια από τις σπουδαιότερες διεργασίες σε ένα διυλιστήριο. Η διαδικασία αξιολόγησης των καταλυτών που χρησιμοποιούνται στη διεργασία αυτή περιλαμβάνει ατμοαπενεργοποίηση των φρέσκων δειγμάτων και στη συνέχεια τη δοκιμασία στη μονάδα MAT για τον προσδιορισμό της ενεργότητας και εκλεκτικότητας των καταλυτών. Στην εργασία αυτή δοκιμάστηκαν 4 εμπορικοί καταλύτες με διαφορετικό ποσοστό σπάνιων γαιών στο κρυσταλλικό πλέγμα. Ιδιαίτερα μελετήθηκε η επίδραση της θερμοκρασίας και η διάρκεια της διαδικασίας ατμοαπενεργοποίησης στην ενεργότητα και εκλεκτικότητα του καταλύτη. Βρέθηκε ότι οι συνθήκες απενεργοποίησης με ατμό επηρεάζουν σημαντικά την ειδική επιφάνεια του καταλύτη, τη μετατροπή της τροφοδοσίας και την επόδοση σε κωκ. Το περιεχόμενο ποσοστό σπάνιων γαιών στον καταλύτη επηρεάζει τη μετατροπή της τροφοδοσίας, την απόδοση σε κωκ και τον αριθμό οκτανίου της βενζίνης που παράγεται.

LITERATURE

1. Gladrow E.M., Kreb R.W., and Kimberlin C.N., Ind. Eng. Chem. 45, 142 (1953)
2. Elliot K.M., and Eastwood S.C., Oil and Gas J., 60(23) 142 (1962)
3. Eastwood S.C., Drew R.D., and Hartzell F.D., Oil and Gas J., 60(44) 152 (1962)
4. Magee J.S., and Blazek J.J., ACS Monograph 171 Zeolite Chem. Catal. (J.A. Rabo, Ed.) p. 615 (1976)
5. Ritter R.E., Creighton J.E., Chin D.S. and Roberie T.G., Catalgram 74 (1986)
6. Annual Book of ASTM Standards 1990, ASTM D-3907, Vol. 05.03, 825 (1990)
7. Annual Book of ASTM Standards 1990, ASTM D-2699, Vol. 05.04, 12 (1990)
8. Muhl J., and Srica V., Fuel 66, 1146 (1987)
9. Rusin M.H., Chung H.S., and Marshall J.F., Ind. Eng. Chem. Fundam, 20, 1951 (1981)
10. Walsh R.P., and Mortimer J.V., Hydrocarbon Process, 50, 153 (1971)
11. Durand J.P., Boscher Y., and Petroff N., J. Chromatography 395, 229 (1987)
12. Cronkright W.A., Butler M.M., and Halter D.A., Paper presented at Ketjen Catalysts Symposium, May 25-28, Kurhaus, The Netherlands, p. F9 (1986)
13. Annual Book of ASTM Standards 1990, ASTM D-4463, Vol. 0503, 870 (1990)
14. Green L.E., Plotczyk L.L. and Pratt J.W., Paper presented at the 32nd Pittsburgh Conference on Analytical Chemistry and Applied spectroscopy, N.J., March 9, 1981

Chimika Chronika, New Series, 20, 159-167 (1991)

VOLTAMMETRIC INVESTIGATION ON CADMIUM-THIOSEMICARBAZIDE-GLYCINE TERNARY COMPLEXES

REFAT ABDEL-HAMID, MOSTAFA K. RABIA and ZANATY R. KOMY
Department of Chemistry, Faculty of Science, Sohag, Egypt.

(Received June 5, 1991)

SUMMARY

Cadmium(II)-thiosemicarbazide-glycine binary and ternary complexes were investigated voltammetrically, cyclic and differential pulse methods, at the isoionic point of glycine in aqueous solutions at 0.1 mol l^{-1} $NaClO_4$. Composition and stability of the complexes formed in solution are determined using POLAG computer program. It was found that, Cd(II) forms a 1:3 binary complex with thiosemicarbazide, while in the ternary system, it gives a mixture of 1:1:1 and 1:2:2 (Cd:gly:tsc) mixed ligand complexes. The ternary complex species are found to have higher stabilities than the binary one. The equilibria exist in solution mixture of the three components are discussed.

Key words: Voltammetry, cadmium(II), thiosemicarbazide, glycine, ternary complexes, equilibria, stability.

INTRODUCTION

Many solid binary complexes of cadmium(II) with thiosemicarbazide are known.[1] Few workers have determined the stability constants of these complexes. Owing to the weak basicity of thiosemicarbazide, its binary complexes have been studied polarographically.[2-6] Although, cadmium(II) ternary complexes involving the ligand are rare, an investigation on complexes of thiosemicarbazide and thiosulphate has been recently reported.[6]

In the present investigation, a detail study is performed on the binary and ternary complexes of cadmium(II)-thiosemicarbazide - glycine at the isoionic point of glycine. The overall stability constants and composition of the complexes liable to form in solution are calculated

from the differential pulse voltammetric data using the approximation-free POLAG computer program.[7] The binary complexes of Cd(II)-thiosemicarbazide are reinvestigated at such conditions.

EXPERIMENTAL

All reagents used (sodium perchlorate, cadmium(II) nitrate, thiosemicarbazide, glycine) were of AnalaR (B.D.H. or Merck) grade. Fresh stock aqueous solution of 0.10 mol l^{-1} $NaClO_4$ was prepared by dissolving the salt in carbon dioxide-free bidistilled water. Fresh thiosemicarbazide and glycine stock solutions (0.10 and 2.00 mol l^{-1}, respectively) were prepared from the fresh electrolyte solution (0.10 mol l^{-1} $NaClO_4$) on the same day that measurements were performed. Stock solution (0.10 mol l^{-1}) of cadmium(II) was prepared by dissolving cadmium nitrate in the electrolyte and it was titrated.[8]

Differential pulse and cyclic voltammograms were taken using an EG & G PAR model 364A Polarographic Analyzer. The measurements were carried out using a conventional three electrodes configuration. An EG & G PAR model SMDE 303 mercury-drop system in small dropping mode was used as working electrode. The electrode area was $1.05X10^{-2}$ cm^2. The reference electrode was $Ag/AgNO_3$ (0.01M) electrode in 0.10 mol l^{-1} sodium perchlorate aqueous solution. An 1.0 cm^2 platinum foil was used as axiliary electrode throughout the experimental work. For differential pulse voltammetric experiments a drop time of 1.0 s, a sweep rate of 2.0 mV/s, and pulse height of -25.0 mV were used. Solutions were purged with pure nitrogen before to take the measurements and an atmosphere of nitrogen was maintained above the working solution. The pH's of all solutions were adjusted using perchloric acid (0.1 mol l^{-1})and sodium hydroxide solutions (0.1 mol l^{-1}) at 6.10.

Calculations were performed using POLAG Computer Program on IBM S/2 Computer.

RESULTS AND DISCUSSION

It was demonstrated that, the POLAG Program is applicable to equilibria of the type:

$$mM + nL \rightleftharpoons M_mL_n \quad ; \quad m,n = 1,2, \ldots m=2, N$$

as well as

$$mM + nL + pL' \rightleftharpoons M_mL_nL'_p \quad ;m, n, p = 0,1,\ldots 2,N(P)$$

whether or not the data are dependent on pH.

It has been noted earlier that, the most common method of extracting stability constants from polarographic data employs the approach detailed by DeFord and Hume.[9,10] The method is based on the following equations:

$$F = \exp [nF/RT (E_{1/2(s)} - E_{1/2(c)})] + \ln (I_{ds}/I_{dc}) \quad (1)$$

$$F = 1 + C_L\beta_1 + C_L^2 \beta_2 + \ldots\ldots C_L^n \beta_N \quad (2)$$

where $E_{1/2(s)}$ and $E_{1/2(c)}$ are the half-wave potentials for the uncomplexed and complexed metal ion, respectively; I_{ds} and I_{dc} are the diffusion currents of the uncomplexed and complexed metal ion; C_L is the analytical concentration of the ligand and β_N is the overall stability constant of the Nth complex.

It is often advantageous to use a second ligand to provide competition for the metal ion. In this situation the method of Schaap and McMasters[11,12] is used.

The exact form of equation (2) is:

$$F = 1 + [L]\beta_1 + [L]^2\beta_2 + \ldots.[L]^n\beta_N \quad (3)$$

which is derived from:

$$F = C_M/[L] \quad (4)$$

POLAG is a non-linear least-square iterative program that seeks to minimize U, the sum of squares of the residual, i.e.,

$$U = \sum_{i=1}^{N} (F_{calc,i} - F_{obs,i})^2 \quad (5)$$

where N is the number of data points; F_{obs} is given by equation (1) and represents the experimental data; F_{calc} is obtained from equation (4).

The values of F_{calc} depend on the particular combination of m, n and p and the values of β_{mnp}. Therefore, various equilibrium models may be fitted to the polarographic data simply by changing the input data values of m, n and p together with appropriate value of β_{mnp}.

Voltammograms of cadmium(II), cadmium(II)-glycine and cadmium(II)-glycine-thiosemicarbazide solutions in 0.1 mol l^{-1} sodium perchlorate at the isoionic point of glycine are recorded at 298K (c.f.Fig. 1). The isoionic point is at pH= $(pK_{a1} + pK_{a2})/2$, $(2.43 + 9.80)/2 = 6.10$.[13] Cadmium(II) is reduced electrochemically at the dropping mercury electrode in binary and ternary systems showing a single diffusion-controlled two-electron wave. The voltammetric wave is found to be reversible. This

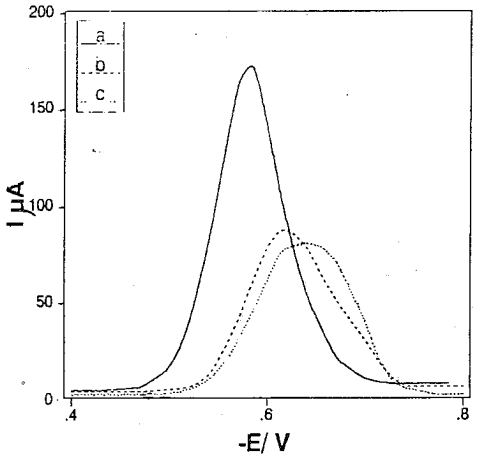

FIG. 1. *Differential pulse voltammograms for a) $5.0x10^{-4}$ mol l^{-1} Cd(II). b) a + $2.5x10^{-2}$ mol l^{-1} gly, c) a + b + $2.5x10^{-2}$ mol l^{-1} tsc.*

is clearly revealed from the shape of the cyclic and differential pulse voltammograms. $E^a_p - E^c_p = 30\pm1.6$ mV (where E^a_p and E^c_p are the peak current potentials of the anodic and cathodic scans, respectively.[14] The anodic to cathodic peak current ratio, i^a_p/i^c_p, reaches unity and $E_p - E_{p/2}$ amounts to 29±2 mV.[14] Furthermore, the peak current potentials do not shift on increasing the sweep rate in the entire range of investigation. Moreover, the half peak width, $w_{1/2}$, of the differential pulse wave is found to be 52±2 mV. The diffusion-controlled nature of the reduction wave is established from the linear variation of the peak current, i^c_p, with the square root of the sweep rate, $\nu^{1/2}$.[14]

I-Cadmium(II)-Thiosemicarbazide Binary System:

Simple system of cadmium(II) with thiosemicarbazide, tsc, is investigated to evaluate the composition and overall stability constants of the complexes liable to form at such conditions. The differential pulse voltammetric peak current potential of Cd(II) ion in 0.1 mol l^{-1} $NaClO_4$ aqueous medium at pH 6.1 is -0.588 volt versus Ag/Ag^+. The E_p does shift to more negative values in the presence of successive amounts of thiosemicarbazide indicating complex formation.

The overall formation constants, log β, quoted are generally for the complex species $[Cd_m(tsc)_nH_j]$, $[Cd_m(tsc)_n(OH)_j]$ and $[Cd_m(tsc)_n]$. It is found that, the hydrogen, hydroxo- and binuclear complex species give high

values of the sum of squares of the residual, U(equation 5), and the refinement of the input data is futil. Hence, only simple complexes $[Cd(tsc)_n]$ have to be considered. On the other hand, when only the species $[Cd(tsc)_n]^{2+}$ where n = 1,2,3 and 4, are considered, the best statistical fit gives low values of U. According to the statistical output, (the values of U, σ_{DATA} and s(log β)), the most likely model of species for the cadmium(II)-thiosemicarbazide binary system is the presence of a $[Cd(tsc)_3]^{2+}$ or $[Cd(tsc)_4]^{2+}$ binary complexes (*c.f.* Table 1). According to Toropova and Naimushina[2] that, thiosemicarbazide in the pH range of 5-7 acts as a NS bidentate ligand with cadmium(II), one can conclude that the most possible complex liable to form in the subject binary system is $[Cd(tsc)_3]^{2+}$. An agreement between the estimated stability constant for the subject system and those from the studies carried out previously[3,4,6] is observed. The slight deviation is due to the difference in the type and ionic strength of the supported electrolyte.

TABLE 1: Overall stability constants for the binary system of cadmium(II)-thiosemicarbazide at 25°C and I=0.10 mol l^{-1} $NaClO_4$ at pH=6.1.

Complex	log β±s	10^4 U	10^3 σ_{DATA}
$[Cd(tsc)]^{2+}$	1.76±0.24	7.97	9.98
	2.4[a]		
	2.71[b]		
	2.3[c]		
$[Cd(tsc)_2]^{2+}$	3.56±0.20	5.77	8.49
	4.38[a]		
	4.32[c]		
$[Cd(tsc)_3]^{2+}$	5.31±0.20	5.07	7.96
	5.66[a]		
	6[b]		
	5.9[c]		
$[Cd(tsc)_4]^{2+}$	7.05±0.21	4.97	7.89

a-ref. 6, b-ref. 4, c-ref. 3.

II-Cadmium(II)-Glycine-Thiosemicarbazide Ternary System:

On the addition of glycine, gly, to the cadmium(II)-thiosemicarbazide, tsc, binary system, its peak current potential, E_p, does shift to more negative potentials greater than in the presence of tsc

alone. This is indicative of the formation of ternary complex. The stoichiometries and overall formation constants of the formed complexes are estimated on trying various possible composition models, $[Cd_m gly_n tsc_p H_j]$, $[Cd_m gly_n tsc_p (OH)_j]$ and $[Cd_m gly_n tsc_p]$ using POLAG program. The hydrogen, hydroxo- and binuclear complexes exhibit high statistical output values indicating that only the simple $[Cdgly_n tsc_p]$ ternary complexes have to be tried by POLAG program. On the other hand, on considering only the simple ternary complexes, the best fit of data gives low statistical output (values of U, σ_{DATA} and s(logβ)) and the other models with high statistical output are rejected. The data obtained are presented in Table 2. It is found that, the most possible model is the model 5, which represents the presence of both [Cd gly tsc] and $[Cd\ gly_2 tsc_2]$ ternary species according to the values of U, σ_{DATA}, and s(log β).

TABLE 2: Overall stability constants for the ternary system of cadmium(II)-glycine-thiosemicarbazide at 298K and I=0.10 mol l^{-1} $NaClO_4$ at pH = 6.1.

Complex	log β±s	10^5 U	10^3 σ_{DATA}
1-[Cd-gly-tsc]	4.76±0.03	4.60	2.40
2-$[Cd\text{-}gly\text{-}tsc_2]$	7.21±0.03	4.50	2.38
3-$[CD\text{-}gly_2\text{-}tsc_2]$	8.40±0.06	27.36	5.23
4-[Cd-gly-tsc];	4.73±0.06		
$[Cd\text{-}gly_2\text{-}tsc]$	3.65±0.76	4.38	2.50
5-[Cd-gly-tsc];	4.81±0.07		
$[CD\text{-}gly_2\text{-}tsc_2]$	8.09±0.07	3.71	2.03

The apparent stabilization of ternary complexes may be expressed on comparing the difference in the stability (Δ log K) for the reactions MA + B and M + B.[15,16] It corresponds to the following reaction:

$$2\ Cd\ gly_3 + 2\ Cd\ tsc_3 \rightleftharpoons 3\ Cd\ gly_2 tsc_2 + Cd \qquad (6)$$

Hence,

$$\Delta \log K = 3 \log \beta_{Cd\ gly_2 tsc_2} - 2 \log \beta_{Cd\ gly_3} - 2 \log \beta_{Cd\ tsc_3} \qquad (7)$$

The computed value of Δ log K is +10.919. This demonstrates that, the ternary complex $[Cd\ gly_2 tsc_2]$ shows significant stabilization.

The results of the subject system and the binary one are summarized in Scheme 1, where log β of the steps is indicated. It is revealed from the Scheme that, the tendency of $[Cd\ gly_3]^-$ or $[Cdtsc_3]^{2+}$ to add the second ligand, thiosemicarbazide or glycine can be compared. The log β values are 6.729 and 2.775 for the addition of thiosemicarbazide and glycine, respectively. This indicates that, the mixed ligand ternary complex formation is favored.

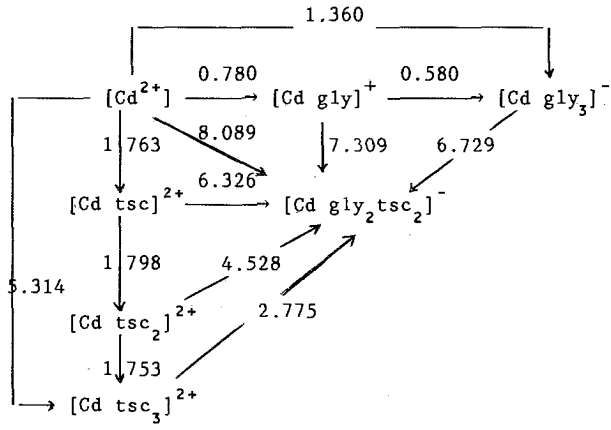

Scheme 1.

From the estimated overall stability constants for the ternary complexes, the percentage concentration, α, of each of the components present in the mixture of cadmium(II), thiosemicarbazide and glycine is calculated. On plotting α values as a function of thiosemicarbazide concentration, a distribution of the metal ions, [Cdglytsc] and $[Cdgly_2tsc_2]$ species is obtained. Typical graphs are illustrated in Fig. 2. It is revealed that, (Cdglytsc) species increases on increasing the concentration of the ligand and gets a maximum, α = 74.6%, at [ligand] = 0.02 mol l^{-1}. On the other hand, the $[Cdgly_2tsc_2]$ complex develops at [ligand] = 0.004 mol dm^{-3} α=1.7% and increases at the expense of the other one on increasing the concentration of the ligand.

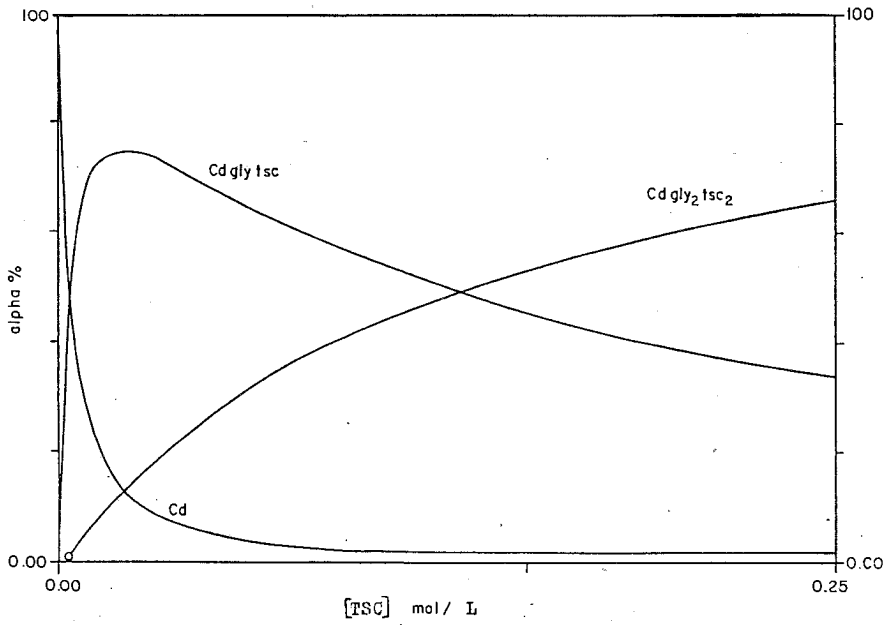

FIG. 2. *Distribution graph for the ternary system,*

ΠΕΡΙΛΗΨΗ

Βολταμμετρική μελέτη τριαδικών συμπλόκων καδμίου - θειοσεμικαρβαζιδίου - γλυκίνης

Μελετήθηκαν τα δυαδικά και τριαδικά σύμπλοκα του καδμίου (II)-θειοσεμικαρβαζιδίου - γλυκίνης χρησιμοποιώντας τις μεθόδους της κυκλικής και διαφορικής παλμικής βολταμμετρίας, στο ισοηλεκτρικό σημείο της γλυκίνης σε υδατικά διαλύματα 0.1 mol l^{-1} $NaClO_4$. Η σύσταση και η σταθερότητα των σχηματισθέντων στο διάλυμα συμπλόκων προσδιορίσθηκε χρησιμοποιώντας το πρόγραμμα POLAG. Ευρέθη ότι το Cd(II) σχηματιζει ένα 1:3 δυαδικό σύμπλοκο με θειοσεμικαρβαζίδιο, ενώ στο τριαδικό σύστημα, προκύπτει ένα μίγμα συστάσεως 1:1:1 και 1:2:2 (Cd:gly:tsc) αναφορικά με τους υποκαταστάτες των συμπλόκων. Τα τριαδικά σύμπλοκα ευρέθη ότι έχουν μεγαλύτερη σταθερότητα από τα δυαδικά. Επίσης διερευνήθηκαν οι ισορροπίες που υφίστανται σε μίγματα διαλυμάτων των τριών αυτών συστατικών.

REFERENCES

1-Nardelli, M. and Chierici, I., *Ricercca Sci.*, **30**, 276(1960).
2-Toropova, V. E. and Naimushina, K. V., *Russ. J. Inorg. Chem.*, **5**, 421(1960).
3-Christensen, A. N. and Rasmussen, S.E., *Acta Chem. Scand.*, **17**, 1315(1963).
4-Goddard, D. R.; Londam, B. D.; Ajayi, S. O. and Campball, M. J., *JCS(A)*, 506(1969).
5-Ajayi, S. O. and Goddard, D. R., *JCS Dalton*, 1751(1973).
6-Ghandour, M. A.; El-Samahy, A. A. and Komy, Z., *J. Indian Chem. Soc.*, **62**, 198(1985).
7-Leggett, D. J., Talanta, **27**, 787(1980).
8-Vogel, A. I., *"A Text Book of Qualitative Inorganic Analysis, Including elementary Instrumental Analysis"*, Longman, LONDON(1978).
9-DeFord, D.D. and Hume, D. V., *J. Am. Chem. Soc.*, **73**, 5321(1951).
10-Hume, D. N., Deford, D. D. and Cave, G. C. B., *J. Am. Chem. Soc.*, **73**, 5323(1951).
11-McMasters, D.L. and Schaap, W. B., Proc. *Indiana Acad. Sci.*, **67**, 111(1958).
12-Schaap, W. B. and McMasters, D. L., *J. Am. Chem. Soc.*, **83**, 4699 (1961).
13-Dhuley, D. G. and Dongre, V. G., *Indian J. Chem.*, **20A**, 208(1981).
14-Nicholson, R. S. and Shain, I., *Anal. Chem.*, **36**, 706(1964).
15-Sigel, H., *Angew Chem. Internal. Edn.*, **14**, 394(1975).
16-Brookes, G. and Pettit, L., *JCS Dalton Trans*, 1224(1976).

Chimika Chronika, New Series, 20, 169-177 (1991)

SHORT PAPER

USE OF BRIJ-35 IN PHOTOGALVANIC CELL FOR SOLAR ENERGY CONVERSION AND STORAGE : METHYLENE BLUE-EDTA SYSTEM

Suresh C. Ameta, Miss Sadhna Khamesra, Miss Anita Lodha and K.M. Gangotri

Department of Chemistry, University College of Science, Sukhadia University, Udaipur 313001, India

(Received October 9, 1989)

SUMMARY

Photogalvanic effect was studied in a photogalvanic cell containing methylene blue ethylenediaminetetraacetic acid, Brij-35 as a photosensitizer, reductant and surfactant, respectively. The photopotential and photocurrent generated by this system were 694 mV and 20 μA respectively. Effect of different parameters on the electrical output of the cell was observed and current voltage characteristics of the cell has also been studied.

Keywords: Photogalvanic cell, Solar energy conversion, Methyle blue, EDTA.

INTRODUCTION

Photogalvanic effect was first reported by Rideal and Williams[1] but it was systematically investigated by Rabinowitch[2]. Later on this type of work was followed by various workers all over the world[3-10]. Hoffman and Lichtin[11] discussed the various problems associated with the growth of this field.

A careful literature survey shows that no attention has been paid to the use of micelles in photogalvanic cell for solar energy conversion and therefore, the present work was undertaken.

EXPERIMENTAL

Methylene blue (BDH), EDTA (EM'GR') Brij-35(SIGMA) and sodium hydroxide (SD'S) were used in the present work. All the solutions were prepared in doubly distilled water.

A mixture of solutions of sodium hydroxide, EDTA, Brij-35 and dye was taken in a H-type cell. Saturated calomel electrode (SCE) was dipped in one limb of the cell and platinum electrode (1x1 cm^2) in the other. The cell was kept in dark till it reaches a stable value (dark potential = -125.0 mV). The platinum electrode was illuminated with a 200 W tungsten lamp and the limb containing SCE was kept in dark. The potential of cell rises on illumination and reaches a stable value at -819.0 mV. A water filter was used for cutting infra-red radiations.

The photochemical bleaching of methylene blue was studied potentiometrically. Digital pH meter (Systronics Model 335) and multimeter (Systronics Model 435) were used to measure the photopotential and photocurrent generated by the system MB/EDTA/OH^-/Surfactant/$h\nu$, respectively. The i-V characteristics of the cell was observed using an external load (log 500 K).

RESULTS AND DISCUSSIONS

Effect of Variation of Concentration of Surfactant

Dependence of electrical output on the concentration of surfactant was studied and results are reported in table 1.

Table 1

Effect of Variation of Brij-35 Concentration

[MB] = 2.00×10^{-5}M [EDTA] = 2.25×10^{-3}M

pH = 11.5 Intensity = 10.4 $mWcm^{-2}$

Temperature = 303 K

[Brij-35]x10^5M	Photopotential (mV)	Photocurrent (μA)
1.0	506.0	10.0
1.5	585.0	14.0
2.0	694.0	20.0
3.2	480.0	16.0
4.8	256.0	13.0

It is clear from the table that there is an increase in electrical output of the cell with the increase in the concentration of surfactant reaching a maximum value (conc. CMC). A further increase in the concentration of surfactant resulted into a fall in electrical output.

The charge on the dye-surfactant system may play a deciding role regarding the probability of photoejection of electrons. The neutral micelle like Brij-35 will play a boarder role between anionic and cationic surfactants.

Effect of Variation of pH

The electrical output of the cell was affected by the variation in pH of the system. The results are summarised in table 2.

Table 2

Effect of Variation of pH

$[MB] = 2.00 \times 10^{-5} M$ $[EDTA] = 2.25 \times 10^{-3} M$

$[Brij\text{-}35] = 2.00 \times 10^{-5} M$ Intensity = 10.4 $mWcm^{-2}$

Temperature = 303 K

pH	Photopotential (mV)	Photocurrent (μA)
11.1	506.0	12.0
11.3	587.0	15.0
11.5	694.0	20.0
11.7	612.0	16.0
11.8	538.0	13.0

The electrical output of the cell was found to increase on increasing the pH values reaching a maximum at pH = 11.5. A further increase in pH resulted into a fall in photopotential and photocurrent. It was observed that the pH for the optimum condition has a relation with pKa of the reductant and the desired pH is slightly higher than its pKa value ($pH > pKa$). The reason may be the availability of reductant in its anionic form which is its better donor form.

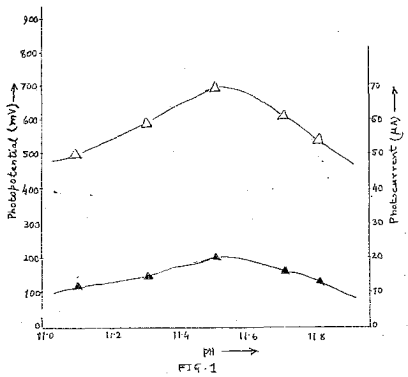

Fig.1

Effect of Variation of Dye Concentration

The effect of variation of dye concentration of electrical output of the cell was also studied and results are given in table 3.

Table 3

Effect of Variation of MB Concentration

[Brij-35] = 2.00×10^{-5}M [EDTA] = 2.25×10^{-3}M

pH = 11.5 Intensity = 10.4 $mWcm^{-2}$

Temperature = 303 K

[MB] x 10^{5}M	Photopotential (mV)	Photocurrent (μA)
0.5	497.0	12.0
1.5	588.0	17.0
2.0	694.0	20.0
3.0	546.0	15.0
4.0	460.0	10.0

Lower concentration of dye resulted into a fall in electrical output because less number of dye molecules are available for the excitation and consecutive donation of the electrons to the platinum electrode. The large concentration of dye again resulted into decrease in electrical output as the intensity of light reaching the dye molecule near the electrode decrease due to absorption of major portion of light by dye molecules present in the path.

Effect of Variation of Reductant Concentration

Dependence of photopotential and photocurrent on the concentration of EDTA was observed and results are summarised in table 4.

Table 4

Effect of Variation of EDTA Concentration

$[MB] = 2.00 \times 10^{-5} M$ Intensity = 10.4 $mWcm^{-2}$

$[Brij-35] = 2.00 \times 10^{-5} M$ pH = 11.5

Temperature = 303 K

$[EDTA] \times 10^{3} M$	Photopotential (mV)	Photocurrent (μA)
1.00	611.0	12.0
1.50	656.0	15.0
2.25	694.0	20.0
2.75	482.0	14.0
3.25	440.0	13.0

The decrease in EDTA concentration resulted into a fall in electrical output because less number of reductant molecules are available for electron donation to dye molecules. The large concentration of EDTA also resulted into a decrease in electrical output because the large number of reductant molecules may higher the dye molecule to reach the electrode in the desired time limit.

Effect of Diffusing Path Length

The effect of variation of diffusing path length on the current parameters of the cell was studied using H-cell of different dimensions. The results are reported in table 5.

Table 5

Effect of Diffusing Path Length

[MB] = 2.00×10^{-5}M [EDTA] = 2.25×10^{-3}M

[Brij-35]= 2.00×10^{-5}M Intensity = 10.4 mWcm^{-2}

pH = 11.5 Temperature = 303 K

Diffusing path length DL (mm)	Maximum photocurrent i_{max} (μA)	Equilibrium photocurrent i_{eq} (μA)	Rate of initial generation of current (μA min^{-1})
35.0	21.0	22.0	1.2
40.0	24.0	21.0	1.7
45.0	27.0	20.0	2.7
50.0	29.0	20.0	3.8
55.0	33.0	19.0	4.4

It was observed that there is a sharp increase in photocurrent (i_{max}) in the first few minutes illumination and then there is a gradual decrease to a stable value of photocurrent. This photocurrent at equilibrium is represented as i_{eq}. This kind of behaviour of photocurrent indicates an initial rapid reaction followed by a slow rate determining step at a later stage.

On the basis of the effect of diffusion length on the current parameters of the cell, it may be concluded that leuco and semi reduced form of the dye and the dye itself are the main electrode active species at the illuminated and dark electrodes, respectively. However, the reductants and its oxidised products behave as the electron carriers in the cell diffusing through the path.

Current-Voltage (i-V) Characteristics, Conversion Efficiency and Performance of the Cell

The open circuit voltage (V_{oc}) and short circuit current (i_{sc}) of the photogalvanic cell were measured with a multimeter(keeping the circuit closed), respectively. The current and potential values in between these two extreme values (V_{oc} and i_{sc}) were recorded with the help

of a carbon pot (log 500 K) connected in the circuit of multimeter through which an external load was applied.

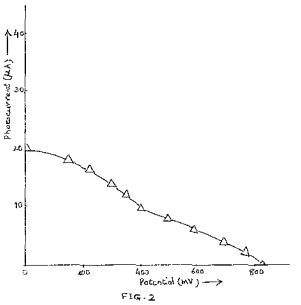

Fig. 2

It was observed that the i-V curve of the cell deviated from its ideal regular rectangular shape. A point in i-V curve called power point (pp) is determined where the product of potential and current is maximum. The values of potential and current at power point is represented as V_{pp} and i_{pp}, respectively, with the help of (i-V) curve, the fill-factor and conversion efficiency of the cell were determined as 0.26 and 0.4060%, respectively, using formula-

$$\text{Fill-factor} = \frac{V_{pp} \times i_{pp}}{V_{oc} \times i_{sc}} \qquad \ldots(1)$$

$$\text{Conversion Efficiency} = \frac{V_{pp} \times i_{pp}}{10.4 \ (\text{mWcm}^{-2})} \qquad \ldots(2)$$

The performance of the cell was studied by applying the external load necessary to have current and potential at power point after removing the source of light. It was observed that the cell can be used in dark at its power point for forty two minutes.

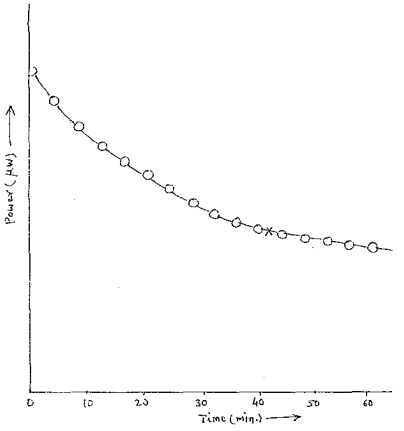

FIG-3

The photovoltaic cell cannot be used in dark even for a second whereas the photogalvanic system has an additional advantage of being used in dark, of course with lower conversion efficiency.

Mechanism

The following tentative mechanism for the generation of photocurrent in photogalvanic cell has been proposed as:

Illuminated chamber

$$MB \xrightarrow{h\nu} MB^* \qquad ..(1)$$

$$MB^* + R \longrightarrow MB^- \text{ (semi or leuco)} + R^+ \qquad ..(2)$$

at Platinum electrode

$$MB^- \longrightarrow MB + e^- \qquad ..(3)$$

Dark chamber

$$MB + e^- \longrightarrow MB^- \text{ (semi or leuco)} \qquad ..(4)$$

$$MB^- + R^+ \longrightarrow MB + R \qquad ..(5)$$

ACKNOWLEDGEMENT

Authors are thankful to the Professor and Head, Department of Chemistry, University College of Science, Sukhadia University, Udaipur for providing necessary laboratory facilities. Thanks are also due to Manju and Sapna for their critical discussion.

ΠΕΡΙΛΗΨΗ

ΧΡΗΣΗ ΤΟΥ BRIJ-35 ΣΕ ΦΩΤΟΓΑΛΒΑΝΙΚΟ ΣΤΟΙΧΕΙΟ ΓΙΑ ΜΕΤΑΤΡΟΠΗ ΚΑΙ ΑΠΟΘΗΚΕΥΣΗ ΗΛΙΑΚΗΣ ΕΝΕΡΓΕΙΑΣ

Μελετάται το φωτογαλβανικό φαινόμενο σε φωτογαλβανικό στοιχείο που περιέχει κυανούν του μεθυλίου, EDTA, Brij-35 ως φωτοευαισθητοποιητή, αναγωγικόν και επιφανειακά ενεργό μέσον αντίστοιχα. Το φωτοδυναμικό και φωτοηλεκτρικό ρεύμα που δημιουργούνται από το σύστημα αυτό είναι 694mV και 20μA αντίστοιχα. Η επίδραση διαφόρων παραμέτρων επί της ηλεκτρικής αποδόσεως του στοιχείου, μελετήθηκε καθώς και τα χαρακτηριστικά του

REFERENCES

Albery, W.J. and Founds, A.W. J. Photochem. 10, 41 (1979).

Ameta, Suresh C., Dubey, G.C., Dubey, T.D. and Ameta Rameshwar, Z. Phys. Chem. (Leipzig), 266, 200 (1985).

Clark, W.D.K. and Eckert, J.A. Solar Energy, 17, 147 (1975).

Fox, M.A. and Kabir-Ud-Din. J. Phys. Chem. Chem. 83, 1800 (1980).

Hoffman, M.Z. and Lichtin, N.N. in Solar Energy(Eds. R.R. Hautala, R.B. King and C. Kutal, 153 (1979).

Kaneko, M. and Yamada, A. J. Phys. Chem. 81, 1213 (1977).

Murthy, A.S.N., Dak, H.C. and Reddy, K.S. Int. J. Energy, Res. 4, 339 (1980).

Potter, A.E. and Thaller, L.H. Solar Energy, 3, 1 (1959).

Rabinowitch, E. J. Chem. Phys. 8, 551 (1940).

Rideal, E.K. and Williams, D.C. J. Chem. Soc. 258 (1925).

Author Index (Volume 20, 1991)

Keyword index (Volume 20) 1991

CHIMIKA CHRONIKA, *NEW SERIES*

CONTENTS

September - December 1991 Volume 20 No 3 - 4